

UNCLASSIFIED

AD NUMBER

AD830297

LIMITATION CHANGES

TO:

Approved for public release; distribution is unlimited.

FROM:

Distribution authorized to U.S. Gov't. agencies and their contractors;
Administrative/Operational Use; FEB 1964. Other requests shall be referred to Army Materiel Command, Alexandria, VA.

AUTHORITY

USAMC ltr, 22 Jul 1971

THIS PAGE IS UNCLASSIFIED

INFORM REFERENCE
LIBRARY SET

18 AUG 1981

RESEARCH AND DEVELOPMENT OF MATERIEL

ENGINEERING DESIGN HANDBOOK

GUNS SERIES GUN TUBES



PROPERTY OF THE U.S. ARMY
REDSTONE SCIENTIFIC INFORMATION CENTER
REDSTONE ARSENAL, ALABAMA

REDSTONE SCIENTIFIC INFORMATION CENTER
5 0510 00197092 7

HEADQUARTERS
UNITED STATES ARMY MATERIEL COMMAND
WASHINGTON 25, D. C.

28 February 1944

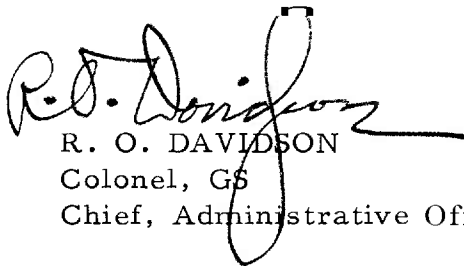
AMCP 706-252, Gun Tubes, forming part of the Guns Series
of the Army Materiel Command Engineering Design Handbook Series,
is published for the information and guidance of all concerned.

(AMCRD)

FOR THE COMMANDER:

OFFICIAL:

SELWYND. SMITH, JR.
Major General, USA
Chief of Staff


R. O. DAVIDSON
Colonel, GS
Chief, Administrative Office

DISTRIBUTION: Special

PREFACE

This handbook is the first of a planned series on Guns. It is part of a group of handbooks covering the engineering principles and fundamental data needed in the development of Army materiel, which (as a group) constitutes the Engineering Design Handbook Series. This handbook presents information on the fundamental operating principles and design of gun tubes.

This handbook was prepared by The Franklin Institute, Philadelphia, Pennsylvania, for the Engineering Handbook Office of Duke University, prime contractor to the Army Research Office—Durham. The Guns Series is under the technical guidance and coordination of a special committee with representation from Frankford Arsenal of the Munitions Command; and Springfield Armory and Watervliet Arsenal of the Weapons Command. Chairman of this committee is Mr. Anthony Muzieka of Watervliet Arsenal.

Agencies of the Department of Defense, having need for Handbooks, may submit requisitions or official requests directly to Equipment Manual Field Office (7), Letterkenny Army Depot, Chambersburg, Pennsylvania. Contractors should submit such requisitions or requests to their contracting officers.

Comments and suggestions on this handbook are welcome and should be addressed to Army Research Office—Durham, Box CM, Duke Station, Durham, North Carolina 27706.

TABLE OF CONTENTS

	<i>Page</i>
PREFACE	1
LIST OF ILLUSTRATIONS	v
LIST OF TABLES	vii
LIST OF SYMBOLS	viii
 CHAPTER 1. INTRODUCTION	 1
A. Scope and Purpose	1
B. Functions	1
C. Types of Guns	1
 CHAPTER 2. REGIONS OF THE GUN TUBE	 2
A. Chamber	2
B. Breech Ring Attachment	2
C. Bore	3
D. Muzzle	3
 CHAPTER 3. TYPES OF GUN TUBES	 5
A. Artillery Tubes	5
1. Monobloc Tube	5
2. Jacketed Tubes	5
B. Small Arms Tubes	5
1. Quasi Two-Piece Tube	5
2. Revolver Type Tube	5
C. Recoilless Tube	7
D. Expendable Tubes	7
 CHAPTER 4. FIRING PHENOMENA AFFECTING GUN TUBES	 8
A. Mechanical Loading	8
1. Propellant Gas Pressure	8
2. Projectile Effects	8
3. Recoil Forces	9
4. Vibration	9

TABLE OF CONTENTS — (continued)

	<i>Page</i>
B. Heating	9
1. Thermal Stresses	9
2. Dimensional Changes	11
3. Cook-Off	11
C. Erosion	12
1. Causes	12
2. Region Affected	12
CHAPTER 5. WAYS OF MINIMIZING HARMFUL EFFECTS TO GUN TUBES	13
A. Mechanical Design	13
1. High Strength Materials	13
2. Vibration Correction Measures	13
3. Vibration Calculations	13
B. Cooling Methods	17
1. Large Tube Masses	17
2. Coolants	18
3. Boundary Layer Cooling	18
4. Low Heat Input	19
C. Low Erosion Measures	19
1. Rotating Band Properties	19
2. Rifling	19
3. Liners and Plating	21
CHAPTER 6. GUN TUBE DESIGN	22
A. Design Objectives	22
B. Interior Ballistics Curves	22
C. Chamber Requirements	22
1. Cartridge Case Fit	23
2. Chamber Slope	24
3. Forcing Cone Slope	24
4. Chamber Geometry — Recoilless Guns	24
D. Nozzle Design, Recoilless Guns	26
1. Parameters	26
2. Nozzle Shape	27
3. Nozzle Pressure Distribution	28
4. Recoil Balancing	28
E. Bore	30
1. Bore Diameter	30
2. Bore Length	30
F. Temperature Distribution	30

TABLE OF CONTENTS—(continued)

	<i>Page</i>
G. Rifling	30
1. Profile	30
2. Rifling Twist	31
3. Rifling Torque	33
H. Determination of Thickness of Tube Walls	38
1. Design Pressures	38
2. Strength Requirements	39
3. Equivalent Stress	40
4. Pressure Stresses	40
5. Rifling Torque Stresses	41
6. Shrinkage Stresses	41
7. Thermal Stresses	44
8. Inertia of Recoil Stresses	45
9. Stress Concentration	45
10. Special Applications for Tube Analyses	45
11. Stress Compensating Measures	60
12. Strain Compensation	62
I. Lincr Design	63
J. Quasi Two-Piece Tube	63
K. Mechanical Features	64
1. Threads	64
2. Rifling Torque Transmitters	66
3. Muzzle Attachments	66
L. Gun Tube Materials	66
1. Steel	66
2. Titanium Alloy	68
3. Aluminum	71
4. Plastics	71
5. Stellite	72
6. Chromium	72
M. Manufacturing Procedures	73
CHAPTER 7. MAINTENANCE	74
A. Corrosion Inhibitors	74
B. Inspection	74
CHAPTER 8. SAMPLE PROBLEMS	75
A. Monobloc Tube, Artillery	75
1. Regular Tube	75
2. Autofrettaged Tube	76
B. Jacketed Tube, Artillery	76
1. Tube With Single Jacket	76
2. Tube With Two Jackets	78

TABLE OF CONTENTS—(continued)

	<i>Page</i>
C. Small Arms Barrel With Shrink Fitted Liner and Cap .	81
1. Shrink Fit Pressure	81
2. Shrink Fit Stresses	82
3. Pressure Stresses	82
4. Combined Stresses	83
D. Small Arms Barrel With Combined Pressure and Thermal Stresses	83
1. Propellant Gas Pressure Stresses	83
2. Shrink Fit Pressure Stresses	83
3. Thermal Stresses	84
E. Recoilless Gun	83
1. Gun Tube	84
2. Chamber	87
3. Nozzle	91
GLOSSARY	94
REFERENCES	99

LIST OF ILLUSTRATIONS

<i>Fig. No.</i>		<i>Page</i>
1	Typical Gun Tube Showing Regions	2
2	Chambers of Various Tube Types	4
3	Jacketed Tube	6
4	Quasi Two-Piece Tube	6
5	Revolver Type Tube Showing Separate Chamber With Round	6
6	Gatling Gun Tubes	6
7	Recoilless Gun Tube	6
8	Temperature Distribution Across Tube Wall	9
9	Temperature Along Outer Surface of Caliber .30 Tube	10
10	Thermal Cracks on Bore Surface	11
11	Dispersion-Frequency Ratio Curve	14
12	Gun Tube Showing Subdivisions	14
13	<i>M/I</i> Diagram of Gun Tube	15
14	Types of Rifling Contour	20
15	Progressive Engraving	20
16	Interior Ballistics of Caliber .30 Gun	22
17	Case-Chamber Stress-Strain Curves	23
18	Chamber With Pertinent Dimensions	24
19	Forcing Cone Study	25
20	Schematic of Recoilless Gun	25
21	Nozzle Entrance Geometry	26
22	Pressure Ratio-Area Ratio Curve	27
23	Lines of Constant Dimensionless Recoil	27
24	Nozzle Shapes—Schematic	27
25	Nozzle Pressure-Area Ratio Curve, M10 Propellant	28

LIST OF ILLUSTRATIONS—(continued)

<i>Fig. No.</i>		<i>Page</i>
26	Groove-Bore Relations	31
27	Standard Rifling Profiles	32
28	Rifling Force Diagram	33
29	Torque Curves for 37 mm Gun	34
30	Effects on Rifling Torque by Varying Exit Angle	35
31	Tipped Parabola	35
32	Rifling Torque Curves for Caliber .30 Barrel	37
33	Wall Ratio-Pressure Factor Curves for Multilayer Tubes	43
34	Thermal Stress Distribution Across Tube Wall	44
35	Equivalent Stress as a Function of Wall Ratio and Temperature Distance for an Internal Pressure of 10,000 psi	46
36	Equivalent Stress as a Function of Wall Ratio and Temperature Distance for an Internal Pressure of 20,000 psi	46
37	Equivalent Stress as a Function of Wall Ratio and Temperature Distance for an Internal Pressure of 30,000 psi	47
38	Equivalent Stress as a Function of Wall Ratio and Temperature Distance for an Internal Pressure of 40,000 psi	47
39	Equivalent Stress as a Function of Wall Ratio and Temperature Distance for an Internal Pressure of 50,000 psi	48
40	Equivalent Stress as a Function of Wall Ratio and Temperature Distance for an Internal Pressure of 60,000 psi	48
41	Design Pressure-Travel Curve	49
42	Typical Recoilless Gun Pressure Design Curves	49
43	Gimbal Ring Loading	53
44	Conical Section Loading	55
45	Toroidal Section Loading	56
46	Toroidal Internal Moment Center	57
47	Toroidal External Loads	58
48	Nozzle With General Dimensions	59
49	Threaded Joint With Butted End	64
50	Thread Profile Types	64
51	Interrupted Threads	65
52	Threaded Joint	65
53	Rifling Torque Reactions	66
54	Gunner's Quadrant Flats	67
55	Effects of Temperature on Tensile Strength of SAE 4150 and Cr-Mo-V Steels	67
56	Effects of Tempering Temperature on Tensile Strength of SAE 4150 Steel	68
57	Effects of Temperature on Tensile Strength of Typical Steels for Recoilless Tubes	69
58	Physical Properties of Steel	69
59	Effects of Aging Processes on Tensile Strength of Titanium at Various Temperatures	70
60	Effects of Temperature on Tensile Strength of Titanium Alloy	70
61	Design Data, Monobloc Artillery Tube	73
62	Design Data, Jacketed Artillery Tube	77
63	Schematic of Tube With Liner	81
64	Tangential Stress of Shrink Fitted Tube	83

LIST OF TABLES

<i>Table No.</i>		<i>Page</i>
1	<i>M/I</i> Calculations for Static Condition	15
2	Area Moments for Static Condition	16
3	Natural Frequency Parameters. Static Condition	16
4	<i>M/I</i> Calculations for Dynamic Condition	17
5	Area Moments for Dynamic Condition	17
6	Natural Frequency Parameters. Dynamic Condition	18
7	Forcing Cone Slopes	24
8	Rifling Torque Calculations for Exponential Rifling	36
9	Ratios of Equivalent Stresses	45
10	Wall Ratio-Pressure Ratio Chart for Monobloc Gun Tubes	50
11	Chemical Requirements of Steel	68
12	Reduction of Area and Impact Requirements	69
13	Heat Transfer Coefficients, <i>h</i>	70
14	Minimum Mechanical Property Requirements of Titanium Alloys	71
15	Properties of Representative Gun Tube Materials	71
16	Thermal Coefficient of Linear Expansion of Stellite 21	72
17	Mechanical Properties of Stellite 21	72
18	Surface Finishes of Gun Tubes. RMS	73
19	Design Data of Theoretical Monobloc Tube	76
20	Design Data of Actual Monobloc Tube	76
21	Design Data of Theoretical Autofrettaged Tube	77
22	Design Data of Actual Autofrettaged Tube	77
23	<i>ESP</i> Calculations for Single Jacketed. 100 mm Tube	79
24	Combined Shrink Fit and Pressure Stresses (lb/in ²)	83
25	Nozzle Stresses	92

LIST OF SYMBOLS

a	= distance from origin of coordinate axes to origin of rifling curve; inner radius; linear acceleration of projectile	F_u	= unit load on breechblock thread
a_m	= maximum projectile acceleration	ΔF	= force increment
A	= area of section; general expression for area	g	= acceleration of gravity
A_a	= nozzle approach area	G	= number of rifling grooves; shear modulus
A_b	= bore area	h	= depth of rifling groove; depth of keyway
A_c	= chamber area	I	= area moment of inertia, general expression
A_e	= nozzle exit area	J	= area polar moment of inertia
A_n	= original nozzle throat area; projected area of nozzle	k	= radius of gyration of projectile
A_t	= nozzle throat area	k_t	= high temperature strength reduction factor
A_x	= nozzle area at distance x from the throat	K	= kinetic energy
ΔA_n	= change in nozzle throat area	K_t	= constant in rifling torque equation for constant twist
b	= twice distance from origin of rifling to point of maximum pressure; outer radius	L	= axial length of rifling curve; length of engaged thread; length of key; length of increment
C	= weight of propellant charge	L_d	= length of diverging cone
CMP	= computed maximum pressure	L_f	= load factor
d_t	= depth of thread	L_n	= length of nozzle cone
D	= diameter varying from D_i to D_o ; mean diameter; general expression for diameter; general expression for flexural rigidity	L_o	= required maximum length of chamber
D_i	= outside diameter of liner; inside diameter of jacket	M	= general expression for moment
D_b	= bore diameter	M_p	= mass of projectile
D_i	= inside diameter	M_r	= recoiling mass; momentum of recoiling mass
D_m	= mean diameter; mandrel diameter	M_{rs}	= specified momentum of recoiling mass
D_o	= outside diameter	ΔM_r	= required change in momentum
ΔD_c	= nominal clearance between bore and projectile	n	= exponent defining rifling curve
E	= modulus of elasticity; propellant potential	n_c	= twist of rifling stated in calibers per turn
E_e	= equivalent modulus of elasticity	N	= induced force normal to rifling curve
E_r	= modulus of elasticity of ring	p	= constant in equation for increasing twist, rifling; general expression for design pressure
ESP	= elastic strength pressure	p_A	= pressure at point A of equivalent bore
f_c	= equivalent stress factor	p_c	= chamber pressure; true computed pressure
f_n	= natural frequency	p_f	= autofrettage pressure
f_r	= firing rate	p_g	= propellant gas pressure
F	= general expression for force; specific impetus; nozzle thrust	p_{gm}	= maximum propellant gas pressure
F_g	= propellant gas force	p_i	= internal pressure
F_n	= nozzle force	p_m	= computed design pressure, based on PIMP
F_r'	= cradle key load induced by rifling torque	p_o	= external or outside pressure; reservoir pressure
F_t	= thread load; thrust at nozzle throat at Mach 50.1	p_s	= pressure induced by shrink fit
		p_t	= design pressure at nozzle throat; pitch
		p_w	= allowable pressure

LIST OF SYMBOLS—(continued)

p_x	= nozzle pressure at point E	x_E	= axial length of rifling in bore
P	= recorded firing pressure	y	= deflection of beam increment; peripheral distance of rifling around bore
$PIMP$	= permissible individual maximum pressure	Y	= yield strength
$PMMP$	= permissible mean maximum pressure	α	= coefficient of linear expansion; angle of twist of rifling; half angle of diverging cone
r	= radius at any point in the wall; general expression for radius	α_E	= exit angle of rifling
r_a	= radius of nozzle approach area	β	= slope of conical surface of chamber; λ equivalent of combined region
r_e	= radius of nozzle exit	γ	= ratio of specific heats
r_t	= radius of nozzle throat	δ	= total deflection; total shrink interference; general expression for deflection; density of steel
R	= radius of pendulum; projectile radius; bore radius	δ_J	= deflection on jacket
R_e	= ratio of effective stresses	δ_L	= deflection on liner
R_f	= frequency ratio	δ_m	= deflection of mandrel
RMP	= rated maximum pressure	δ_{rs}	= deflection of ring due to shrink fit
s	= constant in equation for increasing twist rifling	δ_t	= deflection of tube
s_a	= length of free run	Δ	= loading density; general expression for relative radial deflection
S_A	= distance from breech of equivalent chamber to A	Δ_i	= required interference between tube and mandrel
S_B	= distance from breech of equivalent chamber to base of projectile	Δ_p	= maximum bag density of propellant
S_f	= factor of safety	ϵ_t	= tangential unit strain
t	= time; thickness; temperature at any point in wall	θ	= slope of wall; angular displacement of projectile; general expression for angular deflection
t_a	= time of propellant gas period	θ_n	= included angle of nozzle
t_i	= temperature at inner wall surface	$\dot{\theta}$	= angular velocity of projectile
t_o	= temperature at outer wall surface	$\ddot{\theta}$	= angular acceleration of projectile
t_r	= required wall thickness	λ	= nozzle divergence angle correction factor
T	= rifling torque; period of pendulum	η_a	= axial stress factor
T_p	= rifling torque component due to pressure	η_t	= tangential stress factor
T_v	= rifling torque component due to velocity	μ	= coefficient of friction
aT	= total temperature gradient	ν	= Poisson's ratio
v	= projectile velocity at any point in bore	ρ	= polar radius of gyration
v_m	= muzzle velocity	σ_a	= principal stress in axial direction
v_r	= recoil velocity	σ_{ap}	= axial stress caused by pressure
V_e	= propellant bag space	σ_{at}	= axial thermal stress
V_e	= nozzle entrance volume	σ_{br}	= bearing stress
V_f	= final gun volume	σ_e	= equivalent stress
V_o	= chamber volume	σ_{ea}	= allowable equivalent stress
W	= weight; wall ratio; dynamic force of beam increment	σ_f	= fillet bending stress
W_c	= weight of propellant charge; corrected wall ratio	σ_r	= principal stress in radial direction
W_i	= wall ratio of finished tube	σ_{rp}	= radial pressure stress
W_J	= wall ratio of jacket	σ_{rs}	= radial shrink fit stress
W_L	= wall ratio of liner	σ_{rt}	= radial thermal stress
W_p	= weight of projectile	σ_t	= principal stress in tangential direction
W_r	= weight of recoiling mass	σ_{tm}	= tangential stress produced by moment
W_t	= weight of tube	σ_{tp}	= tangential pressure stress
x	= axial length of rifling curve; linear amplitude of pendulum		

© Fortschreibung des ggf. abgewandten RT

[illegible]

CHAPTER 1

INTRODUCTION

A. SCOPE AND PURPOSE

1. The term gun tube, or simply tube, is used throughout this handbook to designate the principal part of a gun; i.e., that part which discharges the projectile. It is used in its general application without limitation as to caliber, and embraces the terms gun barrel or barrel frequently employed, especially in small arms terminology. The material in this handbook discusses procedures for the design of the various types of gun tubes. It is intended to present various problems facing the tube designer and in this light discusses the present approach in tube design. This handbook should prove helpful in familiarizing new personnel with the many phases of tube design and also should be a useful reference for the experienced.

B. FUNCTIONS

2. The tube is the primary component of a gun. Basically it is a tubular pressure vessel, closed at the breech and open at the muzzle; except in a recoilless gun in which the breech also has controlled openings. The tube determines the initial activities of the projectile. Before firing, it provides space for

the complete round. During firing, it restrains the propellant gas in all directions except that of projectile travel, thus directing the impetus of the gas against the projectile. In recoilless guns part of the gas impetus is directed rearward to counteract recoil. The azimuth and elevation determine the direction of flight. In rifled tubes the rifling imparts the necessary rotation for projectile stability. In brief, the mission of the tube is to direct the projectile toward the target with a specified velocity.

C. TYPES OF GUNS

3. Generally, the tube bears the label of the weapon. Tubes are placed in three general classes, namely: artillery, small arms, and recoilless. Artillery includes guns of over 30 mm in bore diameter, such as guns, howitzers and mortars. Small arms include automatic and semiautomatic, single fire, guns which generally do not exceed 30 mm in caliber. A few automatic weapons of caliber larger than 30 mm, such as the 37 mm Vigilante and the 90 mm Sky-sweeper, make specific classification difficult. Recoilless guns are those of any caliber whose recoil forces are neutralized by the reaction of propellant gas escaping rearward.

CHAPTER 2

REGIONS OF THE GUN TUBE

4. A gun tube may be divided into four regions: the front portion or bore through which the projectile travels when the round is fired; the rear portion or chamber which houses the round before firing; the rear opening or breech through which the ammunition is loaded; and the front opening or muzzle from which the projectile emerges. In recoilless guns the rear opening or nozzle provides for recoillessness. Exceptions do prevail with respect to the functions of these regions particularly with breech opening and loading technique. For example, most mortars are muzzle loaded and have permanently closed chambers. Figure 1 is a typical tube showing the regions applicable to conventional gun tubes.

A. CHAMBER

5. After loading but prior to firing, the part of the projectile forward of the rotating band or its equivalent is located in the bore, and in the case of recoilless ammunition, the pre-engraved band also rests in the bore. The remainder of the round rests in the chamber, which, except for revolver type guns, is integral with the bore and consists of the chamber body, the first shoulder, the centering cylinder for artillery or the neck for small arms, the second shoulder, bullet seat, and the forcing cone, (Fig. 2a). The forcing cone is a conical frustum whose slope extends through the origin of rifling and intersects the bore surface. Engraving of the rotating band occurs here. The section immediately to the rear of the bullet seat is called the centering cylinder or neck. It is just large enough to receive the rotating band or the neck of the cartridge case. This feature is not always found in heavy artillery

tubes. The main and largest compartment, the chamber body, houses the propellant and igniter. Parts b, c, d, and e, of Figure 2 show complete rounds positioned in various tube chambers. Artillery tubes using separate loading ammunition have the inner chamber wall cylindrical or conical, the minimum diameter of either contour being limited to the maximum diameter of the forcing cone. If conical, the inner surface may be the extension of the forcing cone. On the other hand, for tubes firing fixed and semifixed ammunition, the clearances between chamber and cartridge case and the slopes of the chamber walls are critical, since the cartridge case walls, by expanding, seal in the propellant gases, but must recover sufficiently after firing to assure easy case extraction. This is particularly true in small arms where small clearances are desired along the tapers including those in which a definite longitudinal interference is desired at the first shoulder. During loading, the force of the breechblock may actually collapse the case slightly in this region to obviate the likelihood of axial failure of the case. This collapsing action is called crush-up and contributes to easy case extraction.

B. BREECH RING ATTACHMENT

6. The chamber is closed by a breechblock or bolt or, as in recoilless weapons, by the nozzle unit. A breech ring supports the breechblock. The breech ring is threaded to the outside of the chamber wall. Its counterpart in some small arms is the receiver which houses the bolt. The nozzle unit of a recoilless tube may be attached directly to the rear of the chamber wall or to a modified breech ring. These elements are attached to the tube so that the re-

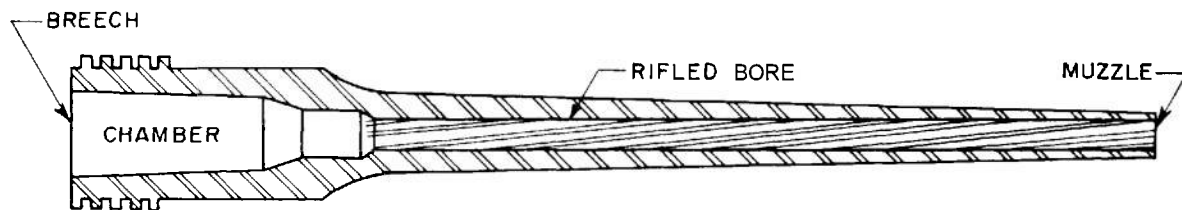


FIGURE 1. Typical Gun Tube Showing Regions.

substant gas force applied to them may be transmitted to the tube. Thus, tube and breech assembly act as a unit in transmitting the resultant force to the structure supporting the tube.

C. MORE

7. The bore is formed by the inner surface of a circular cylinder. It is the accelerating tube for the projectile. Early firearms were smooth bore and inherently inaccurate. Eventually, either by accident or design, it was discovered that spinning the projectile about the flight axis increased accuracy. Several methods have been introduced to achieve this rotation. One method utilizes the behavior of air impinging on canted fins attached to projectiles such as projectiles fired from smooth bore mortars. Another method uses rifling to impart the rotation. Rifling consists of splines which spiral along the bore surface. The raised portions are called lands; the spaces between them are called grooves. The spiral may have a constant angle of twist, i.e., a helix, or it may have a variable angle of twist conforming to some exponential expression. As the projectile moves through the bore, it turns with the rifling at an angular velocity proportional to the linear velocity and to the tangent of the angle of twist.

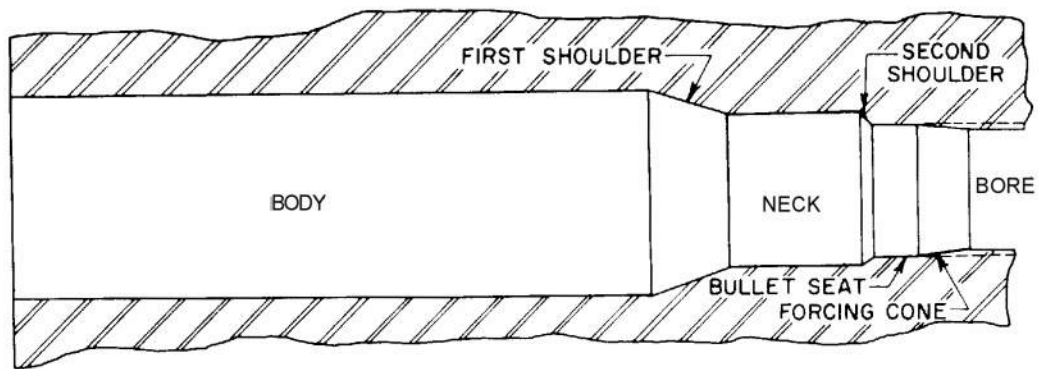
8. Contact with the rifling is assured by having the diameter of the jacket of a bullet or the rotating band of a larger projectile at least equal to the groove diameter. Then, just as the projectile starts to move, the band or jacket is forced into the rifling. This process is called engraving and takes place at the beginning, or origin, of rifling. For recoilless guns, rotating bands are preengraved to eliminate the large engraving forces which are undesirable in this type weapon. Some mortar projectiles have a flaired skirt, or sabot, at the base which is pressed into the rifling by the propellant gas pressure. Rotating

bands can be of a reactive soft material which are welded, bonded, or mechanically attached to the projectile. Jackets may be considered as bands which cover the bullets completely. Either jacket, rotating band, or sabot is necessary to transmit to the projectile the angular accelerating force induced by the rifling, and to serve as a seal to prevent propellant gases from escaping past the projectile.

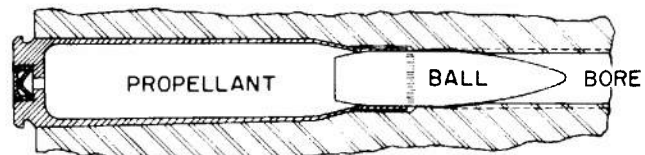
9. Tapered bores (squeeze bores) have been used in the past as a means to increase muzzle velocity. An oversize bore at the chamber was gradually tapered to a much smaller diameter near the muzzle. The larger bore diameter exposed a larger pressure area to the propellant gases thereby increasing the projectile acceleration. The projectile relied on two rotating bands having oversize diameters to keep it centered and in contact with the rifling. The bands, spaced far enough apart to form an effective whellbase, were squeezed inward toward the base of the projectile as it traveled along the tapered bore. This concept was proved impractical and now has no more than historical significance. A more logical use of the tapered bore is that practiced in small arms. In order to decrease its diameter slightly as the muzzle is approached, the bore is provided with a shallow taper along its entire length. This design concept, better known as choke bore, has been adopted to compensate for the anticipated erosion. In shotguns, choke bore is applied to a short distance at the muzzle to control the area of spread, or shot pattern.

D. MUZZLE

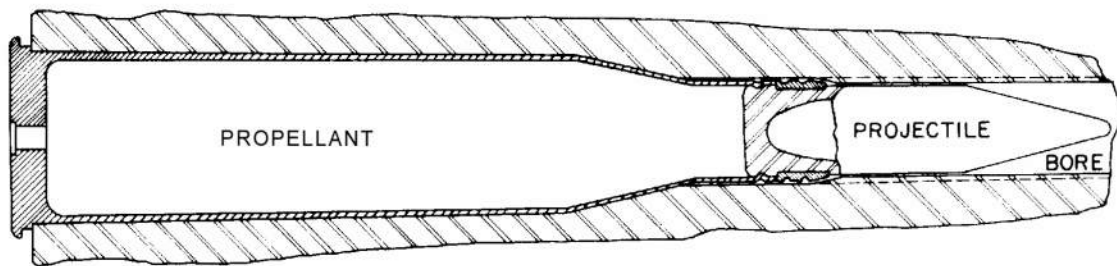
10. The muzzle end of the tube serves as the attachment for front sights, blast deflectors, and muzzle brakes. Blast deflectors do not apply severe loads to the tube. However, muzzle brakes develop large forces which usually are transmitted to the tube by a threaded attachment near the muzzle.



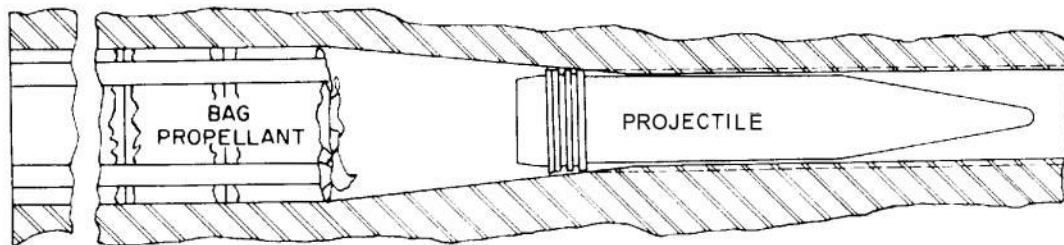
(a) CHAMBER SHOWING COMPONENTS



(b) SMALL ARMS CHAMBER CONTAINING FIXED ROUND



(c) ARTILLERY CHAMBER CONTAINING FIXED ROUND



(d) ARTILLERY CHAMBER CONTAINING SEPARATELY LOADED ROUND

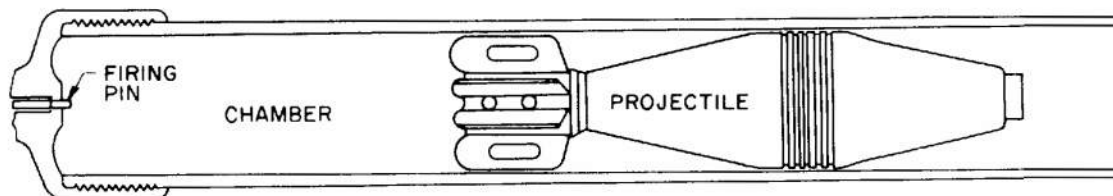


FIGURE 2. Chambers of Various Tube Types.

CHAPTER 3

TYPES OF GUN TUBES

11. Gun tubes are generally classified according to weapon, i.e., artillery tubes, small arms tubes, and recoilless tubes. Each is subdivided according to method of construction although a particular construction need not be confined to any one weapon type.

A. ARTILLERY TUBES

1. Monobloc Tube

12. Artillery tubes fall into two categories, monobloc and jacketed. The true monobloc tube (Figure 1) is made of one piece of material. A variant is the lined tube which deviates only slightly in principle from the true monobloc because the liner is usually not a major contributor of strength to the tube wall. Liners may be assembled by shrink fit or they may be a loose fit. They may extend along the full length of the bore or for only a short distance at and beyond the origin of rifling where erosion is most severe. Liners may prolong tube life by being made of material which is highly resistant to erosion. Loose fitting liners prolong tube life by being replaceable in the field. Most of the shrink fitted type serve throughout the life of the tube. The length is determined by the ability to maintain proper clearances while the liner is being inserted into the tube.

Monobloc tubes are also used for mortars, an adjunct of artillery. Mortars are usually emplaced manually and are often transported manually, therefore low weight is essential. In this respect, mortar tube requirements are similar to those of recoilless tubes.

2. Jacketed Tubes

13. The jacketed, or built-up, type (Figure 3) is constructed of two or more close fitting, concentric tubes not of the same length. (It may, or may not, have a replaceable liner.) The jackets do not extend to the muzzle where pressures are low but are only long enough to provide the built-up tube with wall thicknesses required by the pressure along the bore. Assembly is usually by shrink fit. Although the jackets are not full-length, the inside tube, including its unreinforced forward end, is still referred to as

the liner. Formerly, jacketed tubes included the wire-wrapped type. The wire, square in cross section, was wrapped under tension on a central tube thereby inducing an initial compressive stress in the tube, the same effect realized from shrink fitting. However, its tendency to droop and whip excessively, improvement in manufacturing techniques, and advances in inspection methods, have all contributed to the replacement of the wire-wrapped tube by the present jacketed type.

B. SMALL ARMS TUBES

14. Small arms tubes may be monobloc or they may be made of two or more components, as are the quasi two-piece and the revolver type tubes.

1. Quasi Two-Piece Tube

The quasi two-piece tube (Fig. 4) is particularly adapted to a machine gun. It consists of two units: a lined tube and a cap. The cap contains the chamber. The units are assembled permanently by a combination of threads and shrink fits to become, virtually, a one piece, lined tube.

2. Revolver Type Tube

Another small arms barrel is the revolver type sketched in Figure 5. It has two primary components, the barrel and the drum. The barrel contains the forcing cone and bore and, in this respect, is similar to other tubes. The drum is the chamber housing. It is made of one piece so that the chambers which may number four, five or six, are integral. These are equally spaced around the axis of the rotating drum and are so indexed that each one, in sequence, becomes aligned with the bore when the drum stops for the round to be fired. A seal, carried by each chamber, precludes the escape of propellant gases between drum and tube.

In contrast, the several tubes of the Gatling type gun (Fig. 6), although operating as a unit similar to the revolver type, are complete conventional tubes, each with its own chamber and bore. The advantage of this type lies in its capability of a high rate of fire while subjecting the individual tubes

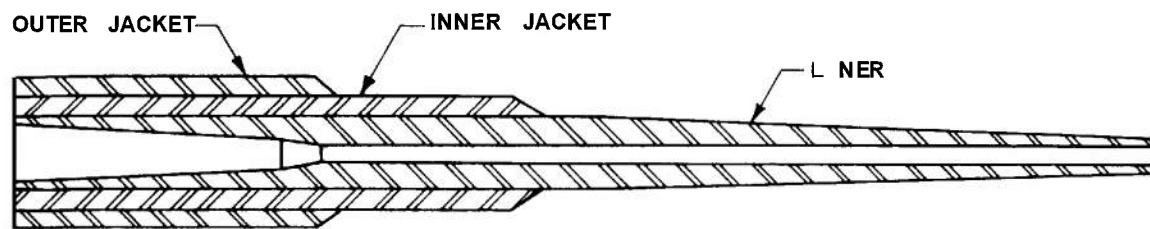


FIGURE 3. Jacketed Tube.

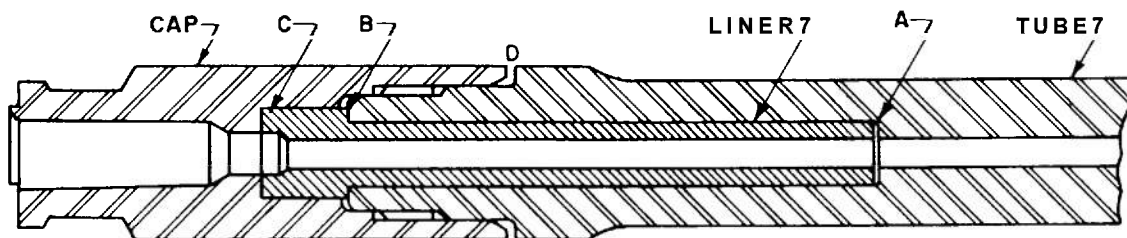


FIGURE 4. Quasi Two-Piece Tube.

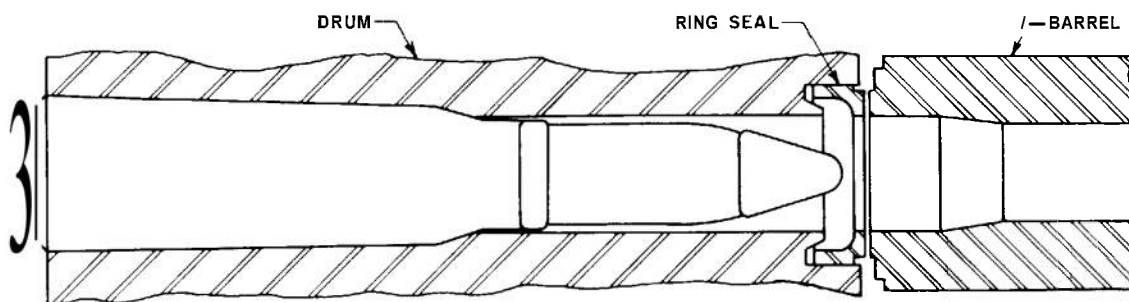


FIGURE 5. Revolver Type Tube Showing Separate Chamber With Round.

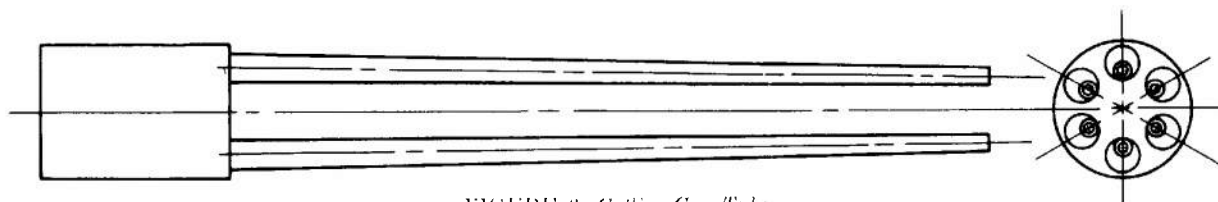


FIGURE 6. Gatling Gun Tubes.

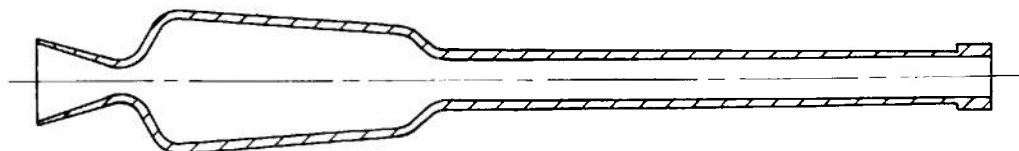


FIGURE 7. Recoilless Gun Tube.

to a relatively low rate. The design criteria differs only to the extent that individual tubes derive considerable rigidity from the assembly and therefore can be made as light as induced stresses, machining operations, and handling abuse will permit. The ring supporting the tubes at the muzzles, one of the parts furnishing this rigidity, has been omitted from Figure 6.

C. RECOILLESS TUBE

15. If practical, monobloc construction is preferred for recoilless tubes. A one-piece tube (Fig. 7) is desirable from the viewpoint of low weight and simplicity. However, to minimize manufacturing complexities, tubes with integral chambers are currently employed with the nozzle being a separate component fastened and sealed to the chamber, usually by some type of threaded joint.

D. EXPENDABLE TUBES

16. Expendable tubes are not a type in the same sense of the preceding ones but may be considered a unique type in terms of application or service. The chief argument for expendability is the saving of weapon weight, resulting in greater mobility and easier handling. A truly expendable weapon might

be considered as being one which would be fired only once, and then discarded. This suggests that the tube could be designed to, or very close to, the point of failure. It is quickly realized, however, that such a design criterion would not be practicable because of the nature of mechanical properties of materials, inconsistencies of material composition, and variations in performance. This leads to consideration of another possibility in the concept of expendability, namely, a limited-life tube.

The real gains accruing to the weapon (reduction in weight, volume, complexity, cost, etc.) are made in changing from extended-life usage. There appears to be little or no gain in reducing the use of the tube from several shots to only one shot. The reasonableness of going from one to a few shots in an expendable system was demonstrated by an experiment involving caliber .50 aluminum tubes. The experiment showed that several rounds could be fired from each tube before the rifling was stripped to the point of not providing sufficient spin stability. It should be recognized that even in these early experiments, the use of a fin-stabilized or possibly a pre-engraved projectile would have resulted in improved useful life. It may be concluded, therefore, that a limited-life, light-weight tube capable of firing several full caliber rounds can be developed.

CHAPTER 4

FIRING PHENOMENA AFFECTING GUN TUBES

17. To be effective, the gun tube must be accurate. Accuracy is directly affected by any change or irregularity in the angular or linear velocity of the projectile as it leaves the muzzle of the gun. Useful life of the tube depends on its ability to withstand the rigors of firing and still maintain the desired muzzle velocity. The ballistic cycle of a gun is extremely short, a matter of milliseconds. During this short period, the tube is subjected to extremely high temperatures, rapidly applied pressures, and inertia forces. Normally a small number of rounds will cause little measurable deterioration. But, after firing a large number of rounds, deterioration becomes evident. High rates of fire accelerate the deterioration. Any phenomenon which reduces accuracy or velocity life, by causing damage or wear in the tube, must be considered deleterious. The adverse effects of some are immediately apparent. Others are less pronounced but are cumulative in nature and eventually will prove harmful. Compensating measures taken during the design stage will minimize many of these ill effects.

A. MECHANICAL LOADING

18. With the exception of rotating band pressure, the effects of mechanical loadings are more predictable than those of heat and erosion, therefore compensating measures can be incorporated in design concepts with considerable confidence.

1. Propellant Gas Pressure

19. From the structural viewpoint, the propellant gas pressure is the predominant influence in the design of the gun tube. Standard procedures for computing wall thicknesses and accompanying stresses are available and are usually sufficient for good tube design. However, stress concentrations due to rifling and stresses due to other phenomena such as heat should not be treated lightly.

2. Projectile Effects

a. Rotating Band Pressure

20. Rotating bands or their equivalent perform two functions when the round is fired. They transmit

the rifling torque to the projectile and seal or obturate the propellant gases to minimize leakage past the projectile. Both functions are performed effectively after the bands are engraved into the rifling. Since engraving is somewhat of a swaging operation, appreciable resistance is offered by the rifling to the rotating band. This resistance is in the nature of a radial force around the periphery and its frictional counterpart. The radial force when distributed uniformly over the band surface becomes the rotating band pressure. The band pressure is higher on the rifling lands than on the bottom of the grooves simply because more material is displaced by the lands.

21. Band pressures may reach considerable proportions and can cause damage to the tube. Unfortunately their intensity can not be predicted accurately. Maximum pressures appear at the origin of rifling and grow smaller as the projectile moves along the bore, mainly because the band is likely to neck to reduce the interference and because the tube walls become thinner farther on and offer less resistance to dilation. Band pressures progress along the tube with the projectile and although they may be very large, the area of application is local and small, and the pressure is present for such a short time that immediate damage is not always apparent. However, repeated application of such band pressures will ultimately damage the bore. Small, imperceptible cracks will develop first and then steadily grow larger as firing continues. This progressive stress damage finally results in tube rupture or in the spalling of rifling lands. Spalling is the outgrowth of cracks starting in the fillets of the rifling grooves and propagating beneath the land. When two such cracks from opposite sides join, the land becomes a floating spline and is then extremely vulnerable to rotating band action. Little effort is then needed to remove it completely from the bore.

Rotating band pressure has a tendency to flatten rifling lands. This swaging effect will happen only if the bearing strength of the bore material is exceeded. Although not as severe a consequence to

the tube life as spalling, the working depth of the rifling is decreased accompanied by a proportionate decrease in its effectiveness.

b. Rifling Torque

22. Rifling torque is another loading condition closely associated with gas pressure. It varies directly as the gas pressure and as a function of the rifling curve. Absolute values of this torque can be large but ordinarily the gun tube is so rigid that the induced torsional stress is inconsequential. However, provision must be made in the mounts for absorbing the torque.

3. Recoil Forces

23. Recoil forces as such are almost incidental to tube design. In single recoil systems, their effects never exceed the axial stresses due to propellant gas pressures. In double recoil systems, the inertia forces created by secondary recoil accelerations bend the tube, but secondary recoil occurs after the projectile leaves the tube thus its influence and that of the propellant gas pressure cannot combine. Alone, the stresses due to secondary recoil are not critical but should be computed to complete the design investigation.

4. Vibration

24. The rapidly applied and released loads to which the tube is subjected are likely to excite vibrations which may prove harmful either structurally by causing failure or operationally by reducing accuracy. There are several sources for these vibrations. Propellant gas and rotating band pressures induce dilative vibrations which produce ringing sounds and may contribute to muzzle cracking. The balloting of a projectile may be another source. Tube whip is another. It is the term designating the motion normal to the longitudinal axis which is attributed to the moment developed by the collateral but directly opposite the propellant gas force and the induced inertial force of the recoiling mass. Another contributor to tube whip, at least a theoretical one, is the tendency of the propellant gases and projectile to straighten the tube of the curvature brought about by bending under its own weight.

25. Generally, the effects on accuracy caused by vibrations in the heavy tubes of slow-fire weapons fall within acceptable limits. These vibrations, affecting only the round being fired, damp out before the next round is fired. Rapid-fire guns are more seriously affected. The rate of fire is high enough

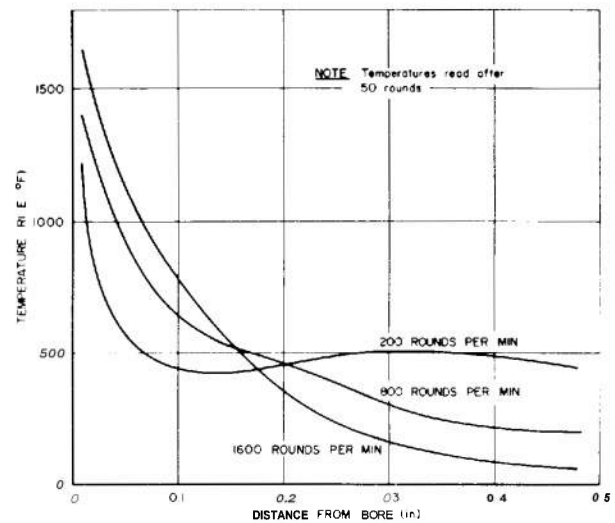


FIGURE 8. Temperature Distribution Across Tube Wall.

that the vibrations initiated in firing each round are not damped out sufficiently between rounds, thus each round may be a resonating influence. Structurally, the tube and mounting should be so designed that vibrations are damped out. This is particularly true for tubes of the recoilless type which must be light for mobility and handling ease. Low weight requirements demand designs of optimum structural efficiency thereby rendering the tube more susceptible to some forces which would otherwise be harmless. A rigorous approach is therefore needed for optimum design. This does not mean that more liberties can be taken with heavy tubes. They too must be designed for maximum structural efficiency. However, their bulk may be sufficient to absorb the disturbances created by vibrations.

B. HEATING

1. Thermal Stresses

26. The burning propellant releases a tremendous amount of heat in the bore. Much of it is absorbed by the tube. The bore surface, being adjacent to the source, receives the brunt of it. If the heat were applied gradually and a reasonable temperature gradient appears through the tube wall, the induced thermal stresses, being compressive in the inner portion, would be analogous to autofrettage and, therefore, beneficial. This, in effect, is what happens in the tube of a rapid fire gun. During prolonged firing, the temperature at the bore surface may reach 2000°F, whereas that at the other surface will be only 1400°F. The temperature distribution across the wall is logarithmic (see Fig. 5), lending credence to the assumption that heat transfer

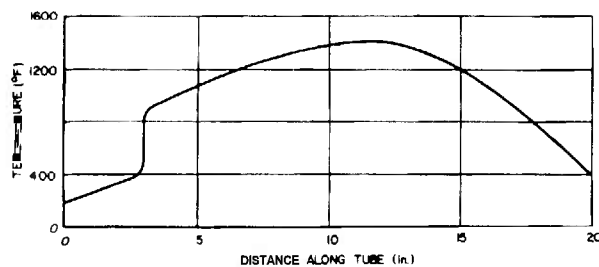


FIGURE 9. Temperature Along Outer Surface of Caliber .30 Tube.

the wall is constant after reaching the steady state condition, the basis for thermal stress calculations of gun tubes. Thermal stresses may be considerable but compensating pressure stresses are available to confine them to the noncritical range. Thermal stresses still prevail after pressures cease but to a lesser extent because bore temperatures drop as soon as hot gases begin to disappear. Since temperatures vary along the tube length (Fig. 9), the gradient too will vary, not only according to the heat input itself but also according to variations in wall thickness. Although the heat input is less at the thin wall regions, the ratio of heat input to wall mass is larger than at the thicker wall regions, thereby increasing the thin wall temperatures. The higher wall temperatures do not necessarily mean higher thermal stresses. The heat follows a shorter path in thin walls, consequently the temperature distribution will show less variation across the wall than for thick walls.

Although thermal stresses are reduced by pressure stresses in a hot gun tube since the thermal tangential stress is compressive near the bore surface and tensile near the outside surface, the converse of thermal stresses reducing pressure stresses should not become a design criterion. The helpful stress pattern depends upon a large negative temperature gradient from the bore surface outward which will exist as long as firing is continued. However, if firing is temporarily ceased, the temperature will rapidly tend to equalize throughout the tube and the whole tube may be at a high temperature level, thereby reducing the yield strength of the metal. If firing is now resumed, the tangential thermal stress will be positive for a short time even near the bore surface, and thus will not lower the pressure induced stress. Therefore, thermal stresses should not be depended upon to help compensate for a reduced yield strength in the tube material when at elevated temperatures.*

* Stated in Conclusions of Reference 1. References are listed at the end of this handbook.

27. Rate of fires as well as total rounds fired play an important role in the heat transfer across the tube wall. A steady state condition exists for every firing schedule. For instance, the maximum temperature of 1400°F on the outer surface of a cal. .30 machine gun tube is reached after firing 7 bursts of 125 rounds each in 14 seconds at a rate of one burst per minute. Adhering to this schedule, continued firing will not increase the tube temperature. Before the steady state condition is reached, rate of fire has an appreciable effect on the temperature gradient. According to Figure 8, the bore surface temperature increases with the rate of fire, but at sonic distance removed from the bore surface, the temperature after 50 rounds is higher for the slower firing rates. This illustrates that time of heat application is an essential parameter in thermal stress considerations.

28. Thermal activity is responsible for another type stress, one confined to a thin layer of tube at the bore surface. No accurate method is available for computing this stress. Its effect is not immediately apparent but cracks will eventually appear on the surface and grow deeper as firing progresses. Figure 10 shows these thermal cracks. Two theories explain this phenomena. The first is metallurgical in nature; the second is mechanical. Both are based on metal contracting after cooling.

29. When a gun is fired, propellant gases heat the bore surface beyond temperatures of 1400° to 1500°F, the transition temperature range of austenite. After the hot gases leave the bore, the relatively cool metal adjacent to the surface and air in the tube quickly cool the bore layer to transform it to martensite. Austenite and martensite have different crystal-line structures and, therefore, have different volumes, austenite having the larger. Upon cooling, the accompanying shrinking induces high stresses. If these stresses exceed the tensile strength of the material, cracks will appear.

30. From the mechanical point of view, if heat at high temperatures is applied for only a short time, a large temperature gradient develops through the tube wall and creates a corresponding compressive stress on the bore surface. When this stress exceeds the yield strength it causes plastic flow. The material at the bore surface having no other escape, moves inward. Upon cooling, the compressive stresses are relieved and the material attempts to return to its original position. However, only tangential and axial

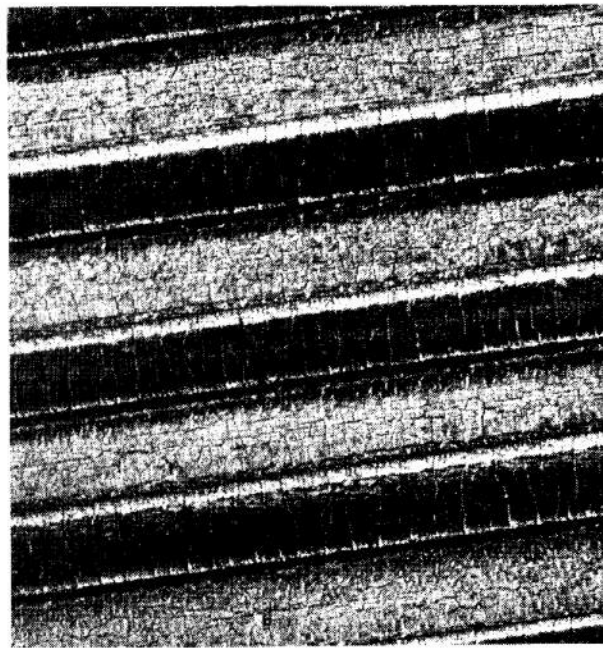
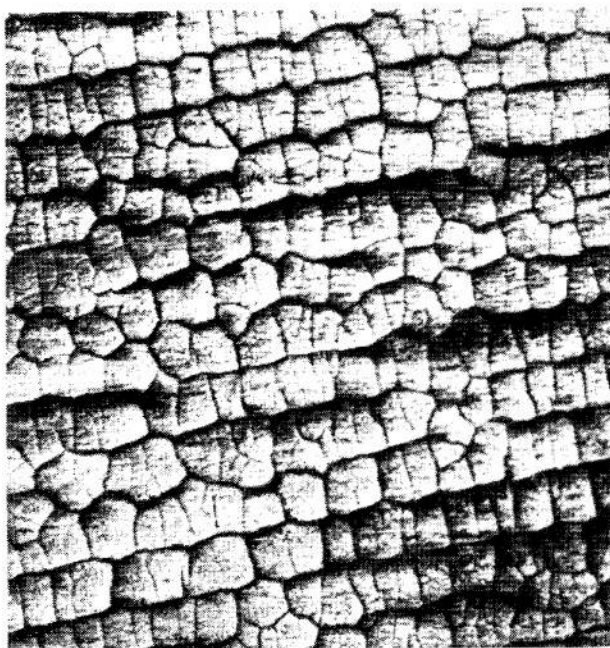


FIGURE 10. *Thermal Cracks on Bare Surface.*

stresses are available to pull the metal back. The new radial growth is proportional to Poisson's ratio, a displacement considerably less than that of the compressive activity which displaced it originally. Effectively, there is not sufficient material to compensate for the elongations created by the newly induced tangential and axial tensile stresses. Hence, when these stresses exceed the tensile strength, surface cracks appear.

2. Dimensional Changes

31. Dimensional changes are also a source of concern to the designer. Solar radiation can cause the top of the tube to become hotter than the bottom. The resulting longitudinal differential expansion will bow the tube downward to be accompanied by a slight reduction in angle of elevation and, therefore, a shortening in range. Conversely, a coolant such as rain will lower temperatures on top and cause the hot tube to bend upward with an accompanying reduction in accuracy. Dilation of the bore caused by elevated temperatures may also reduce accuracy simply by increasing the clearance between bore surface and projectile to permit gas leakage and to create a greater tendency toward balloting. A likely cause of malfunction due to unequal dimensional changes concerns cartridge cases. The clearance between unfired case and chamber is large enough to permit easy loading. On firing, the propellant gas

pressure expands the case and presses it tightly against the chamber wall. After the pressures ceases, the case recovers from the distortion sufficiently to provide ready extraction. The difference in thermal coefficients of expansion of case and chamber wall must be considered to avoid cancellation of the recovery tendencies of the case by this factor.

3. Cook-Off:

32. A phenomenon which plagues gunners during prolonged firing is cook-off. Cook-off is the deflagration or detonation of ammunition caused by the absorption of heat from its environment. Usually it consists of the accidental and spontaneous discharge of, or explosion in, a gun or firearm caused by an overheated chamber or barrel igniting a fuze, propellant charge, or bursting charge. Cook-off is confined mostly to automatic guns and to mortars. Muzzle-loaded mortars when hot have a tendency to fire the propelling charge before the round reaches the breech; sometimes even before it drops completely through the muzzle. The danger in automatic weapons stems from the live round left in the chamber to start the next burst.

33. When cook-off occurs, the consequences may be disastrous. The propellant, its primer, or any of

* Reference 2.

the explosive components in a round may ignite. If it is the propellant within a round in battery, the projectile passes out of the barrel. In this instance, primary danger is to personnel and equipment in line of fire. However, if projectile cook-off occurs in battery, i.e., with round in chamber and all weapon components in their firing positions, or if in the ram or loading position in a small arms weapon, severe damage is almost certain. The gun undoubtedly will be rendered inoperative. Furthermore, the explosion may damage the carrier or injure the crew. In contrast, the danger in slow-fire weapons should be negligible for these need not be kept loaded for any appreciable time.

34. Although cook-off is a safety hazard of some importance, no method has been devised for designing a tube that is safe from this complex heat-transfer problem. In acceptance, all high rate-of-fire weapons must be tested to make certain that the cook-off threshold of their ammunition is not exceeded, and attempts made to introduce corrective measures if needed. For example, in the 20 mm revolver gun, M39, cook-off was eliminated when the chamber-to-barrel seal was redesigned to remove the heat sink (see Figure 5). The approach is necessarily empirical, after the need for corrective measures is determined.

C. EROSION

1. Causes

35. Erosion is literally the wearing away of the bore surface and of all phenomena unfavorable to long tube life, it is the worst offender. Erosion is primarily a physical activity although chemical action can increase its rate. The abrasive effects of propellant gases and rotating hands are the most damaging. The gases impinging at high velocities on the bore surface sweep away sonic of the metal.

This phenomenon is called gas wash. The rotating bands have two contributory influences on erosion; the first is induced by gas wash, the second by ordinary sliding friction. Intense heat also contributes indirectly to erosion, by melting an extremely thin layer of the bore surface, thus making it easier for the gases and band to carry off the material. Also, because of high heat, sonic constituents of the propellant gases may combine with the metal at the bore surface. The newly formed compound, probably a nitride and therefore brittle, may crack and peel off under the action of rotating bands and propellant gases.

2. Regions Affected

36. The region at the origin of rifling suffers most from erosion. Here the factors conducive to high erosion rates are most destructive. Temperatures are highest, engraving takes place here, and frictional forces are highest. Tests have shown that engraving, friction, and gas wash contribute approximately one-third each to the total wear*. This proportion occurs only when relatively cool-burning propellants are used. When the charge consists of hot-burning propellants, the erosion induced by the gases is so great that wear due to other causes becomes relatively insignificant. Although propellant gases move faster farther along the tube and should be more erosive than at the origin of rifling, the other contributing causes diminish considerably, with a subsequent lower rate of erosion. The rate increases again at the muzzle but not nearly as much as at the origin of rifling. The actual cause of the accelerated muzzle erosion has never been determined. However, it may be considered secondary, for the damaging effects sustained by the projectile at the origin can never be completely undone by corrective measures introduced at the muzzle.

* Reference 3, page 599.

CHAPTER 5

WAYS OF MINIMIZING HARMFUL EFFECTS TO GUN TUBES

There are a number of measures which may be incorporated either in tube design or in the ammunition to eliminate completely or reduce the effectiveness of those firing phenomena which shorten tube life.

A. MECHANICAL DESIGN

1. High Strength Materials

37. A gun tube should have all the physical properties required for efficiency and durability. Since some of the ideal physical properties may not be congruous, a compromise may have to be made, reducing the resistance against one adverse phenomenon in order to retain the effectiveness against another. It is not good design practice to compromise strength in a gun tube. A tube should always be strong enough to support its loads including pressure and inertia forces. Failure attributed to these forces renders the tube beyond salvage regardless of its resistance to heat and erosion. The attractive feature of high strength materials, particularly steel, is the ability to withstand other destructive agents to an acceptable degree. Even if these properties are less than adequate, corrective measures discussed earlier in the chapter are available to overcome the deficiency.

2. Vibration Correction Measures

38. Structural failures due to vibrations are infrequent and highly unpredictable. From the viewpoint of economy, corrective measures are usually adopted only after failure occurs. This is particularly true for muzzle cracking due to dilative vibrations. However, one must be aware that tubes are inherently weaker at the muzzle because of the open end effects and failure here may be due to normally applied pressures. An overall thicker wall or a gradual thickening at the muzzle to form a muzzle bell will increase tube strength. The vibrations which disturb accuracy are corrected by a change in the mass or shape. A heavier tube may also absorb the adverse effects of balloting but activity of this nature should be eliminated or moderated at the source,

namely, the projectile. Size or shape of tube wall can contribute nothing toward this end this, placing the burden entirely on the projectile designer.

3. Vibration Calculations

39. Accuracy dispersions due to tube vibrations have been measured and correlated with the natural frequency of the tube and the firing rate of the gun*. Figure 11 shows how dispersion varies with the frequency ratio of the tube which is expressed as

$$R_f = \frac{f_n}{f_r} \quad (1a)$$

where

f_n = natural frequency of the tube, cycles/sec

f_r = firing rate, rounds/sec

To avoid large dispersions, the tube is designed for a natural frequency so that $R_f > 3.5$ or, if the size of the tube, hence its stiffness, precludes a frequency ratio of this magnitude, attempts should be made to direct the frequency ratio toward a value approaching one of the minima in the curve of Figure 11.

40. Calculations for the natural frequency are based on the Stodola Method of Calculating Critical Speeds of Multimass Systems†. Generally

$$\omega = \sqrt{\frac{g \sum W y}{\sum W y^2}} \quad (1b)$$

where

g = acceleration of gravity, 386.4 in/sec²

W = dynamic force of each beam increment, lb

y = deflection of beam increment, in.

ω = critical speed, rad/sec

The critical speed may be written in terms of natural frequency,

$$f_n = \frac{\omega}{2\pi} \text{ cycles per sec} \quad (1c)$$

* Reference 4.

† Reference 5, page 156.

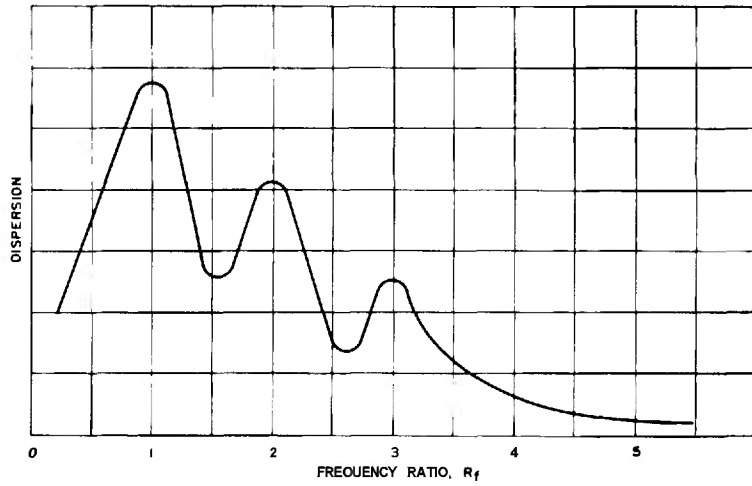


FIGURE 11. Dispersion-Frequency Ratio Curve.

The tube is considered a cantilever beam loaded dynamically by vibratory motion. For the first approximation, ω is usually selected as unity and the deflection, y , is obtained for the beam bending under its own weight. For the analysis, divide the tube into a convenient number of sections, each section representing a uniformly applied load. Then determine the deflection curve. The example shown below follows the area-moment method.

41. For the example, assume Figure 12 to represent a gun tube, 36 in. long, consisting of three cylindrical sections of equal length: A, B, C. Subdivide each section into lengths of 4 inches and compute the deflection at the center of each of the nine increments. The effect of the bore is assumed negligible, thus the analysis is for a solid bar. Area moments of inertia of the sections are

$$I_A = \frac{\pi}{64} d^4 = \frac{\pi}{64} 1.5^4 = .249 \text{ in}^4$$

$$I_B = \frac{\pi}{64} d^4 = \frac{\pi}{64} 1.75^4 = .46 \text{ in}^4$$

$$I_C = \frac{\pi}{64} d^4 = \frac{\pi}{64} 2.0^4 = .785 \text{ in}^4$$

The tube being steel, the weight of each increment is

$$W_{oa} = W_{ab} = W_{bc} = 6 \frac{\pi}{4} d_A^2 L = 2.0 \text{ lb}$$

$$W_{cd} = W_{de} = W_{ef} = 8 \frac{\pi}{4} d_B^2 L = 2.72 \text{ lb}$$

$$W_{fg} = W_{gh} = W_{hi} = 8 \frac{\pi}{4} d_C^2 L = 3.56 \text{ lb}$$

where

$L = 4 \text{ in.}$, length of each increment

$\delta = .283 \text{ lb/in}^3$, density of steel

Calculations of M/I at each station on the beam as indicated in Figure 13 are arranged in Table 1.

Now calculate the area moment of the M/I curve. The moments of the area are found at the mid-span of each increment as indicated numerically in Figure 13. The M/I curve represents a new loading condition, the load on each increment being trapezoidal. The calculations are arranged in Table 2. The moments of the simulated beam are taken from left to right.

Showing the calculations for Station 6,

$$\Sigma_{A6} = \Sigma_{A7} + A_{R8} + A_{L7}$$

$$= 2455 + 609 + 589 = 3653 \text{ lb/in}^2$$

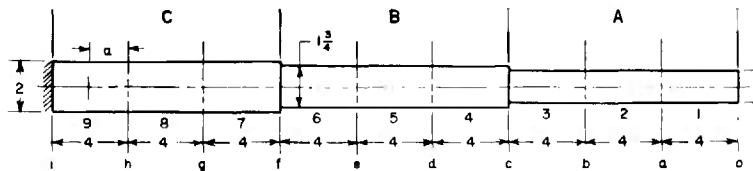


FIGURE 12. Gun Tube Showing Subdivisions.

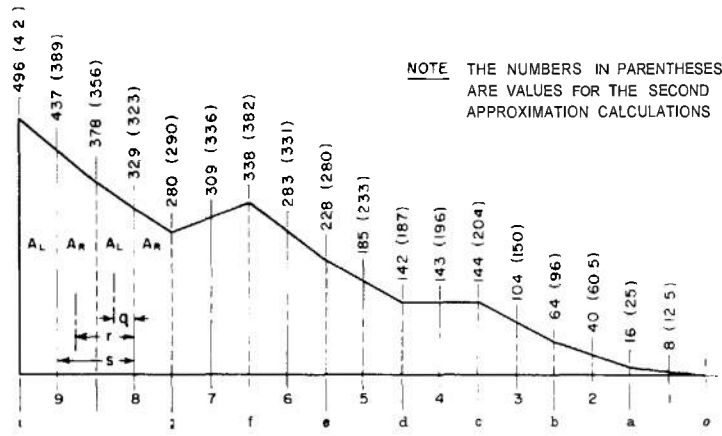


FIGURE 13. M/I Diagram of Gun Tube.

$$\begin{aligned}
 M_{A6} &= q_6 A_{L6} + r_6 A_{R7} + s_6 \Sigma A_6 \\
 &= 1.03 \times 621 + 2.98 \times 647 + 4 \times 3653 \\
 &= 640 + 1930 + 14610 = 17180 \text{ lb-in} \\
 \Sigma M_{A6} &= \Sigma M_{A7} + M_{A6} \\
 &= 20100 + 17180 = 37280 \text{ lb-in}
 \end{aligned}$$

The actual deflection at any station

$$y = \frac{\Sigma M_A}{E} \text{ in} \quad (2)$$

where

$$\begin{aligned}
 E &= 29 \times 10^6 \text{ lb/in}^2, \text{ modulus of elasticity} \\
 \Sigma M_A &= \text{the summation of the area moments at the station}
 \end{aligned}$$

Now compute the items necessary to find the natural frequency and arrange them in Table 3.

$$\Sigma W y_1 = 49.26 \times 10^{-3} \text{ lb-in},$$

$$\Sigma W y_1^2 = 182.9 \times 10^{-6} \text{ lb-in}^2$$

From Equation 1b, the first approximation for the critical speed is

$$\omega_1 = \sqrt{\frac{g \Sigma W y_1}{\Sigma W y_1^2}} = \sqrt{104,200} = 323 \text{ rad/sec}$$

where

$$g = 386.4 \text{ in/sec}^2$$

Now repeat the calculations but this time with the dynamic loading based on ω_1^2 . Thus

$$W_1 = \frac{\omega_1^2 W y_1}{g} = \frac{104200}{386.4} W y_1 = 270 W y_1$$

Table 4 will be similar to Table 1.

TABLE 4. M/I CALCULATIONS FOR STATIC CONDITION.

Sta	Sect	W (lb)	ΣW (lb)	a (in)	Δx (in)	aW (lb-in)	$\Delta x \Sigma W$ (lb-in)	M (lb-in ²)	M/I (lb-in ³)
a	oa	2.0	0	2	0	4.00	0	4.00	16
b	ab	2.0	2.0	2	4	4.00	8.0	16.0	64
c	bc	2.0	4.0	2	4	4.00	16.0	36.0	144
d	cd	2.72	6.0	2	4	5.14	24.0	65.1	142
e	de	2.72	8.72	2	4	5.14	34.9	105	228
f	ef	2.72	11.44	2	4	5.14	45.8	156	338
g	fg	3.56	14.16	2	4	7.16	56.6	220	280
h	gh	3.56	17.72	2	4	7.16	70.9	298	378
i	hi	3.56	21.28	2	4	7.16	85.1	390	496

W = weight of each increment, assumed concentrated at center of section

ΣW = the shear at the right end of section contributing to the moment at the station being considered

a = moment arm of distributed weight for each section

Δx = moment arm of total shear at right end of section

M = $\Sigma(aW + \Delta x \Sigma W)$, total moment at station.

TABLE 2. AREA MOMENTS FOR STATIC CONDITION.

Station	A_L (lb/in ²)	A_R (lb/in ²)	ΣA (lb/in ²)	g (in)	r (in)	s (in)
9	933	815	0	1.02	0	0
8	707	609	933	1.02	3.02	4
7	589	647	2455	.98	3.02	4
6	621	511	3653	1.03	2.98	4
5	413	327	4921	1.04	3.04	4
4	285	287	5845	1.0	3.04	4
3	248	168	6457	1.05	3.0	4
2	104	56	6992	1.07	3.07	4
1	24	—	7264	1.11	3.14	4

Station	qA_L (lb/in)	rA_{R-1} (lb/in)	$s\Sigma A$ (lb/in)	M_A (lb/in)	ΣM_A (lb/in)
9	950	0	0	950	950
8	720	2460	3730	6910	7860
7	580	1840	9820	12240	20100
6	640	1930	14610	17180	37280
5	430	1550	19680	21660	58940
4	280	990	23380	24650	83590
3	260	860	25830	26950	110540
2	110	520	27970	28600	139140
1	30	180	29060	29270	168410

A_L = area to the immediate left of the station

A_R = area to the immediate right of the station

ΣA = represents the total simulated shear at the preceding station

qA_L = moment of the area to the immediate left of the station

rA_{R-1} = moment of the area to the immediate right of the preceding station

$s\Sigma A$ = moment of the simulated total shear at the preceding station

M_A = area moment

The calculations of the area moments of the M/I curve in Figure 13 are listed in Table 5.

The deflection at each station due to the dynamic loading is found according to Equation 2. The deflection and the natural frequency parameters are listed in Table 6.

TABLE 3. NATURAL FREQUENCY PARAMETERS, STATIC CONDITION.

Station	y_1 (in)	W (lb)	$Wy_1 \times 10^3$ (lb-in)	$Wy_1^2 \times 10^6$ (lb-in ²)
1	.0058	2.0	11.60	67.3
2	.0048	2.0	9.60	46.1
3	.00382	2.0	7.64	29.2
4	.00288	2.72	7.84	22.6
5	.00203	2.72	5.52	11.21
6	.001287	2.72	3.50	4.50
7	.000694	3.56	2.47	1.715
8	.000273	3.56	.97	.265
9	.000033	3.56	.12	.004

$$\Sigma Wy_1 = 49.3 \times 10^{-3} \text{ lb-in};$$

$$\Sigma Wy_1^2 = 190.0 \times 10^{-6} \text{ lb-in}^2$$

From Equation 1b, the second approximation of this critical speed is

$$\omega_2 = \sqrt{\frac{g\Sigma Wy_1}{\Sigma Wy_1^2}} = \sqrt{100,500} = 317 \text{ rad/sec}$$

This differs from ω_1 by less than 2% and is therefore considered to be a sufficiently close figure for the natural frequency. Expressed in terms of natural frequency

$$f_n = \frac{\omega_2}{2\pi} = 50.5 \text{ cycles/second}$$

For a gun firing 1200 rounds per minute

$$f_r = \frac{1200}{60} = 20 \text{ rounds/second}$$

From Equation 1a, the frequency ratio is

TABLE 4. M/I CALCULATIONS FOR DYNAMIC CONDITION.

Sta	Seet	W_1 (lb)	ΣW_1 (lb)	a (in)	Δx (in)	aW_1 (lb-in)	$\Delta x \Sigma W_1$ (lb-in)	M (lb-in)	M/I (lb/in ³)
a	oa	3.13	0	2	0	6.26	0	6.26	25
b	ab	2.59	3.13	2	4	5.18	12.5	23.9	96
c	bc	2.06	5.72	2	4	4.12	22.8	50.9	204
d	cd	2.11	7.78	2	4	4.22	31.9	86.2	187
e	de	1.49	9.89	2	4	2.98	39.6	129	280
f	ef	.94	11.38	2	4	1.88	45.5	176	382
g	fg	.67	12.32	2	4	1.31	49.3	227	290
h	gh	.26	12.90	2	4	0.56	52.0	279	356
i	hi	.03	13.25	2	4	0.06	53.0	332	422

$$R_f = \frac{f_n}{f_r} = \frac{50.5}{20} = 2.52$$

Checking this value on the curve (Figure 11) shows that it falls on a minimum dispersion portion of the curve and may be acceptable. However, frequency ratio greater than 3.5 is preferred. This would require that the tube be made stiffer (and heavier) to increase its natural frequency if the firing rate of 750 rounds per minute is to be retained. Firing tests eventually determine whether the dispersion caused by tube vibration is acceptable. If not, the tube is modified to change its stiffness and firing tests are

performed for each modification until a trend is established. With the aid of Figure 11, this trend readily predicts the tube stiffness necessary for minimum dispersion.

B. COOLING METHODS

1. Large Tube Masses

42. Heat effects the tube adversely, and conversely, cooling effects are beneficial. The tube can be kept relatively cool by rapid heat dissipation or by insulation of the bore surface. Most methods are ineffective during prolonged firing although some do provide

TABLE 5. AREA MOMENTS FOR DYNAMIC CONDITION.

Station	A_L (lb/in ²)	A_R (lb/in ²)	ΣA (lb/in ²)	q (in)	r (in)	s (in)
9	811	715	—	1.01	0	0
8	679	613	811	1.0"	3.01	4
7	626	718	2235	.98	3.02	4
6	713	611	3474	1.02	2.98	4
5	513	420	4905	1.03	3.03	4
4	383	400	6029	.99	3.03	4
3	354	246	6832	1.05	2.99	4
2	156	85.5	7586	1.07	3.07	4
1	37.5	—	7988	1.11	3.14	4

Station	qA_L (lb/in)	rA_{R-1} (lb/in)	$s\Sigma A$ (lb/in)	M_A (lb/in)	ΣM_A (lb/in)
9	819	0	0	819	819
8	693	2240	3240	6170	6990
7	613	1850	8940	11400	18100
6	728	2140	13900	16770	35900
5	528	1850	19600	21980	57100
4	379	2170	24100	25750	82900
3	372	1200	27330	28900	111800
2	167	156	30340	31260	143000
1	42	268	31950	32260	175300

TABLE: 6. NATURAL FREQUENCY PARAMETERS,
DYNAMIC CONDITION.

Station	y_1 (in)	it' (lb)	$W y_1 \times 10^3$ (lb-in)	$W y_1^2 \times 10^6$ (lb-in ²)
1	.00605	2.0	2.10	73.20
2	.00493	2.0	9.86	48.60
3	.00386	2.0	7.72	29.75
4	.00286	2.72	7.78	22.25
5	.00197	2.72	5.36	10.58
6	.00121	2.72	3.29	3.98
7	.000635	3.56	2.26	1.41
8	.000241	3.56	.86	.21
9	.000028	3.56	.10	

some compensating features. One of these involves large tube masses acting as heat sinks. Heat is conducted rapidly from the bore surface into the tube mass. Transfer of the heat to the air surrounding the tube is a slower process but, at any given firing rate, the tube eventually reaches a steady state condition. Heavy tubes or light tubes with cooling fins will reach steady state later than plain light tubes. If the yield strength at steady state temperature approaches the firing stresses, continued firing becomes dangerous. Gun steels begin to lose strength above 600°F. A wall thicker than needed for a tube in which thermal stresses are not present will be stressed correspondingly lower, to a value where a lower yield point can be tolerated. But, regardless of tube wall strength, the bore surface can not escape the deterioration attributed to other sources. The solution here then is to select a material not subject to damage by heat, as well as of required strength.

2. Coolants

43. The use of a coolant helps to increase the permissible duration of sustained firing but arrangements for their application are too awkward to be practical. One of these, the forced convection process, has fluid flowing through a jacket or tank surrounding the barrel. If nucleate boiling, i.e., active boiling, can be maintained, the rate of heat transfer is higher than for film boiling with its insulated film of vapor between the fluid and outer barrel surface. The forced convection equipment makes a good laboratory apparatus but is hardly acceptable for the field. Weight and bulk of a circulating system built to sustain the inertia forces of recoil become more burdensome than the advantage of cooling warrants. However, a weapon still finding some favor in the field is the early concept of a water cooled

machine gun. In this version, the tank forms a cooling system with no provision for a continuous incoming flow of cool water. The tank is vented to prevent high steam pressures. So long as water is present, surface temperatures can be held to reasonable limits.

44. Another application of coolant involves water spray injected into the bore after each round or short burst. However, the time lost during spraying reduces the rate of fire, probably to that of normal slow fire activity. That this method of cooling offers any writable advantage in prolonging tube life is questionable. The same viewpoint can be applied to a type of construction referred to as a jacketed liner. This type of construction has thin steel liners reinforced by thicker jackets of copper or aluminum. The high thermal conductivity of the jacket is expected to keep the barrel cooler than if it were made entirely of steel. However, neither copper nor aluminum is acceptable structurally because of low strength. Although considerably stronger, their alloys do not have the heat conducting capacity of the parent metal and actually approach that of steel, thus forfeiting the only advantage that this structure can offer.

3. Boundary Layer Cooling

45. Boundary layer cooling introduces the practice of insulating the bore surface from the heat of the propellant gases. Two techniques have been investigated; one involving ammunition, the other involving tube design. The first or smear technique provides a protective bore coating. The latest application of this cooling concept has a small plastic capsule of silicone oil located in a recess in the base of the projectile. A plunger, sliding in the recess, crushes the capsule when the round is fired and squeezes the oil outward upon the bore surface. This is a one-shot function, the oil deposit being carried off by the next round. Tests show that 0.08 cc of 80,000 centistokes silicone oil reduces the heat input into a 20 mm barrel by 60 percent*. Two difficulties remain: one is to make a suitable capsule that will neither leak nor affect the ballistics too much; the other is the tremendous difficulty of retrofit, i.e., adapting it to existing materiel, a task which is not practical. However, the activity associated with smears does not constitute any part of tube design but rather one associated with preventive maintenance. On the other hand, transpiration cooling does involve tube design. This process de-

* Reference 2, page 120.

depends on a porous tube liner of sintered metal to carry fluid under pressure to the bore surface where it forms a protective coating. Two major disadvantages are an intricate injection system is required to maintain even flow on the bore surface during the time that the highly transient gas pressure is present and still not supply an overabundance of fluid between rounds, and although the principle of transpiration cooling has merit, the sintered liner does not have the strength to survive the severe punishment to which it is subjected during firing.

4. Low Heat Input

46. The best means for retaining relatively cool equipment during firing is to hold the amount of heat generated to a minimum. This can be done within limits by employing cool burning rather than hot burning propellants. A cool burning propellant has a flame temperature of less than 2000°K whereas hot burning ones may reach as high as 3600°K. Although even 2000°K is higher than desirable, it does offer an appreciable advantage over the higher temperatures inasmuch as tube strength will decrease at a slower rate than if it were subjected to hot burning propellants during sustained firing. The lower temperature also aids in reducing gas wash and other types of erosion.

C. LOW EROSION MEASURES

47. Many attempts have been made to discover techniques or material capable of resisting erosion. One method involves the removal or restraint of phenomena responsible for erosion. Heat being one of these, any means of curbing its destructiveness will help. Under this circumstance, the various cooling methods above, if effective, will reduce erosion. Methods other than cooling are available for moderating erosion, but these involve projectiles and propellants rather than gun tubes and further discussion on these items is not within the scope of this handbook.

1. Rotating Band Properties

48. The erosion caused by rotating band action can be checked to sonic extent by selectivity in design and materials. Materials should be easily engraved, have low abrasive and good bearing properties, and should have low coppering tendencies, i.e., should leave little or no metallic deposit on the bore surface. Soft materials including copper, gilding metal (brass), pure iron, and many plastics fall into this category. Some plastics have exhibited excellent ability in retarding corrosion. The metals above show

about equal tendencies toward erosion and tube life. The big problem is work hardening developed during the assembly of band to projectile. Conventionally, metal bands are swaged into peripheral grooves called band seats. This operation work hardens the metal, thereby increasing its engraving resistance and erosion tendencies. Banding methods are available which circumvent work hardening; some by welding, others by mechanical means. Plastics avoid most fabrication problems by being molded directly into the band seat. However, some problems still remain including the malleability of most plastics to meet rotating band requirements such as retention during projectile flight, dimensional stability during temperature changes, and imperviousness to aging characteristics during long periods of storage.

49. Band contour and size directly affect engraving. The optimum band diameter is just large enough for adequate obturation but not so large that excessive engraving effort is needed or high band pressures develop. The use of preengraved bands in recoilless weapons eliminates both engraving effort and band pressure whereas, in other weapons, indexing difficulties while loading, and the added cost cannot be tolerated. Band width too is critical but band diameter is somewhat more significant. In the development of new weapon systems, the tube designer should cooperate with the projectile designer to incorporate the most compatible design features in rotating band and rifling.

2. Rifling

50. The bore erodes most severely at and near the origin of rifling. Attempts have been made to alleviate this condition by varying the design of the rifling itself, introducing sonic variations to ease the engraving process and to reduce band pressures, and to reduce rifling torque. Depth of rifling and width of groove are usually determined from the dynamics of the projectile while in the bore, with little leeway extended toward modification of these parameters. However, there is considerable leeway in selecting the cross-sectional contour of the rifling. For instance, the lands and grooves may be sharply rectangular in one extreme or the grooves may be circular segments in the other (Fig. 14). Experimental firing data on rifling profiles are lacking but by inspection it appears that engraving resistance and band pressures would increase as the profile varies from rectangular to circular grooves because band material displaced during engraving increases, i.e.,

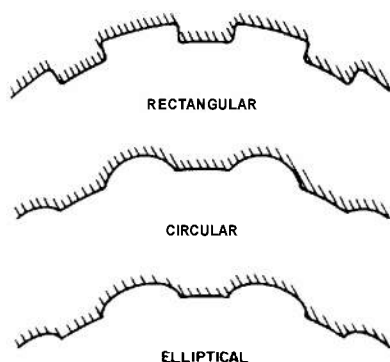


FIGURE 14. *Types of Rifling Contour.*

interference between band and rifling increases. However, the susceptibility to large stress concentration suggests large fillets and a trend toward rounded contours.

51. The slope of forcing cone and rifling at the origin has a decided influence on engraving force. The force diagram is equivalent to that of a wedge; consequently, the gentler the slope, the less resistance offered to translation, hence engraving. Since the total amount of band material displaced is independent of slope, final band pressure too is independent although its rate of increase will vary with slope. A rapidly applied load creates higher stresses than one applied more slowly, therefore, the relatively slow rate of band pressure rise is another favorable characteristic of a gentle forcing cone slope.

52. Ease of engraving is not always an asset. Engraving, generally requiring fairly high propellant gas forces, delays travel in the bore to maintain the design density of loading until burning rate and gas pressure are optimum for maximum efficiency. If engraving resistance is materially reduced, reaching the desired burning rate may be delayed, and peak pressure will appear farther along the bore with the added possibility of not realizing maximum values of pressure and velocity. This may not be serious in highly charged rounds but when conditions are marginal such as in low zone firing, muzzle velocities may be too low. A larger propellant charge will restore the velocity but at reduced efficiency. Another means of compensating for delayed peak pressures resulting from low engraving resistance is the use of faster burning propellants, if feasible, as in recoilless weapons.

53. Variation in the rifling curves are sometimes used to lower erosion rates. Most are concerned with

reducing rifling torque at the origin. The mechanics of rifling curves and rifling torque are discussed later in Chapter 6. Low torque itself will not inhibit erosion but it does delay rotational activity until the undamaged rifling farther along the bore is reached. A new gun with constant twist rifling presents no problem. Engraving is complete, with rifling and rotating band mating perfectly to impart torque to the projectile. On the other hand, a worn gun or a revolver type weapon presents a difficult problem. In these, the projectile begins to move before the rifling is engaged, i.e., it has free run. If the rifling twist is uniform, the theoretical instantaneously acquired angular velocity during engraving creates a torsional impact which may cause rotating band failure. Furthermore when it first reaches the rifling of a worn gun the band barely touches the lands and the shallow contact is not sufficient to carry the load. The rifling here may act as a cutting tool, machining off the top band surface. Or, perhaps the contact is light enough and the slope shallow enough that the rifling swages the band rather than engraves it. The problem is to find a rifling capable of minimizing the abuse.

54. To minimize the damage to rotating bands caused by free run or wear, wear compensating rifling is introduced. This type is so named because it reduces the rifling torque near the origin of rifling where erosion is most severe. The location of the origin remains unchanged but the rifling is without twist for a short distance, usually a length of about one inch in small arms. Then, a length of increasing twist leads to the final angle at a short distance from the muzzle from which point the rifling assumes uniform twist. In a variate application the rifling curve starts at the origin also with a zero angle of twist. Either method relieves the band of the rifling torque at the origin where most of the damage takes place and does no worse at the muzzle where constant twist is retained. Currently, increasing twist rifling is confined to small arms but the practice should

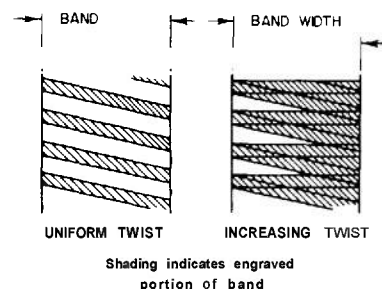


FIGURE 15. *Progressive Engraving.*

not be abandoned for larger gun tubes if favorable characteristics can be used to advantage. Increasing twist rifling has been used successfully in some large guns such as the 14 in., M1920 MII and the 16 in., M1900 guns.

55. Wear compensating rifling decreases the shock after free run which is experienced in revolver type guns and in worn guns of uniform twist. Loads on rifling, rotating band, and fuze are thereby eased. It permits the use of free run without rifling or with rifling of zero height at the origin and continuing in a very gradual slope until it reaches the normal height of land at the bore. For the benefits gained, the price is a higher torque farther along the tube which, in itself, is not necessarily a serious disadvantage. A disadvantage which may prove serious involves the rotating band whose width and therefore load carrying capacity is limited by the continuous engraving produced by the changing slope of the rifling. Figure 15 shows the results of this progressive engraving. After being engraved, the effective band material remaining must be capable of transmitting the induced torque.

3. Liners and Plating

56. The most effective means of moderating erosion entails the use of materials which resist wear. These materials must be hard so as to resist abrasive activity, have good thermal properties to resist heat, and must be chemically inert to retain the original physical properties. Unfortunately, those materials which are erosion resistant seldom have

sufficient strength. In this respect, high strength steel serves a dual purpose. The strength provides an obvious need whereas the accompanying hardness decreases the susceptibility to wear although this advantage applies only to guns firing relatively slowly. For rapid firing guns, the increased life derived from high strength steel is not enough to class it as a low erosion material. However, steel tubes with plated or lined surfaces have increased the durability to the extent where the special effort in manufacturing has become worthwhile.

57. Plating the bore surfaces with a hard, heat resistant material such as chromium reduces erosion and helps keep the tube clean but it still is not totally satisfactory. It is not impervious to gas wash and has a tendency to chip and spall, particularly near the origin of rifling. Liners are far more satisfactory but assembly difficulties limit their length. Figure 4 shows a liner assembly. Being restricted to short lengths is only a minor disadvantage because rifling erodes fastest in the region adjacent to the origin. Present practice exploits the advantages offered by both plating and liner by applying each to different sections of the bore. The liner, containing forcing cone and a short length of rifling, comprises the bore adjacent to the chamber. The remaining length of bore, comprising the parent metal of the tube, is plated. The thickness of the plating gradually increases from the front end of the liner to the muzzle to realize the shallow taper of the choke bore. The gradual restriction thus compensates for erosion, particularly at the muzzle where it can be severe.

CHAPTER 6

GUN TUBE DESIGN

A. DESIGN OBJECTIVES

58. Establishment of the basic performance requirements for a gun tube belongs to the ballisticians and the ammunition designer. They establish the weight, size and shape of the projectile plus its muzzle velocity and spin. The tube designer takes over after all ammunition and interior ballistics data become available. It is his task to design a tube sufficiently strong and durable to meet the ballistic requirements and to design adequate attachments for sights, breech ring or receiver, a recoil brake rod and cradle adapters, and where required, muzzle brakes and flash hiders.

B. INTERIOR BALLISTICS CURVES

59. The tube designer is primarily interested in the pressure-travel and velocity-travel curves. The interior ballistics information is ordinarily available as pressure-time and pressure-travel curves from which the velocity-time and velocity-travel curves are easily derived. Typical examples of all four curves are shown in Figure 16. However, the pressure here is chamber pressure. If used as a design parameter, it yields conservative results since actual pressures along the tube are lower. The conservative approach is acceptable since its effect is to introduce a small safety factor. If desired, the actual propellant

gas pressure along the tube can be calculated by Equation 3.

$$p_A = p_c \left[1 - \frac{W_c}{2W_p - W_c} \left(\frac{S_A}{S_B} \right)^2 \right] \quad (3)$$

where

- p_A = pressure at point A of bore
- p_c = chamber pressure
- S_A = distance from breech of equivalent chamber to point A
- S_B = distance from breech of equivalent chamber to base of projectile
- $S_B = S_A$ for maximum pressure at A
- W_c = weight of propellant charge
- W_p = weight of projectile

The equivalent chamber is a hypothetical chamber of bore diameter having the actual chamber volume. It is obtained by extending the actual bore rearward which establishes a new breech location.

C. CHAMBER REQUIREMENTS

60. Chambers are designed to be compatible with the ammunition and ballistic data. If the gun is to fire existing ammunition, the chamber is designed accordingly so that no difficulty should arise in loading the round or extracting the case whether

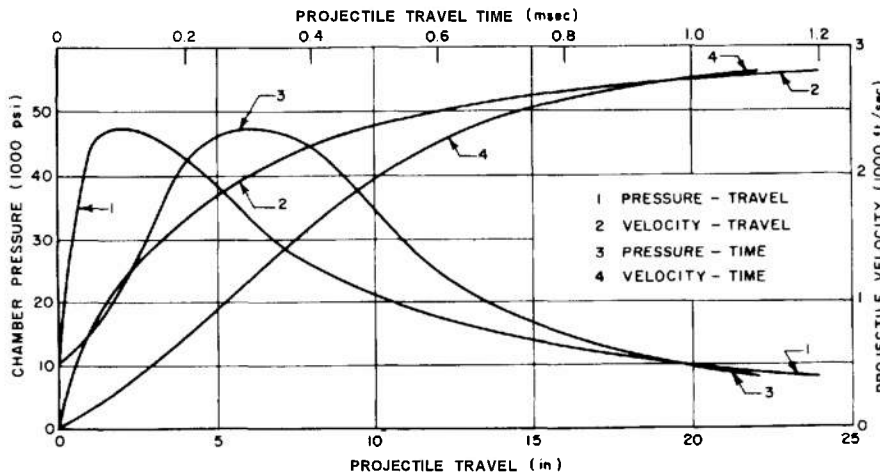


FIGURE 16. Interior Ballistics of Caliber .30 Gun.

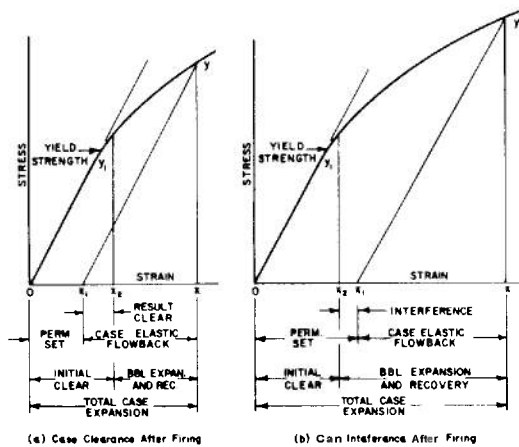


FIGURE 17. Case-Chamber Stress-Strain Curves.

this activity is manual or mechanical; whether single shot, semiautomatic, or automatic. If the ammunition is newly designed and not finalized, any early difficulty in handling or firing should be resolved by the ballistecian, the ammunition designer, and the tiibc designer to their mutual satisfaction. Not only shoild the chamber be designed to control density of loading, but also its interior should be so shaped as to promote the most effective gas flow from chamber to bore. Usually chamber geometry is such that it is compatible with the remaining tube structure, otherwise some measures must be taken to compensate for discontinuities. This is readily done in heavy tubes by arbitrarily extending the large outside chamber diameter beyond the origin of rifling region. In thin tubes where weight is critical, rigorous analyses are necessary to provide adequate strength without excess weight.

1. Cartridge Case Fit

61. The shape of the chamber for fixed and semi-fixed ammunition is somewhat more critical than that for the separately loaded type. Here both processes of loading the round and of extracting the cartridge case must be considered. Chamber slope and clearance aid both activities. Clearance between case and chamber should tie sufficient for easy loading but the space should not tie so large as to permit excessive plastic deformation or rupture. When the round is fired, propellant gas pressure expands the case to the chamber wall. As the case itself is not strong enough to withstand the pressiirc of the chamber miist be designed to prevent excessive dilation, as detailed below.

62. The mechanics of case recovery is demonstrated by the stress-strain curves of Figure 17. It

must be assumed that the chamber recovers completely from the dilation due to propellant gas pressures otherwise the chamber too would be stressed beyond its yield strength and therefore improperly designed. The yield strength of quarter hard 70-30 cartridge case brass is 40,000 lb/in².* The case, being too thin to contain the gas pressures, will expand beyond the initial clearance to the dilated inner wall of the chamber. The total case expansion is represented by the distance, ox , on the stress-strain curves. The corresponding stress is indicated by y . Assume that the initial clearance equals the strain, ox_1 , which is beyond the strain corresponding to the yield strength of the case. As the gas pressure falls to zero, the chamber will recover totally from its expansion, x to x_1 . In the meantime, the case, being stressed beyond its yield strength, will not return to o but to x_1 , the clastic flow back, which is found by drawing a line through y parallel to the modulus oy_1 . If ox_1 is less than the initial clearance, ox_2 (Fig. 17a), a resultant clearance, ox_2x_1 , is available, making the case free for extraction. If ox_1 is greater than the initial clearance, an interference x_2x_1 (Fig. 17b) develops, claiming the case and rendering the extraction difficult. Assuming the same case and pressure for both curves, Figure 17b obviously is based on a thinner chamber wall. By observation, the logical way to prevent interference caused by excessive dilation of the case is to increase the chamber wall thickness or to reduce temperatures in the chamber region thereby maintaining small clearances between case and chamber. The accompanying lower stress and strain shifts xy toward the ordinate so that x_1 will fall to the left of x_2 thereby ensuring the clearance necessary for extraction. Small initial clearances are also helpful. However, for a small permanent set (ox_1), case elastic flowback (x_1x) must be a minimum.

63. Longitudinal clearance is also involved in loading procedures. If this clearance is too large, cases may pull apart, delaying extraction in slow-fire guns but jamming automatic weapons. Dimensional relationships are established to provide automatic small arms with longitudinal interference between case and chamber and invite crush-lip. Sufficient residual energy must be available in the moving breechblock or bolt to perform this function. The amount of required energy is not predictable, hence, tests must be made on a prototype to assure proper action. If crush-up demands too much of the available energy, the chamber is deepened to relieve the

* Reference 6, Table 26.

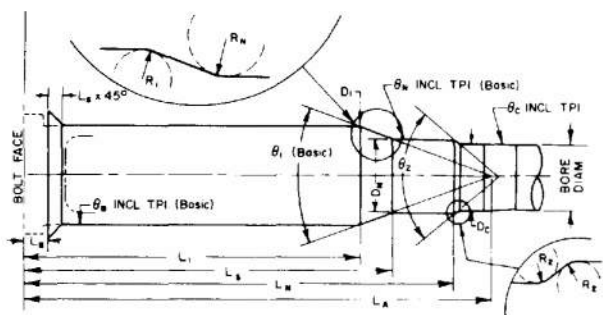


FIGURE 18. Chamber With Pertinent Dimensions.

interference. In some designs, a nominal interference is determined by allowing metal-to-metal contact for a minimum case and a maximum chamber. This provides crush-up for all conditions except the one where the contacting surfaces just meet. Present practice does not provide crush-up in artillery; a nominal clearance of 0.010 inch being currently used. Figure 18 shows the details of a chamber including the longitudinal dimensions to the bolt or breech face where the base of the cartridge case bears against it. All pertinent dimensions are shown, most of which are dictated by the size and shape of the case. The radii at the first and second shoulders are tangent to the straight lines but their locations are determined from the points of intersection of these lines. The arcs conform to their counterparts on the cartridge case but, according to existing chambers, are not correlated with chamber size. In addition, the second shoulder in the chamber of many artillery tubes extends directly to the forcing cone or is totally absent.

2. Chamber Slope

64. Chamber slope is an added precaution to ensure ready extraction. If, for some reason, the case retains contact with the chamber after propellant gases disappear, the slightest motion of the case will break the contact, freeing the case for extraction

without further interference. Some leeway can be exercised for chamber slope which is demonstrated by 10 contemporary guns having diametral tapers varying from 0.0064 to 0.035 in/in. A chamber slope having any of these tapers may be used if both case and chamber have the same nominal taper. Diametral taper is also referred to as included taper per inch (TPI).

3. Forcing Cone Slope

65. Great variety is found in the slopes of forcing cone angles. These vary from 0.040 to 0.3350 included TPI. Table 7 shows the included taper per inch of the forcing cones of a number of small arms and artillery guns.

A shallow taper permits a relatively long projectile travel before rotating band contacts forcing cone which increases the length of free run to invite a high impact velocity. A steep taper reduces this travel thereby providing a short free run and holding the impact velocity to moderate speeds. Figures 19a and 19b illustrate the two types. A double taper forcing cone (Fig. 19c) embodies the favorable aspects of both; the short distance before contact is made and the gradual engraving by the rifling. The interferences between band and forcing cone are purposely exaggerated in order to demonstrate clearly the dimensions which control the length of free run.

4. Chamber Geometry—Recoilless Guns

66. Theoretical and experimental data have been collected to study the behavior of different chamber shapes but more work is needed before optimum chamber shapes can be finalized for general requirements alone*. The present trend in design is toward the conical shape†. It has the ability to meet the gas flow requirement which stipulates that the

* Reference 7.

† Reference 8.

TABLE 7. FORCING CONE SLOPES.

Tube	Included TPI in/in	Tube	Included TPI in/in
Cal. .30 Machine Gun	0.040	37 mm Gun M3A1	0.1514
Cal. .30 Rifle	0.200	75 mm Gun M3	0.1367
Cal. .50 Machine Gun	0.040	76 mm Gun M1A2	0.2000
Cal. .50 Rifle	0.082	90 mm Gun M1A1	0.2680
20 mm Machine Gun	0.2036	105 mm Gun M3T4	0.3350
30 mm Machine Gun	0.050	120 mm Gun M1	0.1333
37 mm Machine Gun	0.100	155 mm Gun M2	0.1000

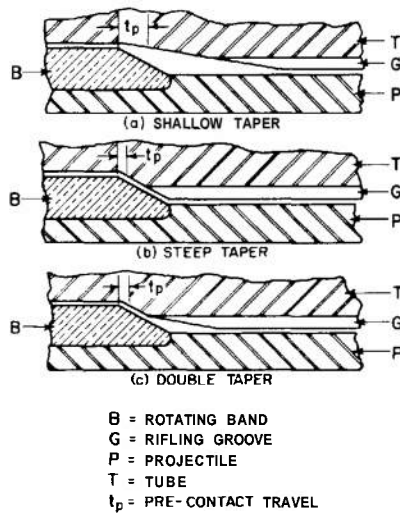


FIGURE 19. *Forcing Cone Study.*

velocity of the gas approaching the nozzle throat should be approximately zero, meaning, in effect, an ideal reservoir of infinite volume. The finite reservoir can closely approximate the ideal by having the chamber approach area adjacent to the nozzle at least four times the throat area or $A_a \geq 4A_t$. In practice, conical chambers having a much lower ratio, of the order of 1.7 to 2.0, can be tolerated with acceptable results.

67. Figure 20 is a schematic of the interior of a recoilless gun tube showing bore, chamber and nozzle. The chamber has three sections consisting of the nozzle entrance, the body, and the forward end leading to the bore. The body is considerably larger than the other two. Chamber volume is determined from interior ballistic requirements. The assigned design data are

- $E = F(\gamma - 1)$, ft-lb/lb (propellant potential)
- F = specific impetus, ft-lb/lb
- ω = ratio, rifle recoil momentum to projectile momentum
- M_p = mass of projectile
- v_m = muzzle velocity
- W_p = weight of projectile
- A = loading density

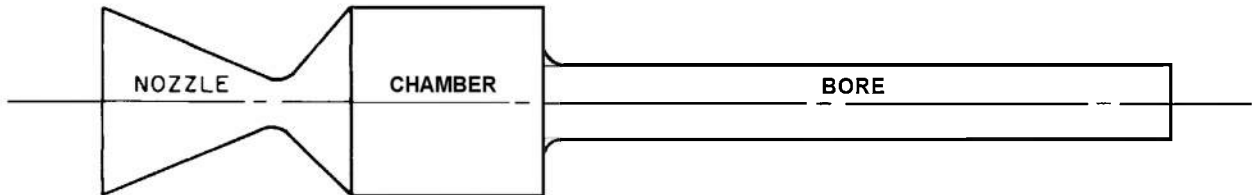


FIGURE 20. *Schematic of Recoilless Gun.*

Δ_p = maximum bag density of propellant (approximately 0.5 for existing chambers)

γ = ratio of specific heats of propellant gases, constant pressure to constant volume

The calculated design data for chamber volume include muzzle energy, weight of charge, and volume of charge. The kinetic energy of the projectile at the muzzle, or muzzle energy

$$K = \frac{1}{2} M_p v_m^2 = \frac{1}{2} \frac{W_p}{g} v_m^2 \quad (4a)$$

The weight of propellant charge

$$C \approx \frac{2K}{E} \left[1 + \frac{(1 - \omega) \sqrt{2gE}}{v_m} \right] \text{ lb}^* \quad (4b)$$

The required chamber volume

$$V_o \geq \frac{C}{\Delta} \geq 27.7 \frac{C}{\Delta} \text{ in}^3/\text{lb} \quad (4c)$$

The bag space, or the space occupied by the propellant package of a round of ammunition

$$V_c = \frac{C}{\Delta_p} \quad (4d)$$

Assuming that the minimum cross-sectional area of propellant charge is the same as the nozzle throat area, the required maximum chamber length

$$L_o = \frac{V_c}{A_t} \quad (4e)$$

When the chamber is a conical frustum whose minor radius is the bore radius, the volume of the chamber body becomes

$$V_o = \frac{\pi L_o}{5} (r_a^2 + r_a R + R^2) \quad (4f)$$

where

r_a = radius of nozzle approach area, A_a , determined from Equation 5b

R = bore radius

This volume is acceptable if it meets the requirements of Equation 4c.

* Reference 9.

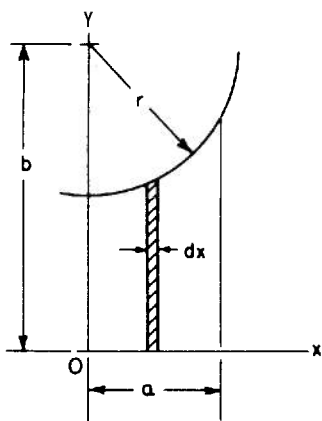


FIGURE 21. Nozzle Entrance Geometry.

68. The nozzle entrance is part of the chamber. It is extremely short, serving merely as a smooth junction between chamber body and nozzle throat. A generous radius of the order of one inch sweeps through the throat and becomes tangent to the nozzle surface to establish a smooth flow path. The volume of the nozzle entrance is the solid of revolution generated by rotating about the x -axis an arc of the fourth quadrant of a circle whose center is at $y = b$ (see Fig. 21). The arc begins at $x = 0$ and extends to $x = a$ with $x = r$ being the upper limit. The volume of this solid of revolution is

$$V_e = \pi \left(ab^2 + ar^2 - \frac{a^3}{3} \right. \\ \left. \sqrt{r^2 - a^2} - br^2 \sin^{-1} \frac{a}{r} \right) \quad (4g)$$

The total chamber volume less nozzle and bore entrance volumes determines the chamber length.

D. NOZZLE DESIGN, RECOILLESS GUNS

69. The recoilless rifle is a gun which overcomes recoil forces by utilizing part of the propellant gases to produce a force in the forward direction. The rearward end of the chamber opens into a converging-diverging nozzle which allows the passage of a fraction of the propellant gas and its associated momentum to the rear. For a given nozzle geometry, the orifice cross section is adjusted until the net pressure forces are of the proper magnitude to neutralize each other. Thus, the rearward momentum of the gases which issue from the nozzle is utilized to counteract the equivalent forces imparting forward momentum to the projectile, and impulses due to other factors, such as projectile friction, engraving resistance, or gas drag.

1. Parameters

70. The design of a recoilless rifle is based on four interrelated parameters: (1) the ratio of rifle bore area to nozzle throat area, (2) the ratio of nozzle approach area to throat area, (3) the divergence angle of the nozzle cone, and (4) expansion ratio of nozzle cone, A_e/A_t . The criteria assigned to the parameters are based on rocket theory, but final nozzle dimensions are adjusted for a given weapon design on the basis of empirical data obtained from balancing experiments (see paragraph 78). These empirical data are:

$$\frac{A_b}{A_t} \approx 1.45 \quad (5a)$$

if

$$\frac{A_a}{A_t} \geq 1.70, \quad (5b)$$

the divergence angle is less than 15° (included angle), and if $A_b/A_t \approx 2$ where

- A_a = nozzle approach area
- A_b = bore area (known)
- A_e = nozzle exit area
- A_t = nozzle throat area

Since a significant portion of the balancing force of a recoilless rifle is caused by the reaction of escaping gases on the cone of the nozzle, the third parameter, the divergence angle of the cone, is significant. The divergence angle influences the component of balancing forces created by the velocity thrust of the nozzle gases. This influence is represented by the divergence angle correction factor

$$\lambda = \frac{1 - \cos 2\alpha}{4(1 - \cos \alpha)} \quad (5c)$$

where

α = half angle of the diverging cone.

Equation 5a may now be corrected to

$$\frac{A_a}{\lambda A_t} \geq 1.45 \quad (5d)$$

However, for values of $\alpha \leq 15^\circ$, λ does not deviate sufficiently from unity to warrant any analysis beyond that provided by Equation 5a.

72. After α has been established, two remaining dimensions of the nozzle are specified for a given type of nozzle, namely, length and exit radius, one being dependent on the other. Other parameters to be considered are

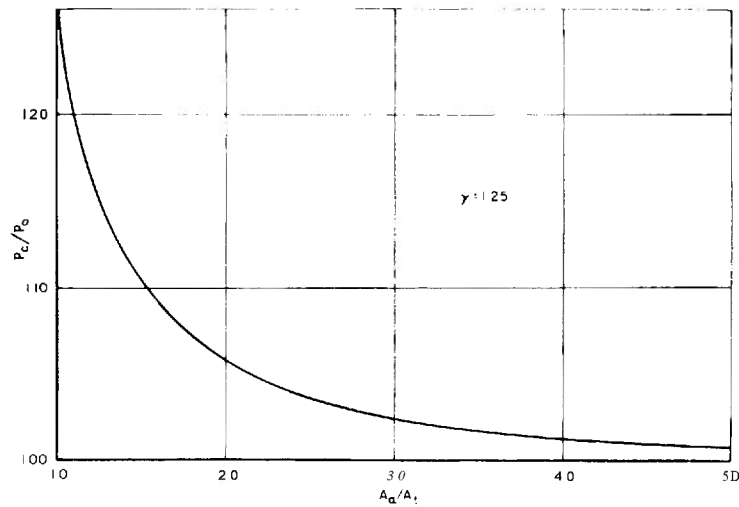


FIGURE 22. Pressure Ratio-Area Ratio Curve.

p_0 = stagnation pressure (pressure at A_n leading to nozzle)

p_c = chamber pressure

The approach area to throat area ratio, A_n/A_t , is determined from Equation 5b. This value, when entered on the pressure ratio-area ratio curve of Figure 22, indicates p_c/p_0 . Since A_n/A_t is known, the ratio $A_n p_c/A_t p_0$ is readily computed. Now refer to Figure 23 and from the curve of the appropriate momentum ratio, ω , locate the corresponding A_e/A_t .^{*} Then, the exit area

$$A_e = \left(\frac{A_e}{A_t} \right) A_t \quad (5e)$$

The radius of the exit area

^{*} Reference 10.

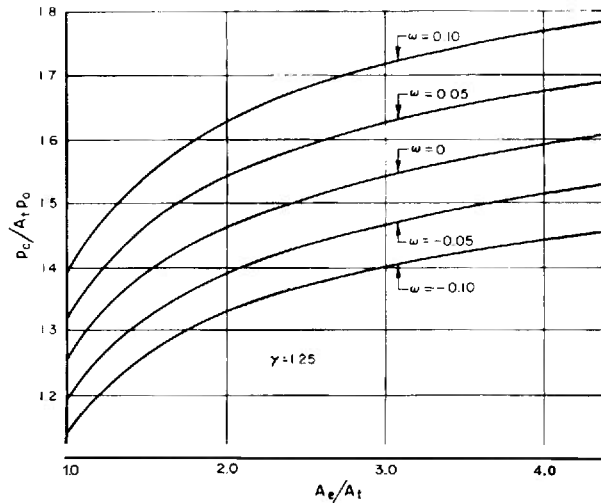


FIGURE 23. Lines of Constant Dimensionless Recoil.

$$r_e = \sqrt{A_e/\pi} \quad (5f)$$

The length of the nozzle cone

$$L_n = \frac{r_e - R}{\tan \alpha} \quad (5g)$$

2. Nozzle Shape

73. A central orifice nozzle (Fig. 24a) is of optimum design in the sense that it is the simplest and lightest. This is most important because low weight is usually

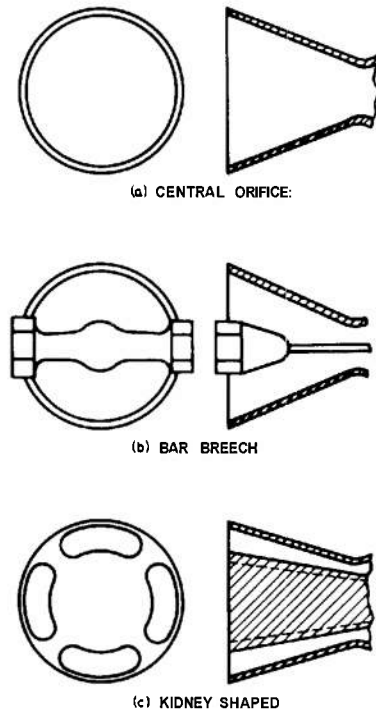


FIGURE 24. Nozzle Shapes-Schematic.

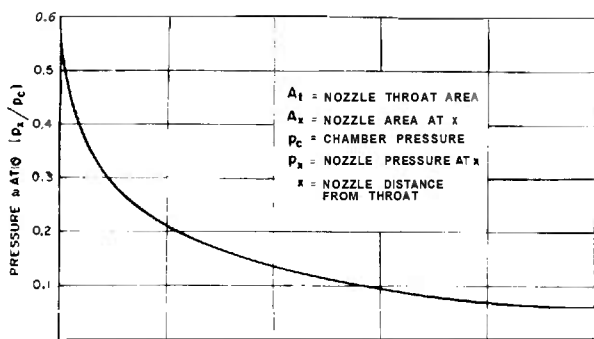


FIGURE 25. Nozzle Pressure-Area Ratio Curve, M10 Propellant.

a critical design criterion. However, a number of problems are associated with this type. It does not permit torque compensation. Normally it loses more unburned propellant through the nozzle, therefore yielding less uniform ballistic performance than is obtained from guns having other type nozzles. Furthermore, some difficulty is presented in providing for ready access to the round for firing. This accessibility can be achieved either by attaching a firing line, commonly called a pig tail, or by housing a centrally located firing device such as that found in a bar breech type nozzle (Fig. 24b).

The bar breech derives its name from the bar which is centered across the nozzle exit and houses the firing device. This arrangement is merely a modified central orifice type nozzle whose basic throat and exit areas must be adjusted to compensate for the bar interference.

74. Another type nozzle is kidney shaped (Fig. 24c). It has the advantage of having a solid center for housing the firing device. Another asset is its adaptability to rifling torque compensation by canting the nozzle sections or channels. Symmetry is essential. Its disadvantages are complexity and extra weight, making it the most costly of all types to produce. It also has the tendency to develop cracks in the webs between the orifices. The number of kidney shaped channels are determined by the available space for the required throat area. To summarize, nozzle shape depends on required throat area, the type firing mechanism, cartridge case geometry, and whether weight and torque compensation are particularly critical.

75. Attachment of nozzle to chamber depends on loading method. If the gun is a muzzle loading type, the nozzle and chamber can be integral. If it is a

breech loading type, the nozzle can be hinged, i.e., be a part of the breech door. A new concept uses a segmented nozzle of 8 pieces held by a circumferential spring. It dilates for the round to be loaded by the radial displacement of the segments. This type requires a pig tail firing line.

76. The nozzle is usually conical, diverging from A_t to A_x . Although the included angle of this cone is theoretically satisfactory to 30° , smaller angles are desirable to prevent detachment of flow. During the development of the nozzle, an included angle of 14° provides a good starting point. However, a small angle such as this means a long nozzle and more weight. By readjusting the angle and length, an acceptable compromise can be reached between weight, included angle, and nozzle effectiveness.

3. Nozzle Pressure Distribution

77. The pressure in the nozzle is controlled by the type propellant and the nozzle parameters. With the aid of the curve in Figure 25 the pressure at any point, in the nozzle for M10 propellant may be obtained. The curve is plotted for the solutions of Equation 5h where γ for M10 propellant is 1.21.

$$\left(\frac{p_x}{p_c}\right)^{-2/\gamma} = \frac{\left(\frac{A_x}{A_t}\right)^2 \left[1 - \left(\frac{p_x}{p_c}\right)^{(\gamma-1)/\gamma}\right]^*}{\left(\frac{\gamma-1}{2}\right)\left(\frac{2}{\gamma+1}\right)^{(\gamma+1)/(\gamma-1)}} \quad (5h)$$

where

- A_t = nozzle throat area
- A_x = nozzle area at x
- p_c = chamber pressure
- p_x = pressure in nozzle at x

4. Recoil Balancing

78. In the recoilless weapon field, recoil is defined as the momentum of the weapon which is derived from the residual impulse between gun tube and nozzle. An ideal nozzle would maintain the weapon motionless during the firing cycle. However, perfection is not sought since variations in performance are always present and slight variations from round to round are unavoidable. In the long run, the progressive wear in the tube and nozzle will aggravate these variations. Hence, a slight amount of recoil is tolerated. In fact, some recoil is deliberately planned since it is desirable, for maximum nozzle life, to have the initial recoil at as high a level as can be tolerated, in the rearward direction. As the

* Reference 11.

nozzle throat wears, rearward recoil diminishes to zero and ultimately forward motion occurs.

The criteria for establishing limits on recoil are determined from the effects on the gunner or on the mount. For shoulder fired weapons, the effect of recoil on the gunner will be reflected in physiological effects of excessive rearward recoil, effects on his stability, and psychological effects of forward recoil. The recoil should not be so severe as to injure him, or to destroy his aim by disturbing his stability or cause him to flinch. Limited tests have indicated that the impulse should not exceed 3.0 lb-sec (rearward), the limit specified for the 90 mm M67 rifle (Military Specification, MIL-R-45511). Experience with conventional weapons leads him to expect rearward recoil of reasonable intensity and he will accept it, but forward recoil will be disconcerting. On a mount, the effects of recoil forces involve stability and strength of structure including attachments such as the mounting trunnions of the gun. Usually, the stability of the system dictates the rearward and forward limits of recoil. When these limits have been established, the effects on structural strength can be absorbed by designing the mount accordingly.

Recoil is usually specified as an impulse. Since impulse and momentum have the same dimensions, the equations associated with recoil may be stated in terms of momentum. On this basis, action and reaction being equal and opposite, the momentum of the recoiling mass plus the impulse of that generated by the nozzle equals the projectile momentum. Expressed as an equation

$$M_r + \int_0^{t_a} F_n dt = M_p v_m \quad (6a)$$

where

F_n = nozzle force
 M_p = mass of projectile
 M_r = momentum of recoiling mass
 t_a = time of propellant gas period
 dt = differential time of application of F_n
 v_m = muzzle velocity (measured)

Firing tests performed with the recoilless rifle suspended as a pendulum provide the data for computing the projectile and recoil momentum of Equation 6a and hence, for recoil balancing. The weapon is freely suspended and fired. Muzzle velocity, amplitude of pendulum swing and period are measured. These measurements are used to determine projectile momentum and recoil momentum of the suspended mass. Thus:

$$M_r = \frac{2\pi W_r x}{Tg} \quad (6b)$$

where

g = acceleration of gravity
 T = period of pendulum
 W_r = weight of suspended mass after firing
 x = linear amplitude of pendulum swing

Recoilless weapons with fixed vents can be adjusted to the desired recoil balance by increasing the throat area to decrease rearward recoil or by decreasing the nozzle length to increase rearward recoil. The former method is simpler and is most commonly used, although in some designs it is necessary to exercise care in determining the location of the throat (minimum cross section for gas flow). Newly designed nozzles should have the throat restricted more than necessary in the test gun to assure a substantial rearward recoil. Subsequent developmental firing tests will indicate the degree of enlargement to meet the specified recoil.

79. The procedure for computing the change in throat area is based on the change in momentum necessary to be compatible with the specified recoil momentum.

$$\Delta M_r = M_r - M_{rs} \quad (6c)$$

where

M_{rs} = specified momentum of recoiling mass
 ΔM_r = required change in momentum

Small changes in recoil momentum are approximately directly proportional to nozzle throat area, thereby forming the relationship:

$$\Delta A_n \approx A_n \frac{\Delta M_r}{M_p v_m} \quad (6d)$$

where

A_n = original nozzle throat area
 ΔA_n = indicated change in throat area

Since this relationship is approximate, variables such as propellant gas pressure and chamber-nozzle configuration may yield even wider deviations. Hence, Equation 6d should be used as a guide only. A more precise relationship becomes available for the individual gun after interpreting the experimental data obtained for this gun during the balancing process.

It is important to note that when the required amount of material is removed from the throat of the nozzle, the remaining sharp corners or discon-

tinuities should be carefully blended into the original entrance radius and the divergent conical surface. Failure to do so will seriously affect nozzle performance. Adjustments that can be made in the field to compensate for changes in recoil due to nozzle wear are desirable. An example is the 57 mm recoilless rifle, a shoulder fired weapon, which provides for recoil balancing by use of replaceable throat rings.

E. BORE

1. Bore Diameter

80. The nominal bore diameter is determined by the combined effort of ballistics and projectile designer in meeting the terminal ballistic requirements of the projectile. Although the tube designer specifies surface finishes and tolerances, practice has set a plus tolerance of 0.002 inch on practically all tubes of 20 mm or larger. Smaller tubes have smaller tolerances, usually 0.0015 inch.

2. Bore Length

81. The length of the bore is determined with the aid of interior ballistics. For a given projectile, a propellant charge is designed which will impart the required velocity within a distance, i.e., bore length, compatible with the particular use of the weapon. If the ballistics of an established round of ammunition meet the requirements of a proposed gun, then the bore length is made to coincide with the travel distance to the point corresponding to the desired muzzle velocity on the velocity-travel curve. An approximate length can be determined provided several data are known. This method is used in recoilless rifle design. Assuming that the data are

- A_b = bore area
- a_m = maximum projectile acceleration
- K = kinetic energy of projectile (Equation 4a)
- M_p = projectile mass
- μ = piezometric efficiency

The maximum propellant gas pressure

$$p_{gm} = \frac{M_p a_m}{A_b} \quad (7a)$$

The bore length

$$x_b \approx \frac{K_e}{\mu p_{gm} A_b} \quad (7b)$$

μ is determined from empirical data from test gun firings. In the absence of such data $\mu = 0.6$ is a reasonable approximation for guns with expansion

ratios, $V_f/V_o \approx 2$. Where V_f/V_o equals the ratio of final gun volume to chamber volume. For higher ratios, μ will decrease.

F. TEMPERATURE DISTRIBUTION

82. The temperature distribution along the tube and across the wall induces thermal stresses which may become appreciable. Although temperatures on the outer surface and through the tube can be readily measured, instrumentation to measure the temperature on the immediate bore surface has still to be perfected. Consequently, temperatures here can only be approximated. This approximation becomes more difficult and less reliable when temperatures must be predicted for a new design since no accurate method is available for computing them. Temperature estimation therefore depends on good judgement and experience. Thermal stress is not a design criterion for tubes of slow-fire weapons, but it is for machine gun type barrels. In a caliber .30 machine gun lined barrel, the maximum differential between bore and outer surface is 600°F at the point of maximum outer temperature. The corresponding bore surface temperature is assumed to be 2000°F. Figure 9 shows the variation along the outer surface. The temperature gradient across the wall is assumed constant at 600°F along the tube from the breech to the point of maximum temperature. From the point of maximum temperature to the muzzle, it decreases as wall thickness decreases. One method of estimating sets the temperature gradient at 600°F for a wall ratio of 2.0 varying to one of 450°F for a wall ratio of 1.5. The temperature distribution curve shows a higher temperature beyond the liner. This demonstrates the insulating effect of the liner-tube intersurface since the bore temperatures of the liner are at least as high as the bore temperatures beyond.

G. RIFLING

1. Profile

83. Rifling and rotating band are intimately associated because of their respective functions—that of imparting torque to the projectile and that of transmitting this torque. The mating lands are the load transmitting members and should be designed so that both rifling and band can support the induced tangential load after engraving. The rotating band, being of softer material than the rifling, will require wider lands. Consequently, the rifling grooves will be wider than the lands. Although no method, either theoretical or empirical, has been established for

determining the ratio of groove to land width, a ratio of 3 to 2 is reasonable, and generally satisfactory in practice.

84. The number of grooves in present guns varies approximately as bore diameter but still no precise method for determining the number can be based on this information. Eight grooves per inch of bore diameter seems to be an appropriate value for the equivalent pitch.

$$G \approx 80, \quad (8a)$$

where

G = number of grooves (to the nearest whole number)

D_b = bore diameter, in.

If the 3 to 2 ratio and the pitch are maintained, the groove width, $b = 0.2356$ in., and the land width, $w = 0.1571$ in., are constants. Since the product 80, will not always be a whole number, the values of b and w will be modified accordingly.

The depth of groove is the third parameter involving the physical aspects of rifling. Here again present rifling offers only a guide, not an exact procedure. Based on present dimensions, a nominal groove depth of

$$h = .01D_b \quad (8b)$$

is in keeping with accepted practice. Generally the smaller bores have groove depths exceeding this dimension whereas for large bores the groove depths are slightly less. Weapons having low propellant gas pressure and low muzzle velocities, such as howitzers and recoilless guns, may need only half this depth but hypervelocity weapons may need considerably more. Rather than vary depth of rifling to correspond to the particular type tube, it may be more feasible to vary the band width to provide the same compensation.

Some option may be exercised in determining the rifling parameters of groove number and size since present weapons have demonstrated that deviations from any rifling pattern can be successfully applied. Heretofore the number of grooves has been restricted to multiples of 3 or 4 to assure proper land or groove alignment for 3 or 4 tipped star gages. Now that air gages are available, this practice is no longer necessary. Figure 26 has the curves of groove depth and number of grooves of present rifling plotted with bore diameter as the abscissa. Many points do not fall on these curves but the trend is general. No such trend is available for either land

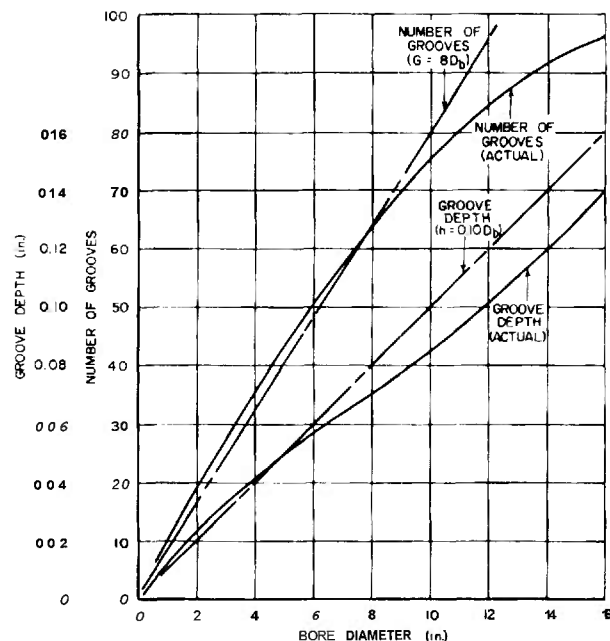


FIGURE 26. Groove-Bore Relations.

or groove width. For a ready reference, the various parameters of standard rifling profiles are provided in Figure 27. For a new tube, the practice is to select the standard rifling profile for that caliber. The standard profiles may not be optimum in strength, durability, and efficiency, but they have been successful in many guns and have become an excellent initial design. For guns which depart drastically from what is considered normal ballistic conditions, the standard rifling may not be adequate, thereby calling for a modified profile. Even so, because of their empirical status, standard forms should be tried first, then, if found wanting, other profiles must be tried. Since rifling and rotating bands work as a unit, considerable attention should be directed toward the band design before any rifling form is finalized. Close collaboration with the projectile designer should yield rifling and rotating band with a high degree of compatibility.

2. Rifling Twist

85. The rotational velocity of the projectile, or bullet spin, varies directly with the tangent of the developed rifling curve. Since two primary requirements of exterior ballistics are the values at the muzzle of velocity and spin rate, the tube designer is given the required exit angle of the rifling or the bullet spin. But the tube designer is also concerned with the rifling characteristics throughout the tube and therefore is also given the interior ballistics curves. The twist of rifling is usually expressed in

calibers per turn, i.e., the bore length measured in terms of calibers in which the rifling makes one complete turn. There are two types of rifling twist, uniform and increasing. In uniform twist, the rifling has a constant angle from origin to muzzle, whereas in increasing twist, this angle varies in accordance with an exponential curve. The general equation

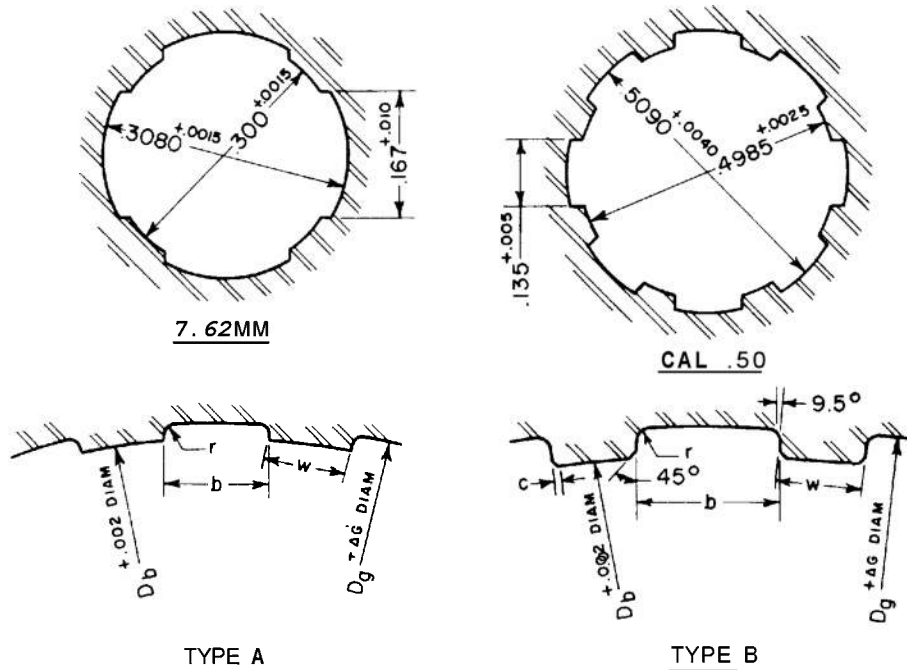
for the rifling curve is

$$y = px^n \quad (9a)$$

where

n = exponent which defines the rifling curve

p = constant determined from the exit angle



BORE	D_b	G	D_g	ΔG	b	w	r	c
20MM	0.787	9	0.817	.004	.205	.205	.01	—
30MM	1.181	16	1.216	.004	.135	.098	.01	—
37MM	1.157	12	1.497	.004	.2314	.15	.01	—
40MM	1.573	16	1.618	.004	.220	.089	.024	—
57MM	2.244	24	2.284	.004	.1736	.120	.02	—
75MM	2.950	28	3.010	.004	.1866	.1444	.015	—
3-IN	3.000	28	3.080	.004	.1866	.15	.015	—
90MM*	3.543	32	3.555	.002	.1978	.15	.002	—
90MM	3.543	32	3.623	.004	.1978	.15	.015	—
105MM†	4.134	36	4.194	.004	.2108	.15	.015	—
105MM*	4.134	36	4.208	.004	.2108	.15	.015	—
105MM	4.134	36	4.224	.004	.2108	.15	.015	—
106MM*	4.134	36	4.208	.004	.2108	.15	.015	—
4.5-IN	4.500	32	4.574	.006	.2945	.1473	.02	—
4.7-IN	4.700	42	4.790	.006	.2016	.15	.02	—
6-IN	6.000	48	6.100	.006	.2193	.1434	.02	.01
155MM	6.100	48	6.200	.006	.2493	.15	.02	.01
8-IN	8.000	64	8.140	.006	.2356	.1571	.02	.01
240MM	9.449	68	9.609	.008	.2619	.1746	.02	.015
10-IN	10.000	72	10.160	.008	.2619	.1744	.02	.015
12-IN	12.000	84	12.200	.008	.2693	.1195	.02	.015
14-IN	14.000	92	14.240	.008	.2868	.1912	.02	.015
16-IN	16.000	96	16.280	.008	.3142	.2094	.030	.015

* Recoilless Exclusively
† Howitzer

FIGURE 27. Standard Rifling Profiles.

x = axial length of rifling curve

$y = R\theta$, peripheral distance of rifling around bore
(Equation 11)

The constant, p , is found by differentiating Equation 9a.

$$\frac{dy}{dx} = pn x^{n-1} = \tan \alpha \quad (9b)$$

where $\tan \alpha$ is the slope of the developed rifling curve. In other words, α is the angle formed by the tangent to the rifling curve and the x-axis which is parallel to the bore axis. For constant twist rifling, $n = 1$ and $p = \tan \alpha$. At the end of increasing twist rifling where α becomes the exit angle, Equation 9b becomes

$$pn x_E^{n-1} = \tan \alpha_E \quad (9c)$$

where

x_E = total axial length of the portion of the rifling curve which follows the assigned equation
 α_E = exit angle of the rifling

$$p = \frac{\tan \alpha_E}{n x_E^{n-1}} \quad (9d)$$

Consequently, the general equation may be written

$$y = \frac{\tan \alpha_E}{n x_E^{n-1}} x^n \quad (9e)$$

$$\frac{dy}{dx} = \tan \alpha = \frac{\tan \alpha_E}{x_E^{n-1}} x^{n-1} \quad (9f)$$

$$\frac{d^2 y}{dx^2} = \frac{d \tan \alpha}{dx} = \frac{(n-1) \tan \alpha_E}{x_E^{n-1}} x^{n-2} \quad (9g)$$

When the required twist of rifling at the muzzle is expressed in calibers per turn, n_c ,

$$\tan \alpha_E = \frac{\pi}{n_c} \quad (9h)$$

Equations 9f and 9g may be written

$$\tan \alpha = \frac{\pi}{n_c x_E^{n-1}} x^{n-1} \quad (9i)$$

$$\frac{d \tan \alpha}{dx} = \frac{\pi(n-1)}{n_c x_E^{n-1}} x^{n-2} \quad (9j)$$

3. Rifling Torque*

86. The rifling torque is derived from the propellant gas pressure applied to the base of the projectile

*The material presented on the mechanics of rifling is based on data made available by Springfield Armory. Reference 12.

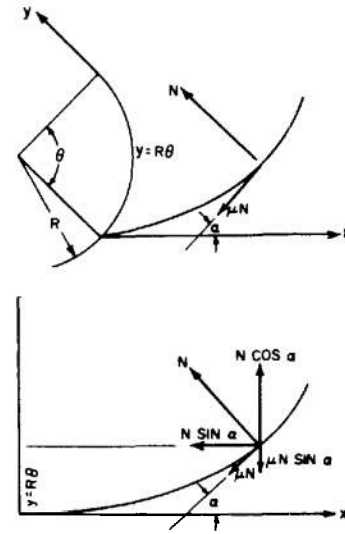


FIGURE 28. Rifling Force Diagram.

and from the slope and change in slope of the rifling curve. Figure 28 is a diagram of the dynamics involved.

N = induced force normal to rifling curve
 μN = frictional force parallel to rifling curve
 R = radius of projectile; bore radius
 e = angular displacement of projectile
 α = angle of twist
 μ = coefficient of friction

The torque on the projectile induced by the rifling is

$$T = \Phi \ddot{\theta} \quad (10)$$

where

$\Phi = M_p \rho^2$, polar mass moment of inertia of projectile
 $\ddot{\theta}$ = angular acceleration of projectile
 ρ = polar radius of gyration of projectile
 M_p = mass of projectile

From Figure 28,

$$y = R\theta \quad (11)$$

$$\frac{dy}{dx} = \tan \alpha = R \frac{d\theta}{dx} = R \frac{d\theta}{dt} \frac{dt}{dx} = R \dot{\theta} \frac{1}{v} \quad (12)$$

where

v = linear velocity of projectile.

The angular velocity or spin rate from Equation 12

$$\dot{\theta} = \frac{v \tan \alpha}{R} \quad (13)$$

The angular acceleration

$$\begin{aligned}\theta &= \frac{d\theta}{dt} = \frac{1}{R} \frac{d(v \tan \alpha)}{dt} = \frac{1}{R} \frac{d\left(\frac{dx}{dt} \frac{dy}{dx}\right)}{dt} \\ &= \frac{1}{R} \left(\frac{d^2x}{dt^2} \frac{dy}{dx} + \frac{dx}{dt} \frac{d^2y}{dx^2} \frac{dx}{dt} \right) \\ &= \frac{1}{R} \left(a \tan \alpha + v^2 \frac{d \tan \alpha}{dx} \right) \quad (14)\end{aligned}$$

where

a = linear acceleration of the projectile.

Substituting the expression for θ in Equation 14 into Equation 10, the rifling torque becomes

$$T = \frac{M_p \rho^2}{R} \left(a \tan \alpha + v^2 \frac{d \tan \alpha}{dx} \right) \quad (15a)$$

By observation, in Figure 28, rifling torque may also be expressed as

$$T = N(\cos \alpha - \mu \sin \alpha)R \quad (15b)$$

Solved for the land force by equating the torques of Equations 15a and 15b

$$N = \frac{M_p \rho^2}{R^2} \left[\frac{a \tan \alpha + v^2 \frac{d \tan \alpha}{dx}}{\cos \alpha - \mu \sin \alpha} \right] \quad (16a)$$

Linear acceleration is equal to the net forward force divided by the mass or the difference between the gas pressure force and two resisting force components indicated in Figure 28.

$$a = \frac{p_o A - N \sin \alpha - \mu N \cos \alpha}{M} \quad (16b)$$

where

A = bore area

p_o = propellant gas pressure

Rewrite Equation 15a by substituting the values for N obtained from Equation 16a after the acceleration, a , in that equation has been expressed in terms of the values of Equation 16b. Thus

$$T = (1 - \mu \tan \alpha)R \frac{p_o A \tan \alpha + M v^2 \frac{d \tan \alpha}{dx}}{\frac{M_p}{\rho^2} + \tan^2 \alpha - \mu \tan \alpha \left(\frac{R^2}{R_o^2} - 1 \right)} \quad (17)$$

87. It is possible to simplify considerably Equation 17 by evaluating, relatively, some of the expressions. $(1 - \mu \tan \alpha)$ can be considered to be nearly equal to unity, as both μ and $\tan \alpha$ are small quantities, and their product would therefore be insignificant. In the denominator, $\tan^2 \alpha$ is also an insignificant quantity. The expression $\mu \tan \alpha (R^2/\rho^2 - 1)$ can be neglected, because $\mu \tan \alpha$, as before, is a small quantity and the value of $(R^2/\rho^2 - 1)$ for a homogeneous cylinder is equal to unity. Equation 17 therefore reduces to its approximate equivalent

$$T = M_p \frac{\rho^2}{R} \left(\frac{A p_o}{M_p} \tan \alpha + v^2 \frac{d \tan \alpha}{dx} \right) \quad (18)$$

For uniform twist rifling, $d \tan \alpha / dx$ is zero, and Equation 18 reduces to

$$T = \frac{\rho^2 A p_o}{R} \tan \alpha \quad (19a)$$

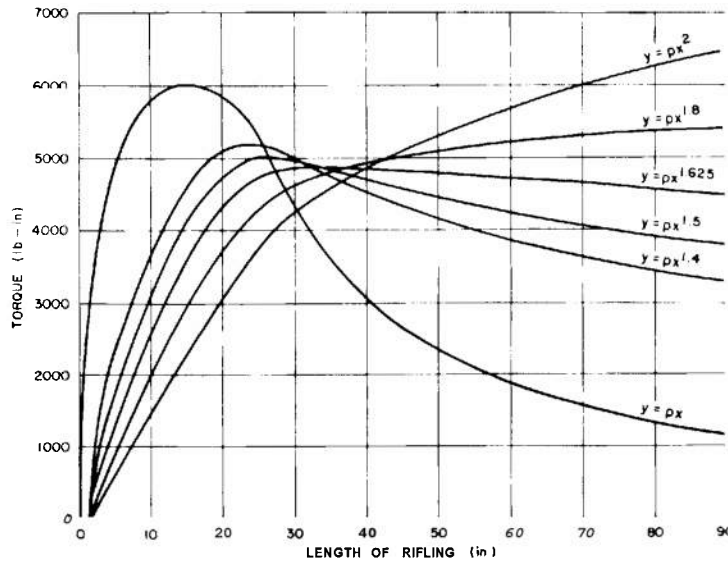


FIGURE 29. Torque Curves for 37 mm Gun.

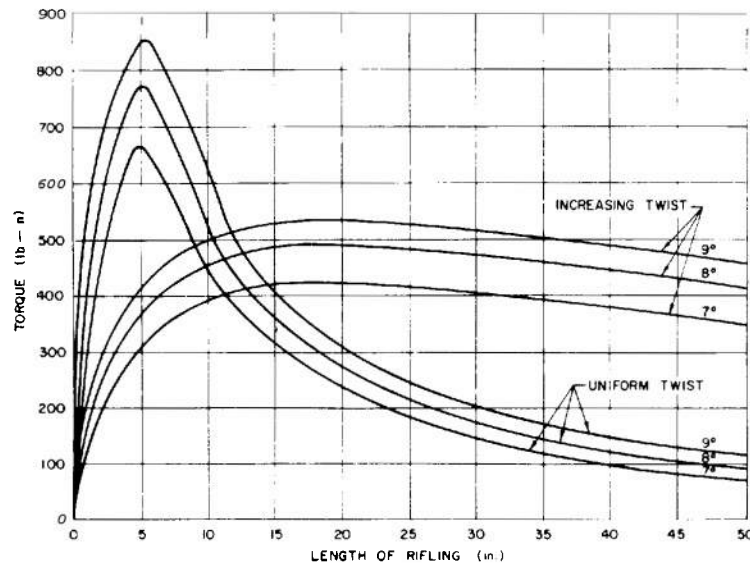


FIGURE 30. Effects on Rifling Torque by Varying Exit Angle.

Since all quantities on the right hand side of the equation, except p_a , are constant for a given gun, Equation 19a may be written

$$T = K_t p_e \quad (19b)$$

where K_t is a constant whose value is $(\rho^2 A_b \tan \alpha)/R$.

88. The advantage of increasing twist rifling is demonstrated in Figure 29. Here a series of curves of computed rifling torques for a 37 mm gun show the distribution along the barrel. They fulfill the purpose of increasing twist rifling by reducing the torque near the origin of rifling where it is most damaging. The curves also demonstrate that just any increasing twist rifling is not the sole answer as higher than necessary torques may still be induced. The ideal is a curve approaching constant torque such as that of $y = px^{1.625}$. Although the remaining curves show less torque at one extremity, the other end, either at origin of rifling or at the muzzle, has unduly high torques to compensate for these corresponding low values. The effects on rifling torque by varying the exit angle for a constant and an increasing twist rifling are illustrated in Figure 30.

As mentioned earlier, some increasing twist rifling with free run have, at least in theory, an infinite torque applied instantaneously at the origin. A curve is available which eliminates the infinite torque. It is the quadratic parabola whose axis of symmetry is rotated from the perpendicular axis*. This tipped parabola is so constructed that the origin of the coordinate axes lies to the left of the

point of tangency on the abscissa, i.e., the origin of the coordinate axes and the rifling do not coincide (Fig. 31). Thus, the variable x will always have a value greater than zero and an infinite torque is avoided. The curve may be written as

$$sx^{1/2} + y^{1/2} = p \quad (20a)$$

or

$$y = p^2 - 2psx^{1/2} + s^2x \quad (20b)$$

The constants s and p are obtained by substituting known values of the first derivative of Equation 20b. These are

$$\tan \alpha = 0 \quad \text{when} \quad x = a$$

and

$$\tan \alpha = \frac{\pi}{n} \quad \text{when} \quad x = a + x_E$$

where

a = arbitrary distance from origin of coordinate axis to origin of rifling curve. Eight calibers is a reasonable value for a .

x_E = axial length of rifling curve in bore.

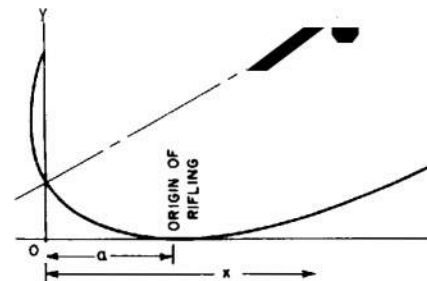


FIGURE 31. Tipped Parabola.

* Reference 13.

TABLE 8. RIFLING TORQUE CALCULATIONS FOR EXPONENTIAL RIFLING.

x (in)	$\tan \alpha$	$\frac{d \tan \alpha}{dx} \left(\frac{1}{\text{in}} \right)$	$p_a \times 10^{-3}$ (psi)	$v^2 \times 10^{-6}$ (ft ² /sec ²)	T_p (lb-in)	T_v (lb-in)	T (lb-in)
0	0	0	10.0	0	0	0	0
1	0.0169	0.01053	41.0	.59	3.9	3.4	7.3
2	0.0260	0.00814	47.5	1.37	6.4	6.1	12.5
3	0.0335	0.00699	45.9	2.10	8.0	8.1	16.1
4	0.0400	0.00626	42.9	2.79	8.9	9.6	18.5
5	0.0461	0.00577	38.4	3.42	9.2	10.8	20.0
6	0.0516	0.00539	33.4	4.04	8.9	11.9	20.8
7	0.0570	0.00509	29.2	4.54	8.7	12.7	21.4
8	0.0619	0.00482	26.0	4.97	8.4	13.2	21.6
9	0.0666	0.00462	23.1	5.38	8.1	13.6	21.7
10	0.0711	0.00445	21.1	5.77	7.8	13.9	21.7
11	0.0755	0.00428	19.2	6.00	7.5	14.1	21.6
12	0.0798	0.00415	17.5	6.25	7.2	14.2	21.4
13	0.0839	0.00402	16.2	6.50	7.0	14.3	21.3
14	0.0878	0.00392	15.0	6.74	6.8	14.4	21.2
15	0.0918	0.00382	13.9	6.89	6.6	14.4	21.0
16	0.0955	0.00372	12.9	7.02	6.4	14.3	20.7
17	0.0993	0.00363	12.0	7.16	6.2	14.3	20.5
18	0.1028	0.00356	11.2	7.29	6.0	14.2	20.2
19	0.1062	0.00349	10.5	7.40	5.8	14.1	19.9
20	0.1096	0.00342	9.9	7.51	5.6	14.1	19.7
21	0.1130	0.00336	9.3	7.59	5.4	14.0	19.4
22	0.1163	0.00330	8.8	7.67	5.3	13.9	19.2
23	0.1198	0.00325	8.4	7.75	5.2	13.8	19.0
24	0.1230	0.00320	8.0	7.84	5.1	13.7	18.8

89. To supplement the information in Figures 29 and 30 and to illustrate the method for computing rifling torque, the torques are computed for several rifling curves of a cal. .30 barrel whose interior ballistic curves appear in Figure 16. These rifling curves are

- uniform twist,
- quadratic parabola with one inch free run
- tipped parabola with one inch free run
- exponential with no free run
- exponential with one inch free run

All exit at an angle of 7 degrees. The torque is computed for each rifling at one-inch increments of travel. In addition to the ballistic curves and the exit angle, other data are

- $L = 24$ in*, distance of projectile travel in bore
 $R = 0.15$ in, bore radius
 $W = 140$ grains = 0.02 lb, projectile weight
 $\rho = .7R$, radius of gyration of projectile.

The design data are incorporated into Equations 18

* Since L is only slightly longer than x_E for the no-free-run condition, the two are assumed equal in this discussion without involving serious error.

or 19 and the torques computed for each rifling. The detailed calculations are listed in Table 8 only for the exponential curve with no free run. Rifling torque curves appear in Figure 32 for all five types. To simplify the tabulation procedure, the torque computed from Equation 18 is divided into two components, the pressure component

$$T_p = \frac{\rho^2 A_b \tan \alpha}{R} p, = 0.00519 \tan \alpha p, \quad (21a)$$

and the velocity component

$$T_v = M_p \frac{\rho^2}{R} v^2 \frac{d \tan \alpha}{dx} = .000548 v^2 \frac{d \tan \alpha}{dx} \quad (21b)$$

The total torque now becomes

$$T = T_p + T_v = \left(51.9 \tan \alpha p_a + 5.48 v^2 \frac{d \tan \alpha}{dx} \right) 10^{-4} \quad (22)$$

a: Uniform Twist Rifling, $y = px$

With no free run, $x_E = L = 24$ in†

From Equations 9b and 9c,

† See preceding footnote.

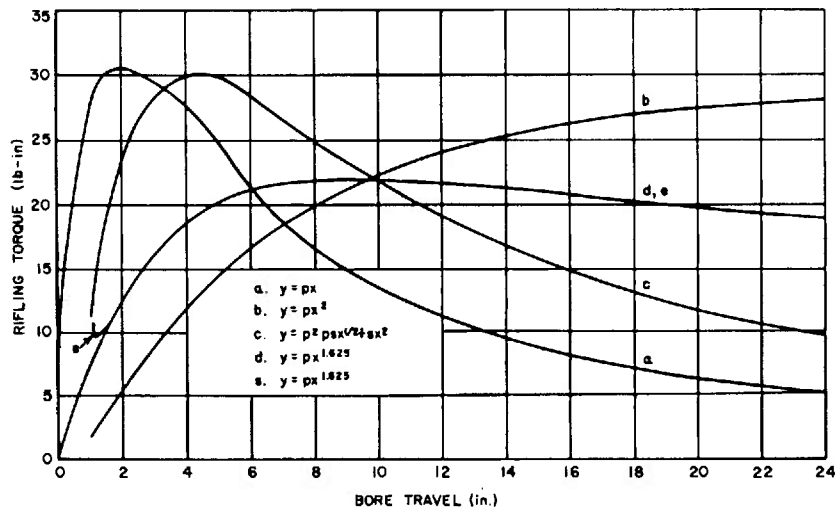


FIGURE 32. Rifling Torque Curves for Caliber .30 Barrel.

$$\tan \alpha = p = \tan 7^\circ = 0.123 \quad \text{and} \quad \frac{d \tan \alpha}{dx} = 0$$

Therefore, from Equation 22,

$$T = 51.9 \times 10^{-4} \times .123 p_v = .00064 p_v \text{ lb-in}$$

b: Quadratic Parabola (1.0 in. Free Run), $y = px^2$

With 1.0 in. free run,

$$x_E = L - 1.0 = 24 - 1.0 = 23 \text{ in}$$

From Equation 9b,

$$\tan \alpha = \frac{0.123}{23} x = 0.00535x$$

From Equation 9c,

$$\frac{d \tan \alpha}{dx} = \frac{0.123}{23} = 0.00535$$

Substituting these values into Equation 22

$$T = (27.8 p_v x + 2.93 v^2) 10^{-6} \text{ lb-in}$$

c: Tipped Parabola (1.0 in. Free Run),

$$y = p^2 - 2psx^{1/2} + s^2 x$$

$$x_E = L - 1.0 = 24 - 1.0 = 23 \text{ in}$$

$$a = 8 \times 2R = 2.4 \text{ in}$$

$$\tan \alpha = \frac{dy}{dx} = -\frac{ps}{x^{1/2}} + s^2$$

$$\frac{d \tan \alpha}{dx} = \frac{d^2 y}{dx^2} = \frac{ps}{2x^{3/2}}$$

When $x = a$, $\tan \alpha = 0$, $s = p/\sqrt{a}$, and $\tan \alpha = -p^2/\sqrt{ax} + p^2/a$.

When $E = a + x_E = 25.4 \text{ in.}$, $\tan \alpha = \tan \alpha_E = .123$.
Substituting these values and solving for p

$$p^2 = \frac{0.123}{\frac{1}{2.4} - \frac{1}{\sqrt{2.4 \times 25.4}}} = 0.426$$

$$p = 0.652; \quad s = \frac{0.652}{1.55} = 0.421$$

$$\tan \alpha = 0.177 - \frac{0.274}{x^{1/2}}$$

$$\frac{d \tan \alpha}{dx} = \frac{0.137}{x^{3/2}}$$

Equation 22 now becomes

$$T = [(4.92 - 7.62x^{-1/2})p_v + 0.75v^2x^{-3/2}]10^{-4} \text{ lb-in}$$

d: Exponential (No Free Run), $y = px^{1.625}$

with no free run, $x_E = L = 24 \text{ in.}$

From Equation 9b,

$$\tan \alpha = \frac{0.123}{24^{0.625}} x^{0.625} = 0.01686x^{0.625}$$

From Equation 9c

$$\frac{d \tan \alpha}{dx} = \frac{0.625 \times 0.123}{24^{0.625} x^{0.375}} = \frac{.01053}{x^{0.375}}$$

According to Equation 22

$$T = (85.8 p_v x^{0.625} + 5.78 v^2 x^{-0.375}) 10^{-6} \text{ lb-in}$$

The increment at 16 inch travel is selected to show the detailed calculation. Here

$$p_v = 12,900 \text{ psi (From curve No. 1, Fig. 16)}$$

$v = 2650$ ft/sec (From curve No. 2, Fig. 16)

$x = 16$ in

$$x^{0.625} = 5.66, \quad \tan \alpha = 0.01686 \times 5.66 = 0.0955$$

$$x^{0.375} = 2.83, \quad \frac{d \tan \alpha}{dx} = \frac{0.01053}{2.83} = 0.00372$$

According to Equation 22

$$T = (51.9 \times 0.0955 \times 12,900 + 5.48 \times 7.02$$

$$\times 10^6 \times 0.00372)10^{-4} = 6.4 + 14.3 = 20.7 \text{ lb-in}$$

e: Exponential (1.0 in. Free Run) $y = px^{1.625}$

With 1.0 in. free run,

$$x_E = L - 1.0 = 21 - 1.0 = 20 \text{ in.}$$

From Equation 9b,

$$\tan \alpha = \frac{0.123}{23^{0.625}} x^{0.625} = 0.0173 x^{0.625}$$

From Equation 9c,

$$\frac{d \tan \alpha}{dx} = \frac{0.625 \times 0.123}{23^{0.625} x^{0.375}} = 0.0108/x^{0.375}$$

For this rifling curve, Equation 22 becomes

$$T = (89.8 p_v x^{0.625} + 5.92 v^2 x^{-0.375})10^{-6} \text{ lb-in}$$

90. The torque curves in Figure 32 indicate that the exponential rifling, $y = px^{1.625}$, either with or without free run are superior to the others inasmuch as their torques are practically constant after reaching a maximum. After free run, the exponential curve (curve d) has an instantaneous infinite torque which is of little consequence since it reduces to 12 lb-in. in less than 5 microseconds. It soon reaches the torque exhibited by its counterpart; the exponential curve with no free run. The two torque curves then continue along the remainder of the bore travel within 3 percent of each other; so close to each other that there would be some difficulty in distinguishing them as being separate.

H. DETERMINATION OF THICKNESS OF TUBE WALLS

1. Design Pressures

91. The fundamental data for the design of the gun tube and its breech closure are given by the pressure-travel curve of the propellant gases. This curve is the plotted results of interior ballistic calculations, and its preparation is usually one of the concluding steps in a feasibility study for the weapon system. Methods followed by the interior ballisticians are available in other sources.*

The lower curve in Figure 41 is a typical pressure-

travel curve. The pressure during the first short portion of projectile travel rises very sharply, reflecting extremely rapid burning of the propellant immediately after ignition. The engraving of the rotating band and the inertia of the projectile create enough resistance to retard projectile travel thereby maintaining the relatively small volume conducive to rapid burning of the propelling charge which is normally complete shortly after peak pressure is attained. Once past the point of peak pressure, the continued rapid increase in volume back of the projectile as it travels in the bore causes a rapid diminution of pressure.

92. In order that gun tubes be designed in accordance with the developed pressure-travel curve and that a measure of uniformity be adopted, agreement is necessary among all tube designers on how the design data should be employed and on the terms by which these data are identified. Many of these data involve design pressures. The various steps in arriving at the pressures employed for the purpose of analyzing gun tubes of slow fire weapons and the definitions of these pressures which appear in the Gun Pressure Code† are:

Computed Maximum Pressure (CMP) is the maximum pressure computed from interior ballistics equations, developed in the gun to achieve rated muzzle velocity during operation at 70°F.

Rated Maximum Pressure (RMP) is the maximum pressure which should not be exceeded by the average of maximum pressure achieved by firing a group of the specified projectiles at the specified muzzle velocity and at 70°F. RMP is obtained by increasing the CMP by 2400 psi. It is used as one of the criteria for acceptance of the propellant.

Permissible Mean Maximum Pressure (PMMP) is the pressure which should not be exceeded by the average of the maximum pressures developed in a series of rounds fired under any service condition.

Permissible Individual Maximum Pressure (PIMP) is the pressure which should not be exceeded by the maximum pressure of any individual round under any service condition. PIMP is the proof pressure for a weapon and is the basis for its design. It is obtained by multiplying the RMP by 1.15.

Information is now available to obtain the gun tube pressure design curve. With the PIMP established as the new maximum chamber pressure and with the weight of propellant charge unchanged, the portion of the curve beyond the previous point of

* References 14, 15, 16.

† Reference 17.

maximum pressure is recalculated. Note that the *PIMP* is the effective pressure from the point of maximum pressure back to the breech. Artillery tube designers currently compute the values for *PIMP* curve directly without first resorting to the computed pressure-travel curve.

93. Basically the design approach of recoilless weapons is similar to that for artillery tubes, but refinements based on statistical treatment of results of actual firing data are then introduced. These refinements are necessary due to the demand for minimum weight while still retaining safety in firing. Therefore, following the preliminary weapon design, a test gun is produced, having the desired interior contour, but with wall thicknesses substantially increased over those calculated as being necessary. With this gun a propelling charge is established to give the desired muzzle velocity with gun aid charge at 70°F. A sufficient number of rounds are fired to give adequate statistical data for establishing the Normal Operating Pressure (*NOP*) which is the average of pressures measured in a test barrel firing an established round to produce the rated muzzle velocity with the temperature at 70°F. The *NOP* then replaces the *CMP* for final prototype weapon design and the gun tube pressure design curve is revised accordingly.

Permissible Individual Maximum Pressure (*PIMP*) is determined more exactly than for artillery tubes. With the firing data from the test weapon, and with the *NOP* established, a new design pressure curve is plotted. The methods for computing *NOP* and *PIMP* appear later with the detailed discussion on design procedures for the respective tubes.

94. For small arms tube design, pressures for computing wall thickness are obtained from pressure-travel curves already established by firing tests or computed by interior ballisticians. As with recoilless and artillery tubes, the maximum design pressure extends back to the breech. Chamber pressures corresponding to the position of the projectile are used rather than the actual pressure at the base of the projectile. The pressure at any point in the bore by being somewhat lower than in the chamber introduces a small factor of safety for stress computation.

2. Strength Requirements

95. Having determined the pressures which will act along the various sections of the gun tube the

required wall thicknesses can now be determined for entire tube length. For this purpose, an allowable stress is assigned, above which no part shall be stressed. This figure must not be greater than the elastic limit of the material at the temperature existing in the material. An exception involving small arms is discussed later (Section 10a). The wall thickness so determined will be minimum and may be increased for handling or machining reasons. The allowable stress assigned to a particular tube depends on the nature of its service. For relatively slow fire artillery weapons it is the elastic limit at 70°F, which is defined as being 10,000 psi less than the yield point. For recoilless tubes, it is necessary to consider the temperature attained in the tube material and design the tube on the basis of the yield point at that temperature. Figures 56 and 58 give properties of steels used in gun tubes at all temperatures of interest. As discussed later in Section 10a, small arms tubes have been assigned an allowable stress of 75,000 psi for approved steels.

96. As a convenience in design, the term Elastic Strength Pressure (*ESP*) has been established. It is defined as the pressure which produces an equivalent stress in the section wall equal to the allowable stress of the gun tube material at 70°F. In a gun tube of changing cross section there is an *ESP* corresponding to each type of section. For recoilless gun tube design an additional term is introduced, called *ESP_{hot}*, the elastic strength pressure of a hot tube. Formerly its value of 0.80 *ESP* was used to compensate for the degradation of material strength at elevated temperatures. Now it is the gas pressure at a point in the tube which produces an equivalent stress at that point equal to the yield point of the material at the permissible maximum tube temperature.

With more experience and additional design data, a more exact approach is available for the design of prototype recoilless gun tubes. Two conditions make this possible. The first is an *ESP_{hot}* computed from the *PIMP* that is based on the anticipated chamber pressure for firing at 125°F, the upper limit of the ambient temperature range for recoilless gun operation. The second is the known degraded yield strength of the tube material at elevated temperature, Y_A . The allowable maximum tube temperature is usually made to correspond to a given rate of fire or the allowable maximum temperature is specified and the rate of fire adjusted to it. The tube is designed in accordance with the reduced strength of the material at these elevated temperatures.

Typical examples of the effect of temperature on strength of recoilless tube material are shown in Figures 57 and 58.

In this procedure, ESP_{hot} for design is determined on the basis of the pressure generated by the firing of a hot (+125°F) round in a gun that is no hotter. A better estimate may be made of the design through the use of data (if available) relating to the effects of inserting a hot round into a hotter gun whose tube temperature is at or near the permissible maximum. The gun could then be designed for the conditions of equilibrium temperature of gun and round. These conditions are entirely system dependent and critically in the past, tests have not been conducted to obtain such data.

97. For any given gun, the inside diameter is the bore diameter and therefore is a constant except in the chamber regions. For rifled tubes, the inside diameter is the groove diameter, also a constant. It is the bore diameter increased by double the depth of groove. Since bore and inside diameter of chamber are fixed, outside diameters and material are the two general variables to be determined. The outside diameter and therefore wall thickness are based on the strength of the tube material. The pressure factor which is the ratio of design pressure to allowable stress has a practical upper limit for single simple tube construction. Equation 55c fixes this limit at 0.5, i.e., the maximum design pressure must not be greater than half the allowable stress of the tube material. When this limit is exceeded, the tube designer must resort to one of two alternatives available. He may use multilayer construction, i.e., having one or more jackets shrunk over the tube, or he may use autofrettage, the prestressing technique practiced in gun tube manufacture. These two design concepts, in addition to the simple tube construction, are later discussed in detail.

3. Equivalent Stress

98. Gun tubes are subjected to the three principal stresses which are produced by applied pressure, shrink fit, and a temperature gradient through the tube wall. Depending on the design technique, pressure stresses may be used alone or they may be combined with either or both thermal and shrinkage stresses. The three principal stresses are

- σ_t = tangential stress
- σ_r = radial stress
- σ_a = axial stress

These stresses are then inserted in the von Mises-Hencky equation following the "Strain Energy Theory of Failure" to find the equivalent stress, σ_e .

$$2\sigma_e^2 = (\sigma_t - \sigma_r)^2 + (\sigma_t - \sigma_a)^2 + (\sigma_r - \sigma_a)^2 \quad (23)$$

The stressed material remains in the elastic range so long as σ_e does not exceed the yield strength in tension.

For an open end cylinder, σ_a becomes zero and Equation 23 reduces to

$$\sigma_e^2 = \sigma_t^2 - \sigma_t\sigma_r + \sigma_r^2 \quad (24)$$

4. Pressure Stresses

99. The stresses induced by the propellant gas pressures are considered for all types of guns but application techniques differ for the different types. The design pressures are adjusted to fit the individual techniques although the stress calculations are identical. According to Lamé, the tangential stress at any diameter due to the design pressure, p , is

$$\sigma_{tp} = \frac{pD_i^2(D_o^2 + D^2)}{D^2(D_o^2 - D_i^2)} \quad (25)$$

where

- D_i = inside diameter
- D_o = outside diameter
- D = diameter at any point (varying from D_i to D_o)

For stress computations, the rifling groove diameter is generally considered to be the inside diameter. The maximum tangential stress occurs at the inner wall

$$\sigma_{tp} = p \frac{W^2 + 1}{W^2 - 1} \quad (26)$$

where

$$W = \frac{D_o}{D_i} = \text{the wall ratio}$$

The general radial stress is

$$\sigma_{rp} = -p \frac{D_i^2(D_o^2 - D^2)}{D^2(D_o^2 - D_i^2)} \quad (27a)$$

The maximum radial stress occurs on the inner wall

$$\sigma_{rp} = -p \quad (27b)$$

Since the tube is not a closed cylinder, the only axial stresses related to pressure are those introduced by the recoil acceleration and the frictional forces induced by the projectile. As later shown in paragraph 107, the axial stress reduces the effective stress, thereby introducing a measure of conserva-

tive design when this component of the stress is omitted from the analysis.

5. Rifling Torque Stresses

100. Rifling torque induces torsional stresses in the tube of

$$\tau = \frac{Tc}{J} \quad (28)$$

where

c = distance from the center to the stress location

J = polar moment of inertia of tube cross section

T = rifling torque

Torsional stresses of this nature are usually low and seldom enter into the stress analysis of the tube.

6. Shrinkage Stresses

101. The jacketed or built-up tube is constructed of two or more concentric cylinders assembled by shrink fit. The shrink fit partly compensates for the nonuniformity of the stresses later induced by the propellant gases. This type construction permits use of thinner walls than a nonprestressed monobloc. A routine procedure based on the maximum shear theory of failure has been developed to determine the wall thickness of tubes with one liner and one jacket provided that similar materials comprise both. This procedure provides a close approximation of the final wall ratio which eventually is determined by iterative calculations.

a. Tube With One Jacket

The known quantities are:

p = design pressure

D_i = ID of liner

σ_u = working stress, may be the elastic limit

The quantities to be determined are:

D_o = OD of jacket

D_1 = OD of liner, ID of jacket

p_s = pressure at D_1 , induced by shrink fit

δ = total shrink interference between liner and jacket

The wall ratios of tube and liner are derived by equating the stresses at each inner surface and solving for the wall ratio of the built-up tube and expressing this ratio in terms of allowable stress and design pressure. Thus

$$W = \frac{D_o}{D_i} = \frac{\sigma_u}{\sigma_w - p}^* \quad (29a)$$

* Based on the solution to Problem 202 found on page 328 of Reference 18.

The liner wall ratio is

$$W_L = \frac{D_1}{D_i} = \sqrt{W}^\dagger \quad (29b)$$

The jacket wall ratio is

$$W_J = \frac{D_o}{D_1} = \frac{WD_i}{\sqrt{WD_i}} = \sqrt{W} \quad (29c)$$

The shrink fit pressure equation is derived by resorting to the Shear Theory of Failure which states that

$$\tau_w = \frac{1}{2}\sigma_w = \sigma_t - \sigma_r^\ddagger \quad (30a)$$

where

σ_r = radial stress

σ_t = tangential stress

σ_u = allowable tensile stress

τ_u = allowable shear stress

According to Lamé,

$$\sigma_t = p \frac{W^2 + 1}{W^2 - 1} - 2p_s \frac{W_L^2}{W_L^2 - 1} \quad (30b)$$

$$\sigma_r = -p \quad (30c)$$

where

p = internal pressure

p_s = shrink fit pressure

W = wall ratio of total wall

W_L = liner wall ratio (inside tube wall ratio)

Substitute the expressions for σ_t and σ_r in Equation 30a. Further, substitute \sqrt{W} for W_L (Equation 29b) and for W in terms of u , (Equation 29a), then solve for p_s .

$$p_s = \frac{p^2}{4\sigma_u - 2p} \quad (31)$$

102. The equations for stresses and deflections of gun tube walls are based on Lamé's equation for thick walled pressure vessels which can be found in most strength of materials texts. The total deflection due to shrink fit is found by adding those of jacket and liner. The diametral deflection of the liner

$$\delta_L = \frac{p_s D_1}{E_L} \left(\frac{W_L^2 + 1}{W_L^2 - 1} - \nu \right) \quad (32a)$$

where ν is Poisson's ratio. The deflection of the jacket

$$\delta_J = \frac{p_s D_1}{E_J} \left(\frac{W_J^2 + 1}{W_J^2 - 1} + \nu \right) \quad (32b)$$

† Based on Equations 414 and 415, page 325 of Reference 18.

‡ Based on Equation 362 and page 314 of Reference 18.

where

W_J = wall ratio of jacket.

If liner and jacket are of the same material, the total deflection becomes

$$\delta = \delta_L + \delta_J = \frac{p_s D_1}{E} \left(\frac{W_L^2 + 1}{W_L^2 - 1} + \frac{W_J^2 + 1}{W_J^2 - 1} \right) \quad (32c)$$

The tangential and radial stresses on the inner wall of the liner due to shrink fit are, respectively,

$$\sigma_{ts} = -p_s \frac{2W_L^2}{W_L^2 - 1} \quad (33a)$$

$$\sigma_{rs} = 0 \quad (33b)$$

The corresponding stresses on the outer surface of the liner are

$$\sigma_{ts1} = -p_s \frac{W_L^2 + 1}{W_L^2 - 1} \quad (34a)$$

$$\sigma_{rs1} = -p_s \quad (34b)$$

The tangential and radial stresses on the inner surface of the jacket are

$$\sigma_{ts2} = p_s \frac{W_J^2 + 1}{W_J^2 - 1} \quad (35a)$$

$$\sigma_{rs2} = -p_s \quad (35b)$$

At the outer surface of the jacket, the stresses are

$$\sigma_{ts3} = p_s \frac{2}{W_J^2 - 1} \quad (36a)$$

$$\sigma_{rs3} = 0 \quad (36b)$$

The stresses caused by the propellant gases are calculated as though the tube were monobloc. These stresses are then combined with those caused by shrink fit. If the resulting principal stresses remain undisturbed from other influences such as heat, the equivalent stress is computed from Equation 25. If the result deviates too far from σ_w , the wall thickness is modified to bring σ_e more in line and the above analysis is repeated to check the modified version.

b. Tube With Two Jackets

103. The known quantities are p , D_i , σ_w , identical to those for the tube with one jacket. The quantities to be determined are:

- D_o = OD of outer jacket
- D_2 = ID of outer jacket, OD of inner jacket
- D_1 = ID of inner jacket; OD of liner
- D_i = ID of liner

p_{s1} = pressure at D_1 , induced by shrink fit

p_{s2} = pressure at D_2 , induced by shrink fit

The wall ratio of the composite tube is based on the working stress and the design pressure.

$$W = \left[\frac{1}{1 - \frac{\sqrt{3p}}{n\sigma_w}} \right]^{n/2} \quad (37)$$

where

n = the number of layers, in this case $n = 3$.

Various values of Equation 37 are plotted in Figure 33. The complete jacketed tube is so constructed that the individual layers have equal wall ratios. If a constant, C , is assigned to the squares of these equal wall ratios, then

$$\left(\frac{D_o}{D_2} \right)^2 = \left(\frac{D_2}{D_1} \right)^2 = \left(\frac{D_1}{D_i} \right)^2 = C \quad (38a)$$

Then

$$\frac{D_o^2 \times D_2^2 \times D_1^2}{D_2^2 \times D_1^2 \times D_i^2} = \left(\frac{D_o}{D_i} \right)^2 = C^3 = W^2 \quad (38b)$$

and

$$C = W^{2/3} \quad (38c)$$

Therefore the individual wall ratios are:

$$W_{1i} = D_1/D_i = W^{1/3} \quad (39a)$$

$$W_{2i} = D_2/D_i = W^{2/3} \quad (39b)$$

$$W_{21} = D_2/D_1 = W^{1/3} \quad (39c)$$

$$W_{o1} = D_o/D_1 = W^{2/3} \quad (39d)$$

$$W_{o2} = D_o/D_2 = W^{1/3} \quad (39e)$$

The shrink fit pressure is found from Equation 31. Half of this pressure is developed at D_1 and half at D_2 so that

$$p_{s1} = p_{s2} = \frac{p_s}{2} \quad (40)$$

Distributed thusly, the shrink fit pressures require approximately the same overlap at D_1 and D_2 . The tangential and radial stresses on the inner surface of the liner due to shrink fit are, respectively,

$$\sigma_{ts} = -p_{s1} \frac{2W_{1i}^2}{W_{1i}^2 - 1} - p_{s2} \frac{2W_{2i}^2}{W_{2i}^2 - 1} \quad (41a)$$

$$\sigma_{rs} = 0 \quad (41b)$$

The corresponding stresses on the outer surface of the liner are

* Based on Equation 23 of Reference 19.

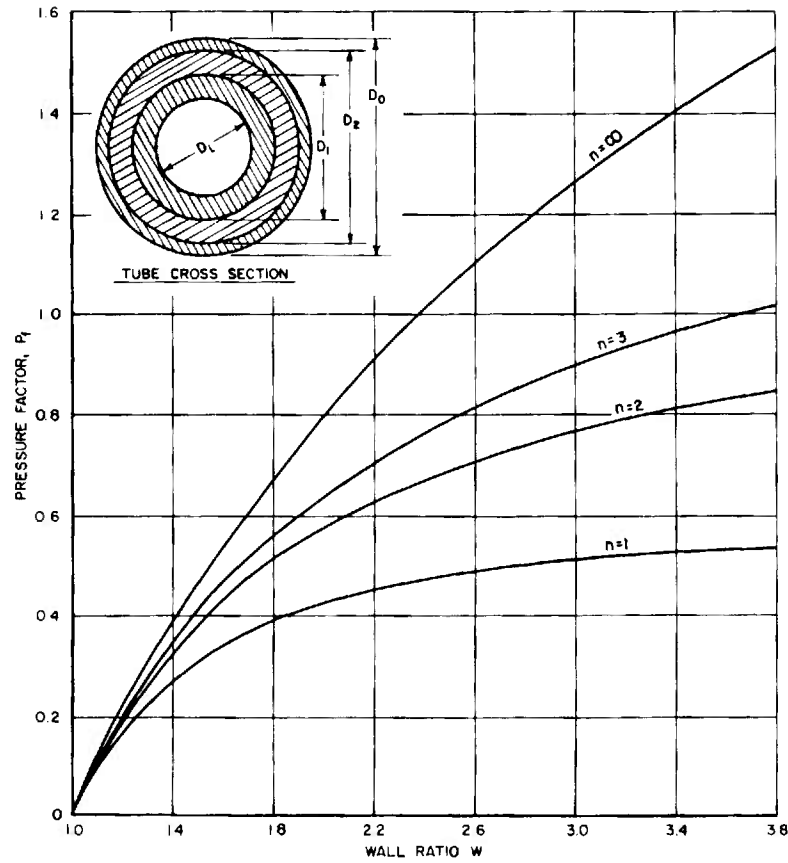


FIGURE 33. Wall Ratio-Pressure Factor Curves for Multilayer Tubes.

$$\sigma_{ts} = -p_{s1} \frac{W_{1i}^2 + 1}{W_{1i}^2 - 1} - p_{s2} W_{21}^2 \frac{W_{1i}^2 + 1}{W_{2i}^2 - 1} \quad (42a)$$

$$\sigma_{rs} = -p_{s1} - p_{s2} W_{21}^2 \frac{W_{1i}^2 - 1}{W_{2i}^2 - 1} \quad (42b)$$

The two stresses on the inner surface of the inner jacket

$$\sigma_{ts} = p_{s1} \frac{W_{2i}^2 + 1}{W_{2i}^2 - 1} - p_{s2} W_{22}^2 \frac{W_{1i}^2 + 1}{W_{2i}^2 - 1} \quad (43a)$$

$$\sigma_{rs} = -p_{s1} - p_{s2} W_{21}^2 \frac{W_{1i}^2 - 1}{W_{2i}^2 - 1} \quad (43b)$$

The two stresses on the outer surface of the inner jacket

$$\sigma_{ts} = p_{s1} \frac{2}{W_{2i}^2 - 1} - p_{s2} \frac{W_{2i}^2 + 1}{W_{2i}^2 - 1} \quad (44a)$$

$$\sigma_{rs} = -p_{s2} \quad (44b)$$

The tangential and radial stresses on the inner surface of the outer jacket

$$\sigma_{ts} = p_{s2} \frac{W_{e2}^2 + 1}{W_{e2}^2 - 1} \quad (45a)$$

$$\sigma_{rs} = -p_{s2} \quad (45b)$$

Finally, the two stresses on the outer surface of the tube are

$$\sigma_{ts} = p_{s2} \frac{2}{W_{e2}^2 - 1} \quad (46a)$$

$$\sigma_{rs} = 0 \quad (46b)$$

When the maximum equivalent stress of each tube component is not equal to the allowable stress, wall ratios and shrink fit pressures may be modified to achieve this objective. Equivalent stresses slightly less than the allowable are acceptable; those only slightly larger are not.

104. Figure 33* shows variations between wall ratios and pressure factors. The pressure factor is

* Computed from Equation 37.

defined as the design pressure divided by the allowable stress: $P_f = p/\sigma_w$. The allowable stress may be the yield strength, the elastic limit, or some other limit of practical significance. In artillery σ_w is the elastic limit. Figure 33 is a guide for determining which type construction is most practical. For example, a tube with a pressure factor of $P_f = 0.80$ will require the following wall ratios:

$$\begin{aligned} W &= 2.0 \text{ for } n = \infty \text{ i.e., cold worked} \\ W &= 2.54 \text{ for } n = 3 \\ W &= 3.25 \text{ for } n = 2 \\ n &= \text{number of layers} \end{aligned}$$

There is no solution for $n = 1$ since $W = \infty$ in Equation 37 for any value of $P_f > 0.577$. The choice would be the cold worked or the three-layered tube. At the lower end of the pressure factor range, the monobloc and two layered construction become the most practical.

A practical approach to determine the effects of shrink fit in small arms tube design (quasi two-piece lined barrel design, Fig. 4) is shown later in Paragraphs 133 and 168. The shrink fit pressure, as a function of the interface fit, is computed first and then applied to the inside cylinder as external pressure and to the outside cylinder as internal pressure.

7. Thermal Stresses

105. Thermal stresses are usually considered for those tubes subjected to high rates of fire such as small arms machine guns where large temperature gradients appear across the tube wall. The low rate-of-fire tubes have sufficient time between rounds to dissipate the heat so that stresses remain comparatively undisturbed by the relatively small changes in temperature. For those tubes which are affected by high temperatures, thermal stresses are combined with pressure stresses to determine the tube wall thickness. Figure 34 shows a typical thermal stress

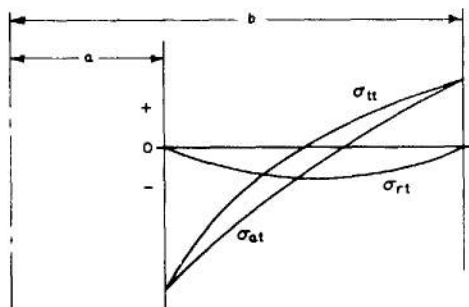


FIGURE 34. Thermal Stress Distribution Across Tube Wall.

distribution across a tube wall. The temperature at any point in the wall is expressed as

$$t = \frac{\Delta T}{\ln W} \ln \frac{b}{r} + t_o \quad (47)$$

where

$$\begin{aligned} a &= D_i/2, \text{ inner radius} \\ b &= D_o/2, \text{ outer radius} \\ r &= \text{radius at any point in tube wall} \\ t_i &= \text{temperature at inner wall surface} \\ t_o &= \text{temperature at outer wall surface} \\ \Delta T &= t_i - t_o, \text{ total temperature gradient!} \\ W &= \text{wall ratio} \end{aligned}$$

Whether the tube is of monobloc or multilayer coil construction, the temperature and thermal stresses are computed as though it were one piece. The tangential thermal stress at r is

$$\sigma_{tt} = \frac{E\alpha\Delta T}{2(1-\nu)\ln W} \cdot \left[1 - \ln \frac{b}{r} - \frac{1}{W^2-1} \left(1 + \frac{b^2}{r^2} \right) \ln W \right] \quad (48a)$$

where

$$\begin{aligned} \alpha &= \text{coefficient of linear expansion} \\ \nu &= \text{Poisson's ratio} \\ E &= \text{modulus of elasticity} \end{aligned}$$

When $r = a$

$$\sigma_{tt} = \frac{E\alpha\Delta T}{2(1-\nu)\ln W} \left(1 - \frac{2W^2}{W^2-1} \ln W \right) \quad (48b)$$

When $r = b$,

$$\sigma_{tt} = \frac{E\alpha\Delta T}{2(1-\nu)\ln W} \left(1 - \frac{1}{W^2-1} \ln W \right) \quad (48c)$$

The radial thermal stress at r is

$$\sigma_{rt} = \frac{E\alpha\Delta T}{2(1-\nu)\ln W} \cdot \left[\frac{1}{W^2-1} \left(\frac{b^2}{r^2} - 1 \right) \ln W - \ln \frac{b}{r} \right] \quad (49a)$$

When $r = a$ or when $r = b$,

$$\sigma_{rt} = 0 \quad (49b)$$

The axial thermal stress at r is

$$\sigma_{at} = \frac{E\alpha\Delta T}{2(1-\nu)\ln W} \cdot \left(1 - 2\ln\frac{b}{r} - \frac{2}{W^2-1}\ln W\right) \quad (50a)$$

When $r = a$,

$$\sigma_{at} = \frac{E\alpha\Delta T}{2(1-\nu)\ln W} \left(1 - \frac{2W^2}{W^2-1}\ln W\right) \quad (50b)$$

When $r = b$,

$$\sigma_{at} = \frac{E\alpha\Delta T}{2(1-\nu)\ln W} \left(1 - \frac{2}{W^2-1}\ln W\right) \quad (50c)$$

106. The methods for computing all the principal stresses are now available; pressure stresses, shrink fit stresses, and thermal stresses. These are combined before the equivalent stress is computed

$$\sigma_t = \sigma_{tp} + \sigma_{ts} + \sigma_{tt} \quad (51)$$

$$\sigma_r = \sigma_{rp} + \sigma_{rs} + \sigma_{rt} \quad (52)$$

$$\sigma_a = \sigma_{at} \quad (53)$$

These stresses, when substituted in Equation 23, will determine the equivalent stress.

8. Inertia of Recoil Stresses

107. Recoil activity in single and double recoil systems introduces axial and bending stresses in the gun tube. Recoilless tubes obviously are not involved. Bending stresses are caused by moments induced by the propellant gas force and its reaction, which is the inertial force of the recoiling parts, when reaction and force have different lines of action, and by the inertia force due to the secondary recoil of double recoil systems. In either case, the stresses are low and unlikely to prove bothersome when either isolated or combined with other stresses. Furthermore, secondary recoil does not begin until gas pressures have dissipated and pressure stresses have ceased to exist. These axial stresses caused by accelerating forces parallel to the bore have little effect on the equivalent stress. To illustrate, Table 9 shows the effect of including the axial stress. Assuming the tube to be a closed cylinder is the most conservative approach since this condition produces the highest axial stress. When σ_{e2} is the equivalent stress of the tangential and radial principal stresses and

TABLE 9. RATIOS OF EQUIVALENT STRESSES.

W	σ_t/p	σ_r/p	σ_a/p^*	σ_{e2}/p	σ_{e3}/p	R_e
3.0	1.25	-1.0	.125	1.948	1.953	1.003
2.5	1.38	-1.0	.190	2.06	2.07	1.004
2.0	1.67	-1.0	.333	2.31	2.34	1.013
1.75	1.97	-1.0	.485	2.57	2.62	1.020
1.5	2.60	-1.0	.800	3.11	3.22	1.035
1.25	4.57	-1.0	1.790	4.83	5.16	1.070

* $\sigma_a = p/(W^2 - 1)$, axial pressure stress of closed cylinder.

σ_{e3} is the equivalent stress of the tangential, radial, and axial principal stresses, their ratio $R_e = \sigma_{e2}/\sigma_{e3}$ indicates conservative design. Although including the axial stress attacks the problem more rigorously, the tabulated results show a maximum overdesign of only 7.0 percent; this for a wall ratio of 1.25. Larger wall ratios give a greater degree of agreement between the two methods, substantiating the accepted practice of using the shorter method of Equation 24 as sufficiently reliable for well designed tubes.

9. Stress Concentration

108. Stress concentration will appear any place in the tube where a discontinuity is present. Normally, generous radii overcome the disturbing influence of reentrant angles and reduce the high stresses in these regions to more acceptable figures. Large radii are not present at the juncture between bottom of groove and land but allowances for stress concentrations are made by using groove diameter instead of bore diameter for stress analysis and by other compensating features in design procedures such as low allowable stresses (see paragraph 50).

10. Special Applications for Tube Analyses

a. Small Arms

109. Small arms tube design, particularly for machine gun tubes, considers thermal and pressure stresses. The methods for determining each have been discussed. Pressures are read from the pressure-travel curve which has been prepared according to prevailing interior ballistic methods. This is chamber pressure and has been obtained by correlating the pressure-time and travel-time data. Although the pressure at the base of the projectile is less than the chamber pressure, the latter is used in design, the differential being accepted as a safety measure. Figures 35 to 40 are graphs from which an approxi-

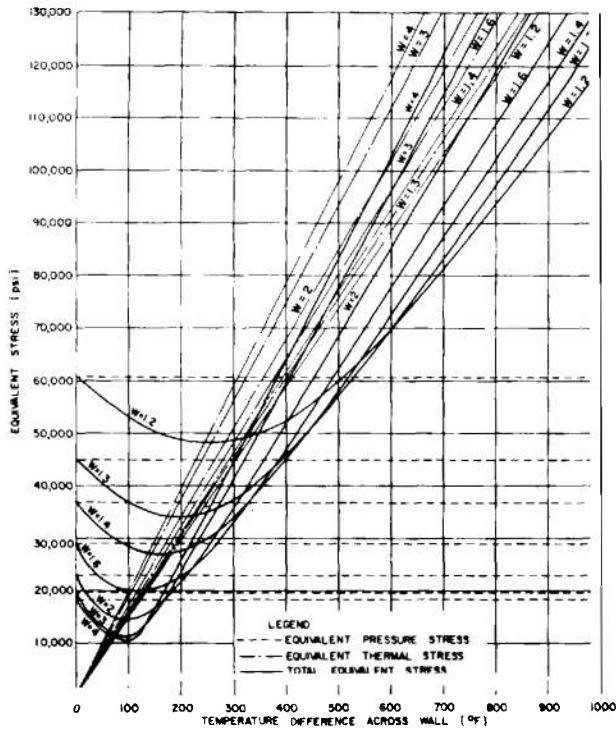


FIGURE 35. Equivalent Stress as a Function of Wall Thickness Ratio and Temperature Distance for an Internal Pressure of 10,000 psi.

mate wall ratio corresponding to a given equivalent stress can be selected for either a given pressure or a temperature gradient or for both. If tube temperatures are relatively low, the equivalent stress may be allowed to approach the yield strength at ambient temperature. If tube temperatures are high, the allowable equivalent stress must be reduced to the yield strength at these temperatures. However, when temperatures are extremely high, such as the 1400°F experienced on the outer surface of machine gun barrels, the static yield strength becomes less than 20,000 psi, far below the allowable equivalent stress. Despite the discrepancy between strength and stress, the gun still fires successfully. One theory advanced for this seeming paradox is that the short ballistic cycle places gun tube firing activity in the field of high rate of loading of short duration where the dynamic responses of materials vary considerably from the static responses. Explicit information in this field involving gun tube design is lacking, thereby placing the burden on previous experience which indicates that, when thermal stresses are included, an equivalent stress of approximately half the yield strength, e.g., 75,000 psi, can be tolerated in steels which have been heat treated to a yield strength of 150,000 psi. The ex-

pression for the allowable equivalent stress under these conditions becomes

$$\sigma_{ea} \approx 75,000 \text{ lb/in}^2 \quad (54)$$

110. To illustrate the use of the graphs, find the wall ratio having an equivalent stress of 70,000 lb/in² for an internal pressure of 40,000 lb/in² and a temperature differential of 600°F. In Figure 38, read up on the 600° line until it intersects the horizontal 70,000 lb/in² line. The wall ratio at this point, is either 1.8 or 4. From Equations 26b and 27b, investigate the thinner wall first

$$\sigma_{tp} = p \frac{W^2 + 1}{W^2 - 1} = 40,000 \frac{4^2 + 1}{4^2 - 1} = 75,700 \text{ lb/in}^2$$

$$\sigma_{rp} = -p = -40,000 \text{ lb/in}^2$$

$$\sigma_{ap} = 0$$

From Equations 48b, 49b, and 50b,

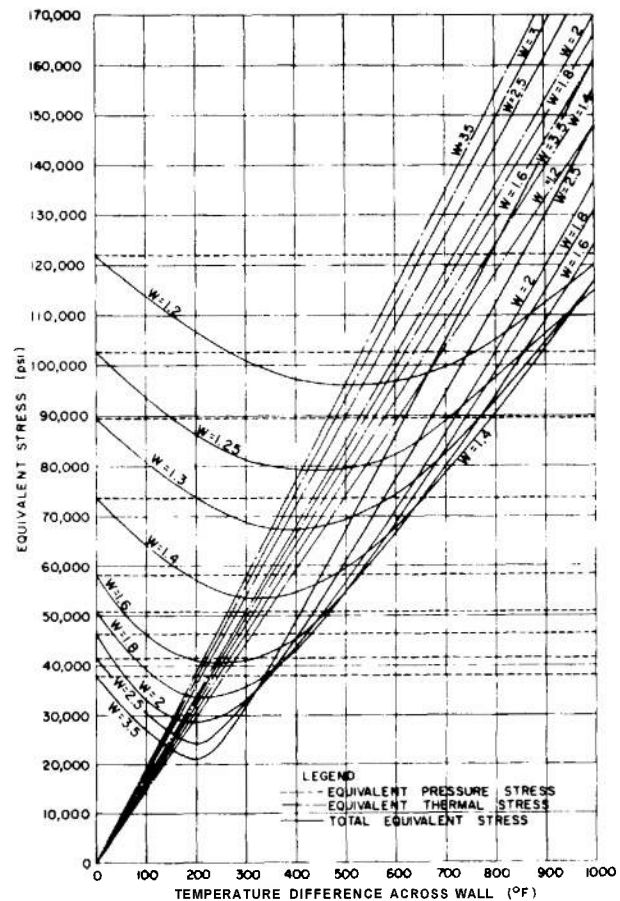


FIGURE 36. Equivalent Stress as a Function of Wall Thickness Ratio and Temperature Distance for an Internal Pressure of 20,000 psi.

$$\sigma_{tt} = \frac{E\alpha\Delta T}{2(1-\nu)\ln W} \left(1 - \frac{2W^2}{W^2-1} \ln W\right)$$

$$= \frac{30 \times 10^6 \times 6.5 \times 10^{-6} \times 600}{2 \times 0.7 \times 0.59}$$

$$\cdot \left(1 - \frac{6.48}{2.1} 0.59\right)$$

$$= -100,700 \text{ lb/in}^2$$

$$\sigma_{rt} = 0$$

$$\sigma_{nt} = \frac{E\alpha\Delta T}{2(1-\nu)\ln W} \left(1 - \frac{2W^2}{W^2-1}\right) \ln W$$

$$= -100,700 \text{ lb/in}^2$$

From Equations 51, 52 and 53 and since there are no shrinkage stresses

$$\sigma_t = \sigma_{tp} + \sigma_{tt} = -25,000 \text{ lb/in}^2$$

$$\sigma_r = \sigma_{rp} + \sigma_{rt} = -40,000 \text{ lb/in}^2$$

$$\sigma_a = \sigma_{ap} + \sigma_{nt} = -100,700 \text{ lb/in}^2$$

From Equation 23,

$$2\sigma_e^2 = (\sigma_t - \sigma_r)^2 + (\sigma_r - \sigma_a)^2 + (\sigma_a - \sigma_t)^2$$

$$\sigma_e = [\frac{1}{2}(2.25 + 36.85 + 57.3)10^8]^{1/2}$$

$$= \sqrt{48.2 \times 10^4} = 69,500 \text{ lb/in}^2$$

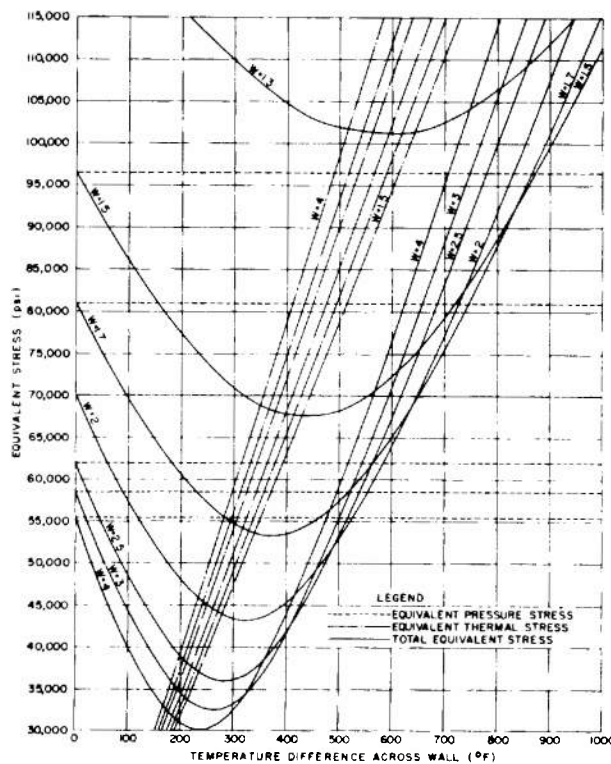


FIGURE 37. Equivalent Stress as a Function of Wall Thickness Ratio and Temperature Distance for an Internal Pressure of 30,000 psi.

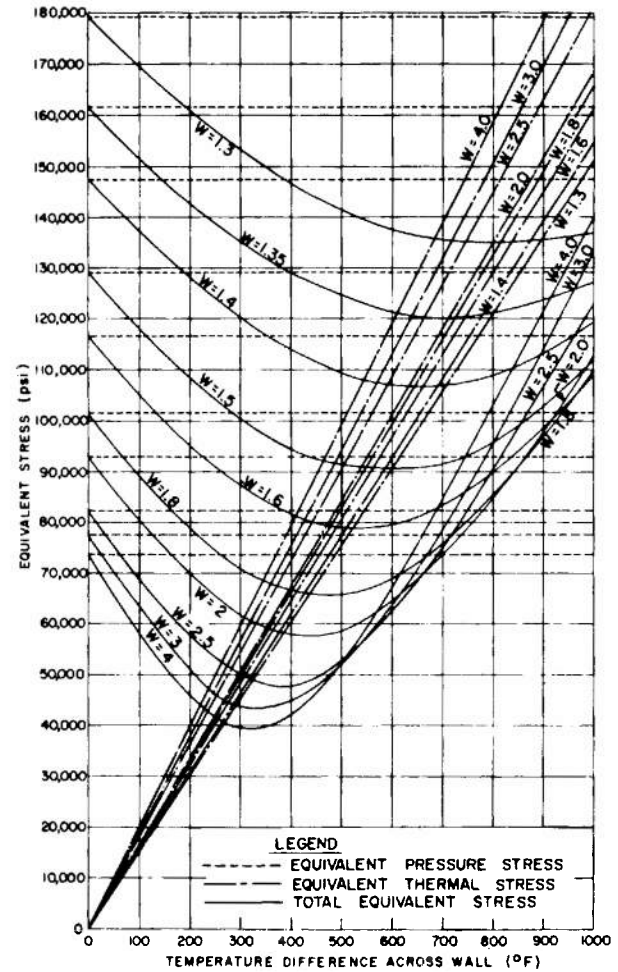


FIGURE 38. Equivalent Stress as a Function of Wall Thickness Ratio and Temperature Distance for an Internal Pressure of 40,000 psi.

Therefore, the indicated wall ratio of 1.8 is satisfactory.

111. When the given design data cannot be located conveniently on the graphs, the unknown data must be interpolated. For example, given:

$$p = 45,000 \text{ psi}$$

$$\Delta T = 450^\circ \text{F}$$

$$\sigma_{en} = 65,000 \text{ psi}$$

From Figure 39 ($p = 50,000 \text{ psi}$), $W = 2.33$

From Figure 38 ($p = 40,000 \text{ psi}$), $W = 1.81$
average $W = 2.07$

The computed equivalent stress for $W = 2.07$

$$\sigma_e = 62,800 \text{ lb/in}^2$$

indicating that a wall ratio slightly smaller than 2.07 may be acceptable.

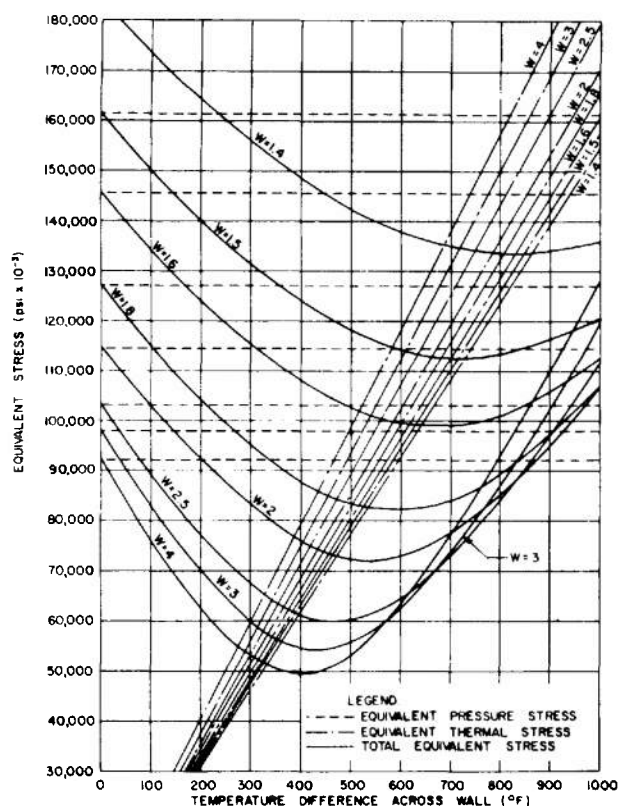


FIGURE 39. Equivalent Stress as a Function of Wall Thickness Ratio and Temperature Distance for an Internal Pressure of 50,000 psi.

b. Artillery

112. Artillery tubes are designed on pressure stresses alone. Thermal stresses not being considered, the equivalent stress is based on the yield strength modified by a small factor of safety. The wall thicknesses along the tube length are governed by a computed design pressure-travel curve. The maximum pressure determines the tube wall thickness from the breech to the point of maximum pressure on the pressure-travel curve. The wall thicknesses of the remaining length of the tube are determined from the maximum value of the computed design pressures, p , corresponding to the various positions. The design pressure-travel curve is a composite of two pressure-travel curves of different shapes. It represents the values of either curve, whichever is maximum at the particular location. Any pressure on the curve is a true pressure which does not incorporate a factor of safety. The maximum pressure coincides with the PIMP at the breech. Computation details of the curve are not considered relevant here. At this stage, a material advantage is achieved if the tube designer knows interior ballistics so that he may compute

the design pressures, become familiar with the complete problem, and thus be in a position to direct logical revisions if necessary.

The strength of the tube is based on the elastic limit of the material which is defined as 10,000 lb/in² less than the yield strength in tension. It is impractical to machine a tube to conform accurately to a given pressure distribution, hence, portions of it, whether straight or tapered, will be stronger than necessary. The pressure necessary to stress any longitudinal increment of the tube to the elastic limit is called the elastic strength pressure. The ratio of elastic strength pressure to actual design pressure is the factor of safety for that increment. If p is the design pressure and ESP is the elastic strength pressure, then ESP must be greater than p at every section. To ensure safe firing, the ratio of ESP/p has been assigned : minimum value of 1.05.*

c. Recoilless Guns

i. Gun Tube

113. Recoilless gun tube dimensions are based on static loading and determined by the same general

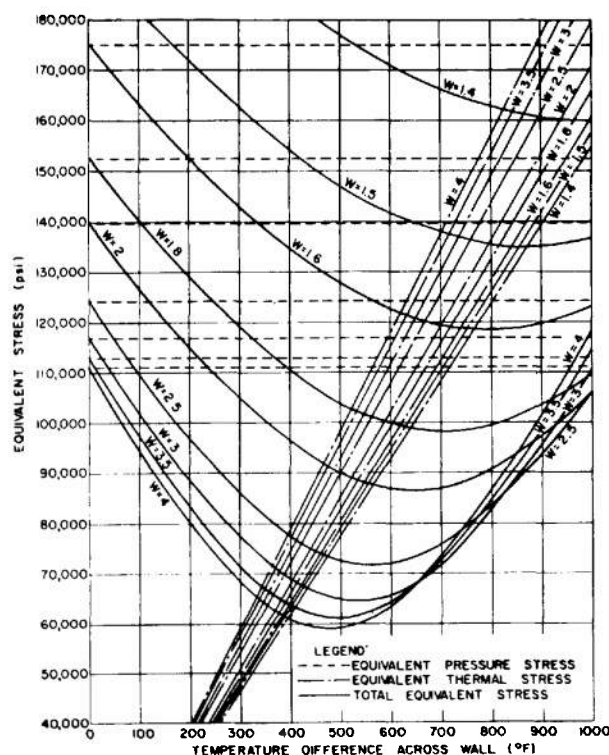


FIGURE 40. Equivalent Stress as a Function of Wall Thickness Ratio and Temperature Distance for an Internal Pressure of 60,000 psi.

* This practice has been established by Watervliet Arsenal.

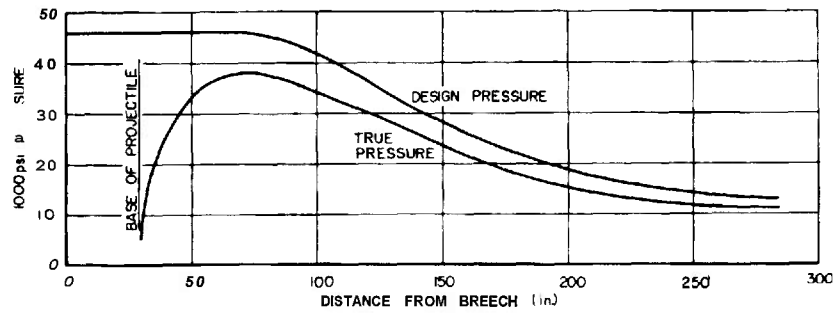


FIGURE 41. Design Pressure-Travel Curve.

procedures involved in the design of other tube types." In regions free from discontinuities, the gun tube is considered to be subjected to two principal stresses induced by the propellant gas pressure, the direct radial compressive stress of Equation 26 and the tangential or hoop tension stress of Equation 27b. For practical purposes, the longitudinal stress is assumed to be zero since the frictional forces of the projectile on the tube are small enough to be negligible.

The maximum distortion-energy theory of failure has proved to be a realistic design criterion primarily because of the ductile materials used for gun tubes. This theory defines the equivalent stresses, σ_e , in materials subjected to combined

loadings. Equation 23 defines the equivalent stress in terms of triaxial principal stresses, whereas Equation 24 defines it in terms of biaxial principal stresses. Failure is indicated by plastic flow which begins when the equivalent stress equals the yield strength of the material. By applying this theory of failure to the gun tube and substituting the expressions of Equations 26 and 27b for the tangential and radial stresses, and the yield strength, Y , for σ_e , Equation 24 becomes

$$Y^2 = p^2 + p^2 \left(\frac{W^2 + 1}{W^2 - 1} \right) + p^2 \left(\frac{W^2 + 1}{W^2 - 1} \right)^2 \quad (55a)$$

Solving for p/Y

$$\frac{p}{Y} = \frac{W^2 - 1}{\sqrt{3W^2 + 1}} \quad (55b)$$

* Reference 20.

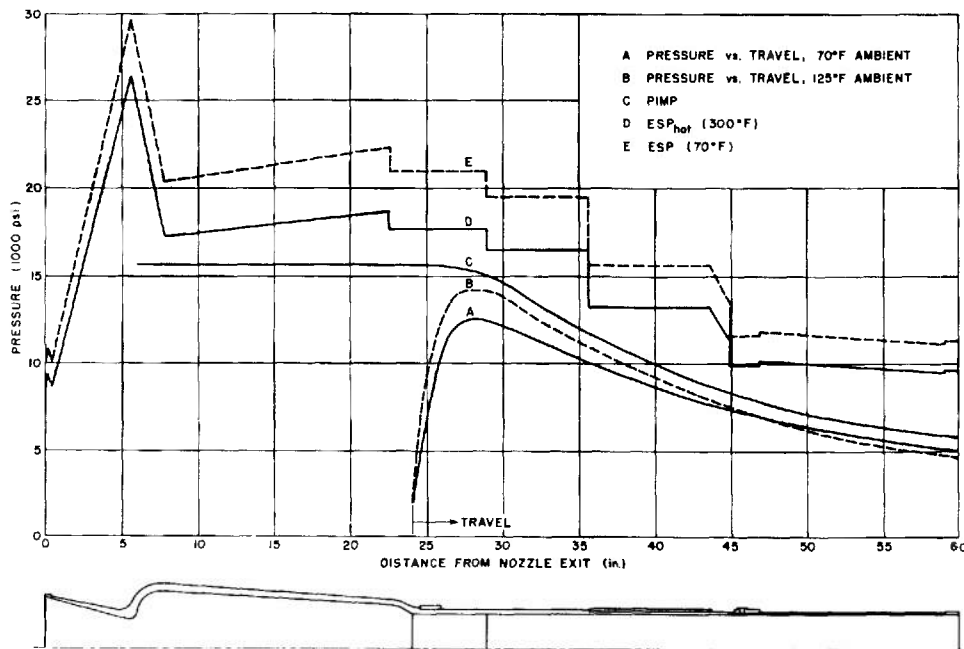


FIGURE 48. Typical Recoilless Gun Pressure Design Curves.
(For hypothetical gun only)

TABLE 10. WALL RATIO-PRESSURE RATIO CHART FOR MONOBLOC GUN TUBES.

$\frac{P}{Y}$	W	$\frac{P}{Y}$	W	$\frac{P}{Y}$	W	$\frac{P}{T}$	W
0.010	1.0101	0.070	1.0755	0.130	1.1513	0.190	1.2417
0.011	1.0111	0.071	1.0767	0.131	1.1327	0.191	1.2434
0.012	1.0122	0.072	1.0779	0.132	1.1541	0.192	1.2451
0.013	1.0132	0.073	1.0790	0.133	1.1555	0.193	1.2468
0.014	1.0142	0.074	1.0802	0.134	1.1569	0.194	1.2485
0.015	1.0153	0.075	1.0814	0.135	1.1583	0.195	1.2502
0.016	1.0163	0.076	1.0826	0.136	1.1596	0.196	1.2518
0.017	1.0173	0.077	1.0838	0.137	1.1610	0.197	1.2535
0.018	1.0183	0.078	1.0849	0.138	1.1624	0.198	1.2552
0.019	1.0194	0.079	1.0861	0.139	1.1638	0.199	1.2569
0.020	1.0204	0.080	1.0873	0.140	1.1652	0.200	1.2586
0.021	1.0215	0.081	1.0885	0.141	1.1666	0.210	1.2761
0.022	1.0225	0.082	1.0897	0.142	1.1680	0.220	1.2942
0.023	1.0236	0.083	1.0910	0.143	1.1695	0.230	1.3131
0.024	1.0246	0.084	1.0922	0.144	1.1710	0.240	1.3328
0.025	1.0257	0.085	1.0934	0.145	1.1724	0.250	1.3533
0.026	1.0267	0.086	1.0946	0.146	1.1738	0.260	1.3717
0.027	1.0278	0.087	1.0958	0.147	1.1753	0.270	1.3971
0.028	1.0288	0.088	1.0971	0.148	1.1767	0.280	1.4205
0.029	1.0299	0.089	1.0983	0.149	1.1782	0.290	1.4450
0.030	1.0309	0.090	1.0995	0.150	1.1796	0.300	1.4709
0.031	1.0320	0.091	1.1007	0.151	1.1811	0.310	1.4980
0.032	1.0331	0.092	1.1020	0.152	1.1825	0.320	1.5267
0.033	1.0342	0.093	1.1032	0.153	1.1840	0.330	1.5571
0.034	1.0352	0.094	1.1045	0.154	1.1855	0.340	1.5892
0.035	1.0363	0.095	1.1056	0.155	1.1870	0.350	1.6234
0.036	1.0374	0.096	1.1069	0.156	1.1884	0.360	1.6599
0.037	1.0385	0.097	1.1082	0.157	1.1899	0.370	1.6989
0.038	1.0395	0.098	1.1094	0.158	1.1914	0.380	1.7408
0.039	1.0406	0.099	1.1107	0.159	1.1928	0.390	1.7859
0.040	1.0417	0.100	1.1119	0.160	1.1943	0.400	1.8347
0.041	1.0428	0.101	1.1132	0.161	1.1958	0.410	1.8878
0.042	1.0439	0.102	1.1145	0.162	1.1974	0.420	1.9457
0.043	1.0450	0.103	1.1157	0.163	1.1989	0.430	2.0094
0.044	1.0461	0.104	1.1170	0.164	1.2004	0.440	2.0800
0.045	1.0472	0.105	1.1183	0.165	1.2020	0.450	2.1585
0.046	1.0482	0.106	1.1196	0.166	1.2035	0.460	2.2469
0.047	1.0493	0.107	1.1209	0.167	1.2050	0.470	2.3472
0.048	1.0504	0.108	1.1221	0.168	1.2065	0.480	2.4628
0.049	1.0515	0.109	1.1234	0.169	1.2081	0.490	2.5976
0.050	1.0526	0.110	1.1247	0.170	1.2096	0.500	2.7578
0.051	1.0537	0.111	1.1260	0.171	1.2112	0.510	2.9524
0.052	1.0549	0.112	1.1273	0.172	1.2127	0.520	3.1960
0.053	1.0560	0.113	1.1286	0.173	1.2143	0.530	3.5134
0.054	1.0571	0.114	1.1299	0.174	1.2159	0.540	3.9512
0.055	1.0583	0.115	1.1313	0.175	1.2174	0.550	4.6116
0.056	1.0594	0.116	1.1326	0.176	1.2190	0.560	5.7824
0.057	1.0605	0.117	1.1339	0.177	1.2206	0.570	8.8720
0.058	1.0616	0.118	1.1352	0.178	1.2222	0.580	∞
0.059	1.0628	0.119	1.1365	0.179	1.2237		
0.060	1.0639	0.120	1.1378	0.180	1.2253		
0.061	1.0651	0.121	1.1392	0.181	1.2269		
0.062	1.0662	0.122	1.1405	0.182	1.2286		
0.063	1.0674	0.123	1.1419	0.183	1.2302		
0.064	1.0685	0.124	1.1432	0.184	1.2319		
0.065	1.0697	0.125	1.1446	0.185	1.2335		
0.066	1.0709	0.126	1.1459	0.186	1.2351		
0.067	1.0720	0.127	1.1473	0.187	1.2368		
0.068	1.0732	0.128	1.1486	0.188	1.2384		
0.069	1.0743	0.129	1.1500	0.189	1.2400		

or, solving for W

$$W = \left[\frac{1 + 2 \frac{p}{Y} \sqrt{1 - 3 \left(\frac{p}{Y} \right)^2}}{1 - 3 \left(\frac{p}{Y} \right)^2} \right]^{1/2} \quad (55c)$$

where

W = wall ratio

p = internal design pressure, psi

Values of W for various ratios of p/Y are listed in Table 10.

For a specified bore diameter or caliber, the wall ratio determines the required outside diameter, thereby establishing a minimum wall thickness. This minimum thickness must be maintained despite any variation that may result from manufacturing tolerances and eccentricities. Thus, the wall thickness obtained by subtracting the maximum inside radius to the bottom of the rifling grooves from the minimum outside radius must be further modified by considering the permissible eccentricity between the bore and outer tube surface. This eccentricity is defined by the manufacturing requirement which states that "The wall thickness at any point shall not be less than 90 percent of the wall thickness at a point diametrically opposite." The wall ratio obtained from Table 10 must be adjusted to an apparent wall ratio

$$W_a = \frac{1.9}{1.8} W - \frac{1}{1.8} \quad (55d)$$

or

$$W_a = 1.0555 W - 0.0555 \quad (55e)$$

The minimum outside diameter is then calculated from the apparent wall ratio.

114. *CMP* serves as the basis for preliminary design. Maximum pressures, after becoming available from firing tests, establish the *NOP*. Unless, by sonic coincidence, the two are equal, the more realistic *NOP* supersedes the *CMP* to become the criterion for filial prototype tube design.

To calculate *PIMP*, determine the standard deviation of *NOP* from the statistical relationship

$$\sigma_{NOP} = \pm \sqrt{\frac{\sum (P - \bar{P})^2}{N - 1}} \quad (56a)$$

where

N = number of rounds

P = recorded pressure of each of N rounds

\bar{P} = *NOP*

The value of $\pm 3\sigma_{NOP}$ establishes a 99.8 percent confidence level for the pressure variation, but since the upper level promotes greater safety in the design, only the plus variation is used and the *PIMP* becomes

$$PIMP = 1.05 NOP + \frac{\Delta p}{\Delta T} (T_h - 70^\circ) + 3\sigma_{NOP} \quad (56b)$$

where

1.05 = factor allowing for 5 percent tolerance on lot to lot propellant variations

$\Delta p / \Delta T$ = pressure change per unit of propellant temperature change, psi/°F, determined from empirical data from test gun firings. In the absence of such data, 20 psi/°F is a recommended approximation.

T_h = upper limit of atmospheric temperature for recoilless gun operation, °F (usually 125°F).

For filial tube design, by definition:

$$ESP_{hot} = S_f \times PIMP \quad (56c)$$

where

S_f = factor of safety.

A factor of safety found to be satisfactory in recoilless gun design is 1.15.

115. To find the wall ratio, either from Table 10 or to compute it from Equation 56b, the degraded yield strength is obtained from curves similar to those in Figure 57 and the expression ESP_{hot}/Y_h is substituted for p/Y . The apparent wall ratio is computed from Equation 55e. The minimum outside diameter becomes

$$D_o = D_i W_a \quad (56d)$$

where

D_i = inside diameter of tube (generally considered to be the rifling groove diameter plus the tolerance).

W_a = apparent wall ratio from Equation 56c.

If desired, the *ESP* of the gun (which is not used in design), i.e., the elastic strength pressure when the gun temperature is 70°F, may be obtained by determining the wall ratio using the expression ESP/Y in place of ESP_{hot}/Y_h . The *ESP* is generally higher than ESP_{hot} .

The wall thickness obtained in the above pro-

cedure does not make allowance for stress concentration at discontinuities such as in the region where barrel joins chamber, hence, it should be used only in regions unaffected by stress raisers.

Additional relationships include:

$$RMP = 1.05 NOP \quad (56e)$$

$$PMMP = RMP + \frac{\Delta p}{\Delta T} (T_h - 70^\circ F) \quad (56f)$$

Before experimental data become available for the final recoilless tube design, a preliminary design of the tube is made. The dimensions are determined by the same procedure as for the final design but based on theoretically computed or estimated design data rather than the more accurate, measured data used in the final design. Theoretical design data includes the *CMP* which replaces the *NOP* in Equation 56. The procedure follows that for filial design, and may be outlined as follows:

1. Obtain *CMP* from ballisticsian.
2. Calculate *PIMP* from Equation 56b which becomes

$$PIMP = 1.05 CMP + \frac{\Delta p}{\Delta T} (T_h - 70^\circ F) + 3\sigma_{CMP} \quad (56g)$$

The ratio $\Delta p/\Delta T$ is the same as in Equation 56b but at this early stage σ_{NOP} is not available from test firings and must therefore be estimated and assigned the value of σ_{CMP} . Past experience indicates that a σ_{CMP} equal to 3 percent of *CMP* is suitable for preliminary design.

3. Calculate *ESP_{hot}* using Equation 56c:

$$ESP_{hot} = 1.15 PIMP$$

4. Determine from temperature degradation data, or estimate the degraded yield strength of the material, Y_s .
5. Compute $ESP_{hot}/Y_h \approx p/Y$ of Table 10.
6. Obtain *W* from Table 10 corresponding to value from 5.
7. Convert to apparent wall ratio by Equation 55e.
8. Calculate minimum outside diameter from Equation 56d.

116. The test weapon from which firing data are established has a much thicker wall than either the preliminary or the final tube in order to provide a tube of unquestionable safety. The wall thickness is derived by arbitrarily increasing the design pressure, usually to $P \geq 2 CMP$. The resulting p/Y

value determines the wall ratio found in Table 10 and, subsequently, the outside diameter. No allowance is made for eccentricity as the overstrength of the wall more than compensates for manufacturing eccentricities. Furthermore, the outside surface is usually made cylindrical, since optimum weight is not a design criterion for test guns.

After sufficient experimental data become available, the design of the filial prototype tube can be established following the same procedure as outlined for the preliminary tube. However, results obtained from Equations 56a through 56d will be more accurate since estimated design data will be largely eliminated and actual values used instead.

Matching the pressure-travel curve with a corresponding stress curve produces a tube whose profile is also curved. A tube conforming precisely to this curve represents optimum design. However, this is impractical because of high machining costs and because of the necessity for thicker sections in the muzzle region to prevent mechanical damage. Present practice approximates the ideal by joining, with a straight taper, the required outer surface at the point of maximum pressure to the minimum surface at the muzzle. Propellant gas pressure at the muzzle of recoilless guns generally varies from approximately $\frac{1}{4}$ to $\frac{1}{2}$ of maximum chamber pressure. Therefore, for preliminary design, $\frac{1}{2} CMP$ replaces *NOP* in Equation 56b for determining the equivalent *PIMP* and eventually the minimum outside diameter at the muzzle. In some cases, simulated firings of the theoretical gun are performed on an analog computer to obtain a theoretical pressure-travel curve for preliminary design. Computer information so obtained has proved accurate to within 5 to 8 percent when compared with experimental data. Wall thickness at the muzzle is calculated on the basis of the pressure curve established by the *NOP*. Although the wall is strong enough to contain the pressure, it usually is not thick enough to provide the rigidity needed during machining and handling. Based on field handling experience, the wall thickness is increased to 0.15 inch for a distance of about 1.5 inches from the muzzle. A straight taper is provided from here to the location of the maximum wall thickness at the chamber end.

The axial stress, σ_a , in the chamber wall is appreciable. An analysis of the chamber wall shows that the wall can be made slightly thinner if the three principal stresses rather than the radial and tangential principal stresses are considered.* This

* Reference 21.

argument is substantiated in paragraph 107. However, the gain is slight and the possibility of discontinuities introducing stress concentrations prevails, and indicates that the slightly more conservative approach applied to the barrel wall also should be applied to the chamber wall.

117. Design data drawings are prepared for each prototype recoilless gun designed, a typical example of which is shown in Figure 42 for a hypothetical gun. Three pressure-travel curves are shown, the first for firing at 70°F air temperature, the second for firing at 125°F air temperature, and the third for the permissible individual maximum pressure (*PIMP*). Two capability curves are also shown. One indicates the pressure which will produce equivalent stresses of 170,000psi at 70°F (*ESP*), and the other indicates the pressure which will produce equivalent stresses of 140,000 psi at 300°F (*ESP_{hot}*). These two curves illustrate the strength capabilities of the tube at ambient and elevated temperatures.

ii. Gimbal Ring—Recoilless Tube

118. Recoilless tubes with shrunk on attachments such as gimbal rings are subjected to discontinuity stresses induced by the lamina. Figure 43 shows the laminated structure and the diagram of induced loads and deflections.

The analysis for the discontinuity stresses is based on a procedure developed for recoilless tubes when these tubes are considered as having thin walls.* The shrink fit pressure is one of the parameters and is assumed to be uniform over the entire cylindrical contact surface between ring and tube. It is determined by equating the radial interference to the sum of the radial deflections of ring and tube produced by the shrink fit pressure and then solving for that pressure, using the formula

$$p_s = \frac{Ar}{\frac{r_o^2}{E_t} + \frac{r_r^2}{E_r t_r}} \quad (57a)$$

Two other parameters include the general expressions

$$D = \frac{Et^3}{12(1-\nu^2)}, \quad \text{flexural rigidity} \quad (57b)$$

$$\lambda = \sqrt[4]{\frac{3(1-\nu^2)}{r^2 t^2}} \quad (57c)$$

The laminated structure is influenced by the individual properties of Region 2 and the ring. Their respective moduli of elasticity are modified to be

* Reference 22.

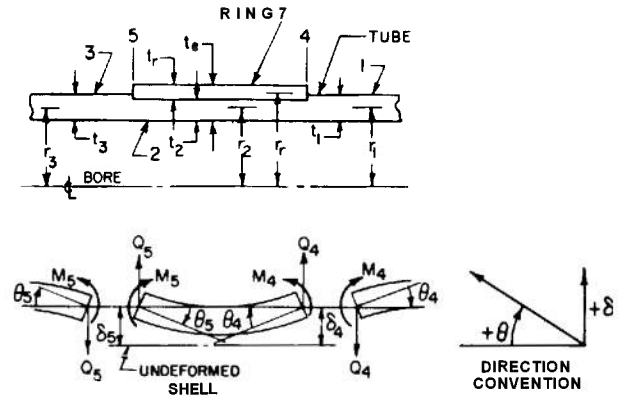


FIGURE 43. Gimbal Ring Loading.

Definitions of Symbols

E, E_r	= moduli of elasticity of tube and ring
\bar{E}_r	= equivalent modulus of elasticity of combined section
M_4, \bar{M}_r	= moment per unit circumference at Stations 4, 5
p	= internal pressure
p_s	= shrink fit pressure
Q_4, Q_5	= shear per unit circumference at Stations 4, 5
r_1, r_2, r_3	= mean radii Region 1, 2, 3 of tube
r_r	= mean radius of ring
Δr	= radial interference between rim and Region 2
t_1, t_2, t_3	= wall thickness of Region 1, 2, 3
t_c	= wall thickness of ring and Region 2 of tube combined
t_r	= wall thickness of ring
δ_4, δ_5	= radial deflections at Stations 4, 5
θ_4, θ_5	= angular deflections at Stations 4, 5
ν, ν_r	= Poisson's ratio for tube and ring

$$E = E/(1 - \nu^2) \quad (57d)$$

$$\bar{E}_r = E_r/(1 - \nu_r^2) \quad (57e)$$

Other properties are determined by treating the two members as an equivalent one-piece structure. Its mean radius

$$r = \frac{r_2 + r_r}{2} \quad (57f)$$

and the product

$$E_r t_r = E t_2 + E_r t_r \quad (57g)$$

are approximate but the error is small enough to be negligible. The flexural rigidity for the equivalent region is

$$D_c = \frac{\bar{E}^2 t_2^4 + \bar{E}_r^2 t_r^4 + \bar{E} \bar{E}_r (4 t_2^3 t_r + 6 t_2^2 t_r^2 + 4 t_2 t_r^3)}{12(\bar{E} t_2 + \bar{E}_r t_r)} \quad (57h)$$

The λ equivalent of the combined region is denoted by β and is defined by

$$\beta = \left(\frac{C}{4D_e} \right)^{1/4} \quad (57i)$$

where

$$C = \frac{(\bar{E}t_2 + \bar{E}_r t_r)^2 - (\nu \bar{E}t_2 + \nu_r \bar{E}_r t_r)^2}{r^2(\bar{E}t_2 + \bar{E}_r t_r)} \quad (57j)$$

Each region of the tube is isolated to determine the angular and radial deflection at the discontinuities. For Region 1 at Station 4

$$\delta_4 = \frac{pr_1^2}{Et_1} + \frac{\lambda_1 M_4 - Q_4}{2\lambda_1^3 D_1} \quad (57k)$$

$$\theta_4 = \frac{2\lambda_1 M_4 - Q_4}{2\lambda_1^2 D_1} \quad (57m)$$

Note that the shrink fit pressure is not applied to this region. For the Equivalent Section e, i.e., Region 2 and the ring combined, at Station 4 the shear and moment as represented in Figure 43 will increase the inside radius of the laminated structure but the shrink fit pressure will tend to decrease it by compressing the inside tube.

$$\delta_4 = \frac{pr_1^2}{E_r t_r} - \frac{pr_2^2}{Et_2} + \frac{\beta M_4 + Q_4}{2\beta^3 D_e} \quad (57n)$$

$$\theta_4 = -\frac{2\beta M_4 + Q_4}{2\beta^2 D_e} \quad (57p)$$

The two components of the equivalent section function as a unit under shear and bending particularly since an initial interference exists between them. At Station 5.

$$\delta_5 = \frac{pr_1^2}{E_r t_r} - \frac{pr_2^2}{Et_2} + \frac{\beta M_5 + Q_5}{2\beta^3 D_e} \quad (57q)$$

$$\theta_5 = \frac{2\beta M_5 + Q_5}{2\beta^2 D_e} \quad (57r)$$

For Region 3 at Station

$$\delta_5 = \frac{pr_3^2}{Et_3} + \frac{\lambda_3 M_5 - Q_5}{2\lambda_3^3 D_3} \quad (57s)$$

$$\theta_5 = -\frac{2\lambda_3 M_5 - Q_5}{2\lambda_3^2 D_3} \quad (57t)$$

119. The shear and moment values are obtained by equating the two expressions for deflections at each side of the discontinuity and solving for Q and M from the two pairs of simultaneous equations. Since general solutions are awkward, the substitution of numerical values will result in equations which are much easier to handle. After the values for shear,

moment, and the two deflections are found, the three components of stress may be computed. The first is the axial stress produced by the moment

$$\sigma_a = \frac{6M}{t^2} \quad (58a)$$

The second is the tangential stress which is made up of two parts. One part is produced by the moment and is given by

$$\sigma_{tm} = \nu \sigma_a \quad (58b)$$

and the other is produced by the radial deflection and is given by

$$\sigma_{td} = \frac{E_r \delta}{r} \quad (58c)$$

The third is the radial stress due to internal pressure

$$\sigma_r = -p \quad (58d)$$

The above stresses are positive when tensile and negative when compressive. Since the maximum equivalent stress may occur at the inner or the outer surface, it is necessary to substitute the set of values of stress at each of these points into Equation 23 to determine which is critical.

Similar stresses on the gimbal ring and the portion of the tube which it covers are determined by first finding the following parameters:

$$B = \frac{(\nu - \nu_r) \bar{E} \bar{E}_r t_2 t_r (t_2 + t_r)}{r(\bar{E}t_2 + \bar{E}_r t_r)} \quad (58e)$$

$$H = \frac{1}{2} \left(\frac{\bar{E}t_2^2 - \bar{E}_r t_r^2}{\bar{E}t_2 + \bar{E}_r t_r} \right) \quad (58f)$$

$$J = \frac{3(\bar{E}t_2^2 - \bar{E}_r t_r^2)(\nu \bar{E}t_2^2 - \nu_r \bar{E}_r t_r^2)}{12r(\bar{E}t_2 + \bar{E}_r t_r)} - \frac{4(\bar{E}t_2^3 + \bar{E}_r t_r^3)(\nu \bar{E}t_2 + \nu_r \bar{E}_r t_r)}{12r(\bar{E}t_2 + \bar{E}_r t_r)} \quad (58g)$$

The three components of stress in Region 2 and the gimbal ring may now be computed. The axial stress produced by the moment is

$$\sigma_a = \frac{E}{D_e} \left[-M(H + At) + \delta \left(\nu \frac{D_e}{r} \right) + J + \frac{B \Delta t}{2} \right] \quad (58h)$$

where At is the distance from the interface of the ring and tube to the point in question and is assumed positive when measured outward from the interface. The tangential stress produced by the moment is

$$\sigma_{tm} = \nu \sigma_a \quad (58i)$$

and the tangential stress produced by the radial

deflection for Region 2 only is

$$\sigma_{t\delta} = \frac{E\delta}{r} \quad (58j)$$

or for gimbal ring only this stress is

$$\sigma_{t\delta} = \frac{E_r(\delta + \delta_{rs})}{r_r} \quad (58k)$$

where δ_{rs} is the deflection of the gimbal ring due to the shrink fit pressure and is computed from the equation

$$\delta_{rs} = \frac{p_s r_r^2}{E_r t_r} \quad (58m)$$

The radial stress due to internal pressure at inner surface of tube is

$$\sigma_r = -p \quad (58n)$$

and at outer surface of tube or inner surface of gimbal ring this stress is

$$\sigma_r = -p_{2r} = -(p_r + p_s) \quad (58p)$$

At the outer surface of gimbal ring the radial stress is

$$\sigma_r = 0 \quad (58q)$$

where p_r , the component of the internal pressure on the inner surface of the gimbal ring is computed from the equation

$$p_r = p \frac{E_r t_r r_r^2}{E_r t_r r_r^2 + E t_2 r_2^2} \quad (58r)$$

Again, since the maximum equivalent stress may occur at the inner or the outer surface, it is necessary to substitute the set of values of stress at each of these points into Equation 23 to determine which is the larger.

iii. Conical Section

120. The analysis of the discontinuity stresses created at the end points of a conical section of a chamber follows the procedure discussed below with reference to Figure 44.

D_c, D_t = flexural rigidity of indicated sections defined by Equation 57h

E = modulus of elasticity

M_1, M_2 = unit bending moments at Stations 1 and 2

p = internal pressure

Q_1, Q_2 = unit shear at Stations 1 and 2

\bar{r} = mean radius of conical section

\bar{r}_c = mean radius of cylindrical section

\bar{r}_t = mean radius of tube

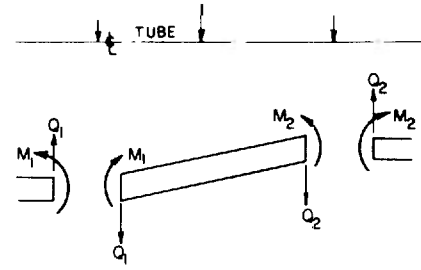


FIGURE 44. Conical Section Loading.

t, t_c, t_t = wall thickness of conical section, cylinder and tube

β = angle of conical slope

λ_c, λ_t = values defined by Equation 57c for indicated sections

The mean radius of the conical section is assumed to be

$$\bar{r} = \frac{1}{2}(\bar{r}_c + \bar{r}_t) \quad (59a)$$

The moment, shear, deflection, and ultimately the stresses at each section are found by showing the compatible relationship of angular and linear deflection of the adjacent sections at the two joints. The relative deflection due to internal pressure between conical and cylindrical section at Station 1

$$\Delta_1 = \frac{p}{E} \left(\frac{\bar{r}^2}{t} - \frac{\bar{r}_t^2}{t_t} \right) \quad (59b)$$

and at Station 2

$$\Delta_2 = \frac{p}{E} \left(\frac{\bar{r}^2}{t} - \frac{\bar{r}_c^2}{t_c} \right) \quad (59c)$$

For simplicity, three expressions which appear in the compatibility equations are represented by a particular symbol

$$C = \frac{12\bar{r}^2}{E(Lt^3 + L^3t \tan \beta)} \quad (59d)$$

$$C_c = \frac{\bar{r}_c \bar{r}}{E t L} \quad (59e)$$

$$C_t = \frac{\bar{r}_t \bar{r}}{E t L} \quad (59f)$$

The terms D and λ are those of Equations 37h and 57c. The compatibility equations are based on

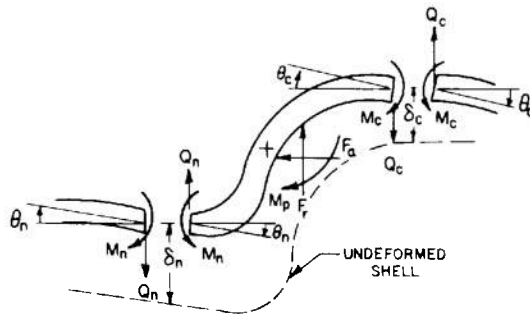
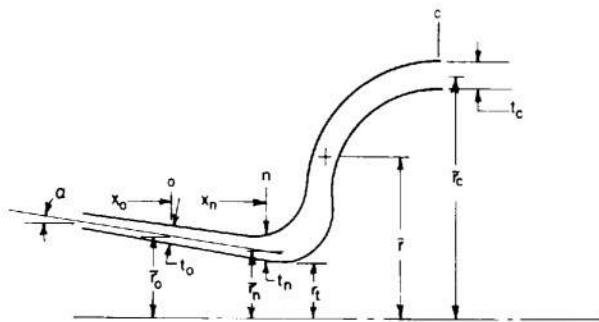


FIGURE 45. Toroidal Section Loading.

Definition of Symbols

A_n	= projected area of nozzle
D_c, D_n	= flexural rigidity of sections indicated defined by Equation 57b
E	= modulus of elasticity
M_c, M_n	= unit moments at Stations c and n
p_c, p_n, p_o	= design pressures at Stations c, n, o
p_t	= design pressure at nozzle throat
Q_c, Q_n	= unit shear at Station c and n
$\bar{r}_c, \bar{r}_n, \bar{r}_o$	= mean radii at Stations c, n, o
r_t	= radius of nozzle throat
t_c, t_n, t_o	= wall thickness at Stations c, n, o
α	= angle of nozzle slope
λ_c, λ_n	defined by Equation 57e for indicated sections
ν	= Poisson's ratio

angular deflections at Sections 2 and 1, respectively, are

$$\left(\frac{CL}{2} - \frac{1}{2\lambda_c^3 D_c}\right)Q_2 - \frac{CL}{2}Q_1 + \left(\frac{1}{\lambda_c D_c}\right)M_2 + CM_1 = 0 \quad (59g)$$

$$\frac{CL}{2}Q_2 - \left(\frac{CL}{2} - \frac{1}{2\lambda_t^3 D_t}\right)Q_1 - CM_2 + \left(C + \frac{1}{\lambda_t D_t}\right)M_1 = 0 \quad (59h)$$

The compatibility equations based on radial deflection at Stations 2 and 1, respectively, are

$$\left(C_c + \frac{CL^2}{4} + \frac{1}{2\lambda_c^3 D_c}\right)Q_2 + \left(C_t - \frac{CL^2}{4}\right)Q_1 - \left(\frac{CL}{2} - \frac{1}{2\lambda_t^3 D_t}\right)M_2 + \frac{CL}{2}M_1 = \Delta_2 \quad (59i)$$

$$\left(C_t - \frac{CL^2}{4}\right)Q_2 + \left(C_c + \frac{CL^2}{4} + \frac{1}{2\lambda_t^3 D_t}\right)Q_1 + \frac{CL}{2}M_2 - \left(\frac{CL}{2} - \frac{1}{2\lambda_t^3 D_t}\right)M_1 = \Delta_1 \quad (59j)$$

By substituting the expressions available in Equations 59b and 59e for A , and Δ_2 and then inserting the known values, Equations 59g to 59j may be solved simultaneously for M_1, M_2, Q_1 and Q_2 which complete the data needed for the radial deflections at Stations 1 and 2. The deflections are found from

$$\delta_1 = \frac{p\bar{r}_t^2}{Et_t} + \frac{M_1}{2\lambda_t^3 D_t} + \frac{Q_1}{2\lambda_t^3 D_t} \quad (59k)$$

$$\delta_2 = \frac{p\bar{r}_c^2}{Et_c} + \frac{M_2}{2\lambda_c^3 D_c} + \frac{Q_2}{2\lambda_c^3 D_c} \quad (59m)$$

The computed data and the given pressure are sufficient to determine the primary stress of Equations 58a to 58d and eventually the equivalent stress of Equation 23.

iv. Toroidal Section

121. The analysis at the toroidal section of the chamber involves pressure stresses and discontinuity stresses induced by shear and bending where cylinder and nozzle join the toroid. Figure 45 shows diagrammatically the various components contributing to the analysis which is based on procedures developed for recoilless rifles.*

Shear and moment are determined by equating the expressions for linear and angular deflections at c and n, the points of discontinuity, Figure 45.

The deflections of nozzle and cylinder are found similarly to those in the gimbal ring analysis (paragraph 118). The radial deflection at n

$$\delta_n = \frac{p_n \bar{r}_n^2}{t_n E \cos \alpha} - \frac{\lambda_n M_n + Q_n}{2\lambda_n^3 D_n} \quad (60a)$$

The angular deflection has a pressure component which is estimated by assuming a straight line variation of radial deflection over a short distance. There-

* Reference 23.

† Derived from Formula for s_2 of Case 3 on page 269 of Reference 24.

‡ Combined from Cases 10 and 11 on page 271 of Reference 24.

fore, the total angular deflection when assuming that the nozzle is conical

$$\theta_n = \frac{p_o \bar{r}_o^2 - p_n \bar{r}_n^2}{E \cos \alpha (x_n - x_o)} + \frac{2\lambda_n M_n + Q_n}{2\lambda_n^2 D_n} \quad (60b)$$

where x_n and x_o are the distances from the end of the nozzle to Stations n and O . At Station C , the radial deflection

$$\delta_c = \frac{p_c \bar{r}_c^2}{E t_c} - \frac{\lambda_c M_c - Q_c}{2\lambda_c^2 D_c} \quad (60c)$$

The angular deflection

$$\theta_c = -\frac{2\lambda_c M_c - Q_c}{2\lambda_c^2 D_c} \quad (60d)$$

122. The analysis of the toroid itself is based on the assumption that its cross section is rigid and subjected only to a uniform angular displacement and to radial deflections. The angular displacement analysis follows the procedure developed for a ring whose width is large in comparison with its mean radius. The hiding stress for the section shown in Figure 46

$$\sigma = \frac{E \theta y^*}{r} \quad (60e)$$

where

r = radius to any fiber of the ring
 y = distance from the neutral axis to the fiber
 θ = angle of rotation

The normal differential force on any differential area of a section subjected to bending is

$$\Delta F = \sigma \Delta A = \sigma \Delta r \Delta y = E \theta \frac{y}{r} \Delta r \Delta y \quad (60f)$$

The summation of forces must be zero since their directions on each side of the neutral axis are opposite

$$F = \sum \Delta F = E \theta \sum \frac{y}{r} \Delta r \Delta y = 0 \quad (60g)$$

Correspondingly, the internal unit moment of the section

$$M_r = \frac{\sum y \Delta F}{\bar{r}} = \frac{E \theta}{\bar{r}} \sum \frac{y^2}{r} \Delta r \Delta y \quad (60h)$$

where

\bar{r} = the mean radius of the section.

In Figure 46, y is measured from the neutral axis

* Page 179 of Reference 25.

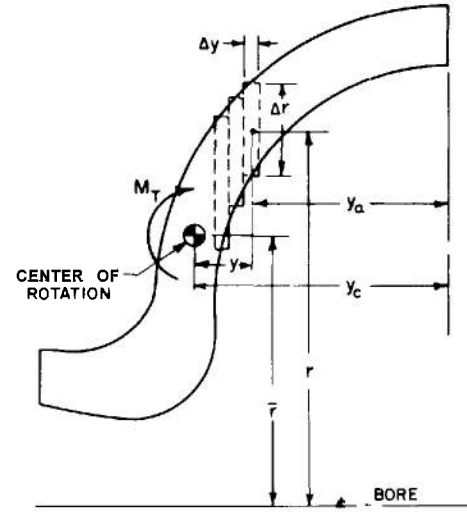


FIGURE 46. Toroidal Internal Moment Center.

in either direction and y_a is measured from the outer fibers so that

$$y = y_c - y_a \quad (60i)$$

where

y_c = distance from neutral axis to outer fiber

Substituting $y_c - y_a$ for y in Equation 60g and solving for y_c , a constant

$$y_c = \frac{\sum \frac{y_a \Delta r \Delta y}{r}}{\sum \frac{\Delta r \Delta y}{r}} \quad (60j)$$

The mean radius of the toroid

$$\bar{r} = \frac{\sum r \Delta r \Delta y}{\sum \Delta r \Delta y} \quad (60k)$$

Both y_c and \bar{r} are found by dividing the irregular area into increments and then performing the numerical integration. The intersection of y_c with the line indicative of the mean circumference is the axis about which all moments of the toroidal section are taken, including those contributed by the pressure as well as those induced by the discontinuity.

123. Before proceeding, the axial pressure forces are found by resorting to numerical integration. Divide the inner surface of the toroid into small circular increments (Figure 47). The total axial force is the summation of the unit axial pressure force on each increment

$$F_a = \sum \Delta F_a = 2\pi \sum r_p \Delta r_p p_i \quad (60m)$$

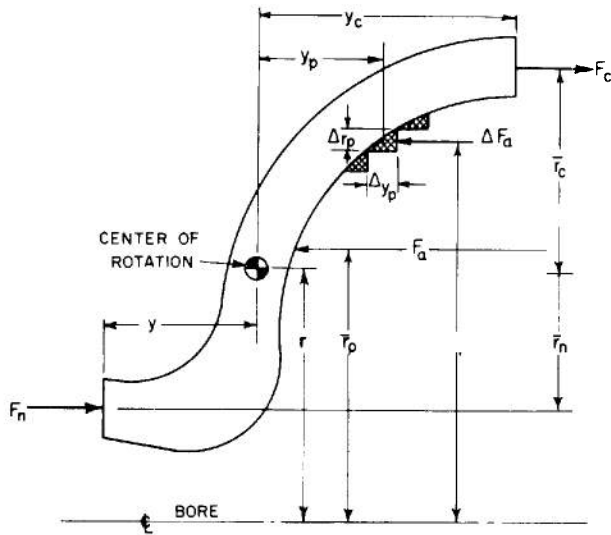


FIGURE 47. Toroidal External Loads.

where

AF_i = pressure force on each increment
 p_i = pressure at the increment

The location of the axial pressure center is found by taking moments of the load increments about the radial axis

$$r_p = \frac{\sum r_p AF_i}{\sum \Delta F_a} \quad (60n)$$

By balancing the axial pressure forces in Figure 47, the axial force at the cylinder joint

$$F_i = F_a - F_n \quad (60p)$$

where

F_n = axial pressure force on nozzle juncture.

Clockwise moments being positive, the unit moment on the toroid produced by the axial pressure forces taken about the center of pressure

$$M_a = [F_c(\bar{r}_c - \bar{r}_p) - F_n(\bar{r}_p - \bar{r}_n)]/2\pi\bar{r} \quad (60q)$$

The unit moment due to pressure exerted radially is computed directly by the summation of incremental moments about the neutral axis

$$AI_i = \frac{\sum r \Delta y_p p_i y_p}{\bar{r}} \quad (60r)$$

where

y_p = distance of center of increment to neutral axis
 Δy_p = width of increment

The total moment due to internal pressure

$$M_p = M_a + M_r \quad (60s)$$

The total externally applied unit moment tending to rotate the toroidal section

$$M_r = M_p + M_c - M_n + y_c Q_c + y_n Q_n \quad (60t)$$

Since the external moment must equal the internal moment, the expression for M_r of Equation 60h

$$\frac{E\theta}{\bar{r}} \sum \frac{y^2}{r} \Delta r \Delta y = M_p + M_c - M_n + y_c Q_n + y_n Q_n \quad (60u)$$

Expressions for the deflections of the toroid completes the information necessary to compute shear and moment values at the points of discontinuity. The radial deflection at each juncture has two components, one being generated by the angle of rotation, 8. The other is caused by the resultant radial shear acting at the mean circumference. Being analogous to pressure in a cylinder, the effective shear on the toroid becomes the resultant of the projected radial loads. The total radial deflection combining the effects of rotation and shear at the cylinder

$$\delta_c = -y_c \theta + \frac{\bar{r}(\bar{r}_n Q_n - \bar{r}_c Q_c)}{EA} \quad (60v)$$

where

$A = \sum \Delta r \Delta y$, the cross-sectional area

At the nozzle, the radial deflection

$$\delta_n = y_n \theta + \frac{\bar{r}(\bar{r}_n Q_n - \bar{r}_c Q_c)}{EA} \quad (60w)$$

Maintaining the assumption that the cross section of the toroid is rigid, the angle of rotation must correspond with the angular deflections at c and n , therefore

$$\theta = \theta_n = \theta_c \quad (60x)$$

Direct substitution for θ_n and θ_c in Equations 60b and 60d puts these equations in terms of unit moment and shear. Radial deflection, δ_n , is eliminated by equating its expressions in Equations 60a and 60w, and δ_c by equating its expressions in 60e and 60v. This manipulation provides four equations with four unknowns, M_c , M_n , Q_c , Q_n , for which values may be obtained by simultaneous solutions. After deflections become available, primary stresses may be computed from Equations 58a to 58d and then the equivalent stress of Equation 23.

v. Nozzle Stresses

124. A procedure with appropriate formulas has been developed to determine the equivalent pressure

stress for the wall of a nozzle at any position.* The equivalent stress considers tangential (hoop) and meridional (axial) stresses and is based on the Hencky-von Mises strain-energy theory of failure. Pressure and pressure loading are obtained from gas dynamics of one-dimensional isentropic flow. A nozzle showing pertinent general dimensions appears in Figure 48.

Corresponding values of the ratios A/A_t , F/F_t , p/p_o , are available for various values of γ .† At any nozzle station

$$\frac{A}{A_t} = \left(\frac{r}{r_t}\right)^2 \quad (61a)$$

Now, from the gas tables,‡ for the appropriate γ , and corresponding A/A_t find the ratio F/F_t . Then

$$\psi = (1 + \gamma) \left(\frac{1}{1 + \gamma} \right) \quad (61b)$$

Similarly

$$\psi_e = (1 + \gamma) \left(\frac{2}{1 + \gamma} \right)^{\gamma/(\gamma-1)} \frac{F_e}{F_t} \quad (61c)$$

From the same table, obtain p/p_o . The axial and tangential stress factors are

$$\eta_a = -\frac{\psi_e - \psi}{2 \frac{r}{r_t} \sin \phi} \quad (61d)$$

$$\eta_t = \frac{r/r_t}{\sin \phi} \left(\frac{p}{p_o} + \frac{r_t}{r_1} \eta_a \right) \quad (61e)$$

By the adaptation of the Hencky-von Mises Theory, the equivalent stress factor

$$f_e = \sqrt{\eta_a^2 - \eta_a \eta_t + \eta_t^2} \quad (61f)$$

The required wall thickness normal to the nozzle profile

$$t_r = \frac{r p_o}{Y} f_e \quad (61g)$$

where Y is the minimum yield strength. The wall thickness normal to the nozzle axis

$$t = t_r / \sin \phi \quad (61h)$$

Referring to Equation 56c the OD of the nozzle including the allowable eccentricity

$$D_r = 2r + \frac{19}{9} t \quad (61i)$$

Ordinarily, the nozzle wall so obtained for high

* Reference 26.

† Reference 27.

‡ Reference 26.

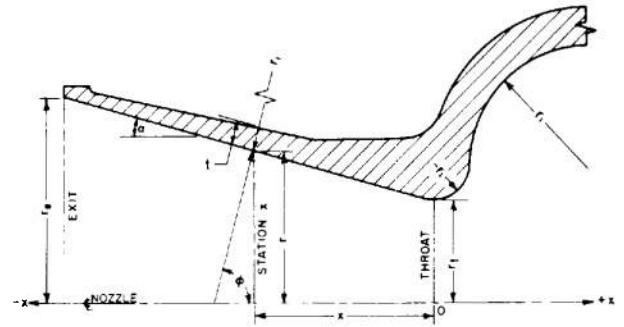


FIGURE 48. Nozzle With General Dimensions.

Definition of Symbols

- A = nozzle area at any station, x
- A_t = nozzle throat area
- F = thrust at any nozzle station
- F_t = thrust at throat where Mach number is unity
- f_e = equivalent stress factor
- p = pressure at any nozzle station
- p_o = stagnation pressure (known)
- r = radius at any station
- r_t = nozzle throat radius (known)
- r_1 = radius of curvature of nozzle wall, meridional (known)
- t = design wall thickness (estimated)
- t_n = nominal wall thickness, final (known)
- x = distance, station to throat. Negative toward exit (known)
- Y = minimum yield strength
- α = nozzle slope (known)
- γ = ratio of specific heats of propellant gases (known)
- η_a = axial stress factor
- η_t = tangential stress factor
- σ_e = equivalent stress
- ϕ = complement of nozzle slope (known)
- ψ = modified thrust factor
- ψ_e = thrust factor at nozzle exit

strength material is much too thin for handling purposes, consequently a heavier wall is provided which will survive handling. The equivalent stresses are then computed for the thicker wall. The equivalent stress now becomes

$$\sigma_e = f_e \frac{p_o r_t}{t_e} \quad (61j)$$

where t_e is the effective wall thickness based on the allowable eccentricity.

The effective wall thickness assumes that the nominal wall thickness normal to the nozzle profile

has incorporated the allowable eccentricity. The apparent wall ratio

$$W_a = \frac{r + t_n}{r} \quad (61k)$$

Then according to Reference 14, the actual wall ratio

$$W = .947W_a + 0.053 \quad (61m)$$

The stresses are based on the wall whose allowable eccentricity now shows a minimum effective wall thickness of

$$t_e = r(W - 1) \quad (61n)$$

11. Stress Compensating Measures

a. Jacketed Construction

125. Gun tubes are high pressure vessels that must be made of high strength material to hold wall thicknesses within reasonable limits. Depending on high tensile strength alone will not always satisfy weight requirements so the designer must resort to other techniques to augment the inherent strength of the tube. The techniques involve mechanical procedures. One such is multilayer construction comprising two or three shrink fitted concentric cylinders. The use of more than three is rare in the gun tube field. Sometimes the nature of the tube structure dictates the method of construction. We find this in the quasi two-piece tube (Figure 4) where the cap is threaded to and shrink over the tube to serve in the multiple capacity of chamber, liner retainer, and the tube jacket.

126. The methods for determining wall thickness and shrinkage pressure are presented in Part II-3, Shrinkage Stresses. The amount of interference between cylinders of a two layered tube is equal to the total deflection of Equation 32c. The equations for determining the interference between cylinders of a three layered tube are derived below. The tangential strain of a cylinder may be expressed as

$$\epsilon_t = \frac{1}{E} (\sigma_t - \nu \sigma_r) \quad (62a)$$

where ν is Poisson's ratio. The change in diameter is

$$\delta = \frac{\pi D \epsilon_t}{\pi} = D \epsilon_t \quad (62b)$$

Substituting for ϵ_t

$$\delta = \frac{D}{E} (\sigma_t - \nu \sigma_r) \quad (62c)$$

From Lamé's solution for thick walled cylinders,*

* Reference 18, page 299.

the general expressions for tangential and radial stresses for internal and external pressures p_i and p_o , respectively, are

$$\sigma_t = \frac{p_i D_i^2 - p_o D_o^2 + \frac{D_i^2 D_o^2}{D_o^2 - D_i^2} (p_i - p_o)}{D_o^2 - D_i^2} \quad (62d)$$

where

D = any diameter, $D_i \leq D \leq D_o$

D_i = inside diameter

D_o = outside diameter

$$\sigma_r = \frac{p_o D_o^2 - p_i D_i^2 + \frac{D_i^2 D_o^2}{D_o^2 - D_i^2} (p_i - p_o)}{D_o^2 - D_i^2} \quad (62e)$$

Substituting for σ_t and σ_r in Equation 62c,

$$\delta = \frac{D}{E} \left[\frac{p_i D_i^2 - p_o D_o^2 + \frac{D_i^2 D_o^2}{D_o^2 - D_i^2} (p_i - p_o)}{D_o^2 - D_i^2} + \nu \frac{p_o D_o^2 - p_i D_i^2 + \frac{D_i^2 D_o^2}{D_o^2 - D_i^2} (p_i - p_o)}{D_o^2 - D_i^2} \right] \quad (62f)$$

where

D_i = ID of liner

D_1 = OD of liner, ID of inner jacket

D_2 = OD of inner jacket, ID of outer jacket

D_o = OD of outer jacket

The first operation is shrinking the inner jacket over the liner. For the liner, $p_i = 0$, $p_o = p_{s1}$, $D_o = D_1$. The change in OD of the liner is

$$\delta_{o1} = -\frac{D_1 p_{s1}}{E(D_1^2 - D_i^2)} [D_i^2(1 - \nu) + D_i^2(1 + \nu)] \quad (63a)$$

For the inner jacket, $p_i = p_{s1}$, $p_o = 0$, $D_i = D_1$, $D_o = D_2$. The change in its ID

$$\delta_{i1} = \frac{D_1 p_{s1}}{E(D_2^2 - D_1^2)} [D_1^2(1 - \nu) + D_2^2(1 + \nu)] \quad (63b)$$

The second operation is shrinking the outer jacket over the liner-inner jacket composite tube. For the composite tube, $p_i = 0$, $p_o = p_{s2}$, $D_o = D_2$. The change in inner jacket OD.

$$\delta_{o1} = \frac{-D_2 p_{s2}}{E(D_2^2 - D_1^2)} [D_2^2(1 - \nu) + D_1^2(1 + \nu)] \quad (63c)$$

For this outer jacket, $p_i = p_{s2}$, $p_o = 0$, $D_i = D_2$. The change in ID is

$$\delta_{i2} = \frac{D_2 p_{s2}}{E(D_o^2 - D_2^2)} [D_2^2(1 - \nu) + D_o^2(1 + \nu)] \quad (63d)$$

The required interferences between liner and inner jacket and between the inner and outer jackets are, respectively

$$\delta_1 = -\delta_{o1} + \delta_{i1} \quad (63e)$$

$$\delta_2 = -\delta_{o2} + \delta_{i2} \quad (63f)$$

b. Autofrettage

127. Autofrettage or self-hooping is a method for prestressing thick-walled cylinders which has been successfully applied to gun tubes. It follows the technique of stressing the inner portion of the wall beyond the elastic region but not exceeding the yield on the outer surface. When the stress inducing agent, either hydrostatic pressure or oversized mandrel is removed, the outer surface will contract in an effort to recover its original size. The contraction will compress the inner wall to induce substantial compressive stresses. Meanwhile, because the recovery from the outer strain is not complete, residual tensile stresses will remain in this region. Prestressed in this manner, the tube will respond elastically and will be safe for any pressure which does not exceed the autofrettage pressure or its equivalent. Tube wall thickness is determined from the allowable stress and the strength of the material. The autofrettage pressure

$$p_f = Y \ln \frac{D_o}{D_i} \quad (64a)$$

where

D_o = outside diameter of tube
 D_i = inside diameter of tube
 Y = yield strength of material

In terms of the elastic strength pressure (*ESP*), the pressure that the tube can sustain, Watervliet Arsenal has found experimentally that this pressure in a finished tube is

$$ESP = 1.08 Y \ln W_f \quad (64b)$$

where W_f is the wall ratio of the finished tube. Since the outer surface is stressed to the yield point by the autofrettage pressure, the residual stress here is

$$\sigma'_i = E - \quad (65a)$$

where, according to Equation 25, the upper limit of the hoop stress is due to the autofrettage pressure, p_f , thus, substituting D_i for D , and p_f for p ,

$$\sigma'_{i0} = p_f \frac{2}{W^2 - 1} \quad (65b)$$

* Reference 18, Equation 332.

Hereafter, the resultant stress on the outer surface induced by the allowable pressure is

$$\sigma_t = \sigma'_i + p_o \frac{2}{W^2 - 1} \quad (65c)$$

By substituting the expressions for σ'_i and then for σ'_{i0} , Equation 65c becomes

$$\sigma_t = Y - (p_f - p_o) \frac{2}{W^2 - 1} \quad (65d)$$

This shows that the tube will be safe for all working pressures which do not exceed p_f .

128. When autofrettage is performed by applying a constant hydrostatic pressure along the full length of the bore, the outside of the tube must be prevented from straining beyond the yield point. Even the thickest part of the tube should be restrained as a safety measure. The restraining cylinder is called a container. Clearance between container and tube should be so arranged that the outer surface of the tube is on the verge of yielding at autofrettage pressure. Since the container induces external pressure on the tube, both internal and external pressures must be included in the analysis. Based on the Maximum-Shear-Stress Theory $Y = 2\tau_w$,† where τ_w is the allowable stress of the material in shear, and is equal to $\frac{1}{2}(\sigma_t - \sigma_r)$. Substituting for τ_w

$$\sigma_r = \sigma_t - Y \quad (66a)$$

and

$$\sigma_r = Y \ln r + C \quad (66b)$$

where r is the general term for radius and C is a constant of integration, whose value is determined from the boundary conditions. When $r = r_o$, the outer radius, $\sigma_r = -p_o$, the external pressure. Therefore

$$C = -p_o - Y \ln r_o \quad (66c)$$

and

$$\sigma_r = Y \ln \frac{r}{r_o} - p_o \quad (66d)$$

or, in terms of diameters

$$\sigma_r = Y \ln \frac{D}{D_o} - p_o \quad (66e)$$

When $D = D_i$, the internal diameter, $\sigma_r = -p_f$. Substituting in Equation 66e,

$$-p_f = Y \ln \frac{D_i}{D_o} - p_o \quad (66f)$$

† Reference 28, page 39.

‡ Reference 18, Equation 427.

The tube wall thickness is determined from Equation 64d. The effective autofrettage pressure

$$(p_f - p_o) = Y \ln \frac{D_o}{D_i} \quad (67)$$

Substituting for σ_r from Equation 66a into Equation 66e, the tensile stress at any point in the tube wall after autofrettage pressure is fully applied

$$\sigma_t = Y \left(1 + \ln \frac{D}{D_o} \right) - p_o \quad (68a)$$

When $D = D_o$,

$$\sigma_t = Y - p_o \quad (68b)$$

and, from Equation 62c, the corresponding outer diametral deflection of the tube is

$$\delta_t = \frac{D_i}{E} [Y - p_o(1 + \nu)] \quad (69a)$$

Where D_i = the nominal OD of the tube and ID of the container. The inner diametral deflection of the container, also from Equation 62c, is

$$\delta_c = \frac{D_i}{E} p_o \left(\frac{W_c^2 + 1}{W_c^2 - 1} + \nu \right) \quad (69b)$$

where W_c = wall ratio of the container which may be any reasonable value provided that its stress remains in the elastic range. The diametral clearance between tube and container preceding autofrettage is

$$A_i = \delta_t - \delta_c \quad (69c)$$

Therefore, the inside diameter of the container is

$$D_{ic} = D_i + A_i \quad (70)$$

129. When autofrettage is performed with an oversized mandrel, the object is to induce stresses equivalent to those developed by the hydrostatic pressure method. Tube size is determined from Equation 64a and the equivalent autofrettage pressure also from Equation 64a, by substituting the allowable pressure, p_u for p_f , and the allowable stress, σ_w for Y . The deflection of the inside diameter of the tube

$$\delta_t = \frac{D_o^2}{4 \sqrt{3GD_i}}^* \quad (71a)$$

where

G = shear modulus

D_i = ID of tube and nominal diameter of mandrel

The deflection of the mandrel

$$\delta_m = p_f \frac{D_i}{E} (1 - \nu) \quad (71b)$$

* Reference 28, Equation 8.5%.

The required interference between tube and mandrel

$$\Delta_i = \delta_t + \delta_m \quad (71c)$$

Therefore, the mandrel diameter

$$D_m = D_i + \Delta_i \quad (71d)$$

12. Strain Compensation

130. Light weight being a major design criterion for recoilless tubes, thin walls and high stresses with corresponding large bore dilations become axiomatic. Such large bore dilations must be compensated for. This was demonstrated by one recoilless gun whose inaccuracy was traced to the balloting of the projectile as it traveled through the tube.† Excessive clearance between projectile and bore surface was responsible. This clearance comprised the nominal clearance, the tolerance, and the tube dilation induced by the propellant gas pressure. Reducing clearance and tolerance did not help materially. Accuracy was eventually improved to an acceptable level by providing a small interference between projectile and bore. This development led to the introduction of strain compensating tubes whose initial interferences compensate for the dilation of the tube resulting from gas pressure.

131. Theoretically, the interference should equal the diametral deflection induced by the propellant gas less the desirable clearance. In practice a nominal interference between front bourrelet and bore of 0.002 inch was found satisfactory. At the rear bourrelet the diametral interference necessary to achieve normal projectile action in the bore is computed to be

$$\Delta D_b = \frac{p_o D^2}{2tE} - \Delta D_c \quad (72)$$

where

D = mean diameter of tube

ΔD_c = desired clearance between bore and projectile during dilation

E = modulus of elasticity

p_o = propellant gas pressure

t = wall thickness

The restricted bore is relieved for a short distance at the start. Here rifling diameters are standard in order to seat the projectile.

Generally only a very highly stressed tube with corresponding large deflection requires strain compensation. The technique of strain compensation as applied to recoilless tubes is fairly new and until

† Reference 29.

more data become available to establish firm design procedures, firing test using prototypes with conventional clearances must be conducted to determine whether or not strain compensation is necessary.

I. LINER DESIGN

132. Where liners are designed solely for the purpose of prolonging tube life, strength is secondary. However, these liners must be strong enough to develop and transmit the rifling torque and to withstand the collapsing pressure of shrink fit. Such liners if made only as thick as required for machining and handling are generally adequate to transmit torque and, being thin and therefore less rigid, have the inherent advantage of developing low shrink fit pressures. For example, the liner for the 7.62 mm machine gun has a wall thickness of approximately $\frac{1}{8}$ inch. However, when the liner of a multilayer tube extends along the full length as shown in Figure 3, it must be as one of the constituent members, subject to the same design requirements as the other members.

Liners should preferably extend through the total length of the bore but if their lengths are restricted, they should at least cover the regions of the forcing cone and the first part of the rifled bore where erosion is normally most severe. The practice of assembling the liner by shrink fit limits its length if, as in small bore tubes, the clearance between heated tube and cool liner is also small. During assembly this clearance may disappear as the liner is inserted. Available insertion time and hence liner length depends on how soon the heat from the tube expands the liner to a diameter which prevents further travel. Liners in small arms are limited to about 6 inches. On the other hand artillery tubes have large diameters, clearances due to heat expansion are correspondingly large, consequently, more time is available for assembly to permit the installation of long liners.

133. Practical shrink fit experience determines the compatibility between interference limits and liner length. For small arms, diametral interference limits vary from 0.0002 to 0.0012 inch. Shrink fit pressures and stresses are computed for the maximum interference to insure against liner collapse. When three tubes are shrunk together, the shrink fit pressure is computed first for the interference between the inside and middle layers. Later, this composite tube is treated as one homogeneous tube to find the pressure between middle and outer layers of tube.* If

* This procedure is practiced at Springfield Armory

the interference for shrink fit has been established through practice, as for small arms, the shrink fit pressure is readily computed. The pressure between two tubes of like material is

$$p_s = \frac{E\delta(b^2 - a^2)(c^2 - b^2)}{aL^3L^2 - 2\gamma} \quad (73a)$$

where

- a = inner radius of assembly
- b = intermediate radius of assembly
- c = outer radius of assembly
- δ = total radial deflection at interface.

If the mating tubes have different moduli of elasticity, the shrink fit pressure becomes

$$p_s = \frac{\delta}{b \left[\frac{1}{E_J} \left(\frac{c^2 + b^2}{c^2 - b^2} + \nu_J \right) + \frac{1}{E_L} \left(\frac{b^2 + a^2}{b^2 - a^2} - \nu_L \right) \right]} \quad (73b)$$

where

- E_J = modulus of elasticity of jacket
- E_L = modulus of elasticity of liner
- ν_J = Poisson's ratio of jacket
- ν_L = Poisson's ratio of liner

Once the shrink fit pressures become known, resultant stresses throughout the composite wall can be computed by applying the appropriate method. A sample calculation demonstrating the procedures appears in Chapter 8, Part C.

J. QUASI TWO-PIECE TUBE

134. The quasi two-piece tube (Figure 4) represents a small arms lined tube which aptly illustrates the advantages of the lined type. Not only does the liner prolong tube life, but the shrink fitted members increase the strength while the arrangement of the structural components inhibits extreme temperatures at the chamber. Referring to Figure 4, gaps at A and D , the ends of the liner and cap, respectively, are arranged so that a positive seal materializes at B , between liner and tube, and at C , between cap and liner. Further benefit is derived from the gap at D . Since the hottest region of the tube is near the forward end of the liner, heat flows from here in either direction. As it reaches the gap, D , the rearward flow to the cap is interrupted, thereby inducing the temperature drop which may be observed in Figure 9. The comparatively cool chamber wall relieves two sources of trouble. One,

† Reference 25, page 242.

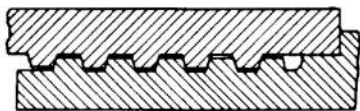


FIGURE 49. Threaded Joint With Butted End.

its low temperature limits thermal expansion and hence clearances between chamber and cartridge case are maintained to limits which preclude case rupture. Two, the small heat flow to the chamber deters cook-off tendencies. The gap may be small since the two members affecting the gap are of the same material, therefore, changes in temperature will not disturb it. The difference in linear coefficients of expansion between steel and liner material require that the gap at the end of the liner be wide enough to compensate for the excess thermal expansion of the liner, since liner materials generally have the larger coefficient. The gap at ambient temperatures should be

$$\Delta L = (\alpha_L - \alpha_t) L \Delta T \quad (74)$$

where

- L = liner length
- ΔT = change in temperatures
- α_L = coefficient of linear expansion of liner
- α_t = coefficient of linear expansion of tube

Present practice has

$$\begin{aligned} \Delta T &= 1000^\circ\text{F} \\ \alpha_L - \alpha_t &= 5 \times 10^{-7} \text{ in/in/}^\circ\text{F} \text{ when liner is} \\ &\text{stellite and tube is steel} \end{aligned}$$

K. MECHANICAL FEATURES

135. The structural components which help to moderate, support, and transmit firing loads to the mount or other supporting structure must have some convenient, functional, and strong means of attachment to the tube. Established methods include threaded connections for axially loaded components and keys for torsionally loaded ones. Screw threads should conform to unified thread standards.* Threads should never be used to align and position a component in an assembly. Wear due to continued take-down and reassembly and local failure at the entering end will advance the travel of the threaded joint at each tightening. Continued alignment and positioning are assured by machining off the incomplete thread so that the two mating pieces will mutually butt against finished surfaces, and by providing sleeve contact, as shown in Figure 49.

* Reference 30.

1. Threads

136. Threads carry their load in shear. A conservative method for computing the shear stress assumes the shear area to be formed at the mean diameter of the thread. Eliminating the space between the threads, only half the length of the engaged threads can be considered. The shear stress becomes

$$\tau = \frac{F}{\frac{1}{2}\pi D_m L} \quad (75)$$

where

- D_m = mean diameter of thread
- F = force on thread, axial expression
- L = length of engaged threads

137. When quick detachable assemblies become necessary, interrupted threads are used. These are usually acme, buttress, or square threads (Figure 50). The latter two are more often used in small arms. Interrupted threads are made by removing half the thread periphery alternately along a various number of segments on the two mating components (Figure 51). After sliding the two pieces together, only a fractional turn (the reciprocal of the number of segments) is needed to realize total engagement. In artillery design, all engaged threads are assumed to be acting whereas in small arms design, a much more conservative philosophy is adopted by assuming that only one thread carries the full load. Shear and bearing stresses determine the feasibility of the design.

138. In artillery, breech ring is attached to tube by interrupted threads. The larger caliber weapons in the small arms category are similarly attached but complete screw threads (UN) are used for the smaller calibers. The maximum load appearing on these threads is based on the maximum propellant gas pressure and the rear chamber area for separate

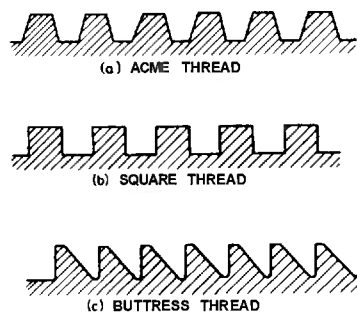


FIGURE 50. Thread Profile Types.

loaded ammunition, or the internal area of the base of the cartridge case for fixed ammunition.

$$F_t = p_{gm} \frac{\pi}{4} D_c^2 \quad (76)$$

where

D_c = rear chamber diameter or equivalent!

F_t = thread load

p_{gm} = maximum propellant gas pressure

139. Threaded joints in the chamber of recoilless tubes are designed on the basis of a Watertown Arsenal Laboratory method which assigns the maximum load on any one thread as one half the total load.* Stress concentrations at the root of the threads are emphasized. Four stresses are involved: the direct shear, the direct bearing, the fillet bending, and the net, section tensile stress. The latter two are influenced by concentrations factors which are readily available.† Figure 52 shows the cross section of a chamber joint with an enlarged view of the thread showing dimensions and loads where

C = clearance

d_t = depth of thread

D_m = mean diameter of thread

p_t = pitch of thread

r = radius of fillet and rounded corner

t = wall thickness at joint

w = width of thread at root diameter

The total load on the threads is computed from Equation 76. Since half the load is assumed to be

* Reference 31.

† References 32 and 33.

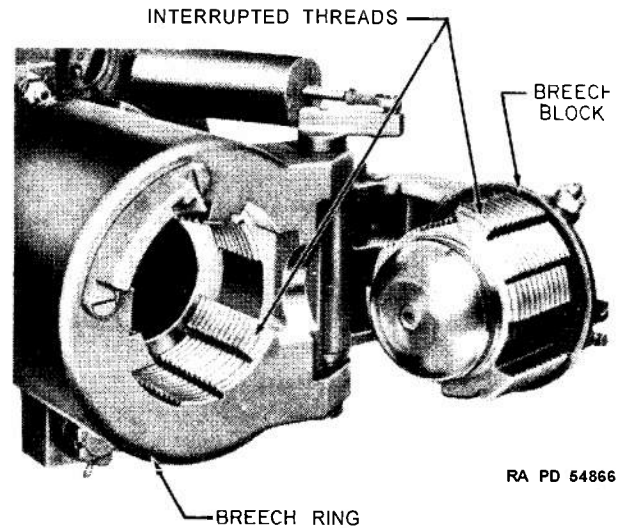


FIGURE 51. Interrupted Threads.

carried by one thread and concentrated on the mean circumference, the unit load

$$F_u = \frac{F_t}{2\pi D_m} \quad (77a)$$

The direct shear stress at the mean diameter

$$\tau = \frac{F_u}{\frac{1}{2}p_t} = \frac{2F_u}{p_t} \quad (77b)$$

The direct bearing stress

$$\sigma_{br} = \frac{F_u}{d_t - C - 2r} \quad (77c)$$

The net tensile stress through the wall

$$\sigma_n = k_c \frac{2F_u}{t} \quad (77d)$$

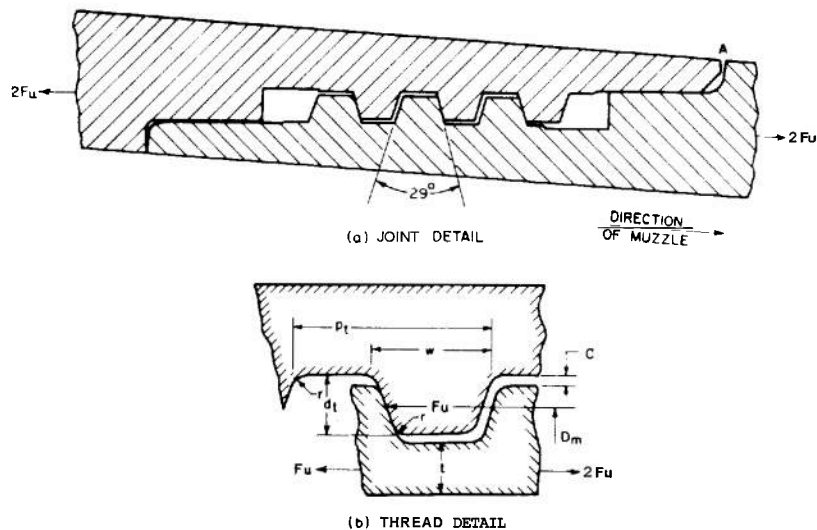


FIGURE 52. Threaded Joint.

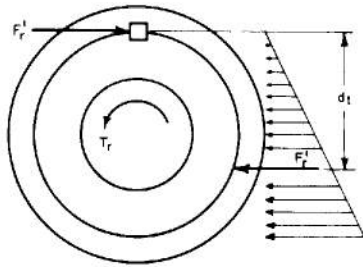


FIGURE 53. Rifling Torque Reactions.

where k_e is the stress concentration factor. The fillet bending stress is based on cantilever beam analogy.

$$\sigma_f = 3k_e \frac{F_r(d_t + C)}{W^2} \quad (77e)$$

2. Rifling Torque Transmitters

140. To transmit rifling torque effectively from tube to cradle and to prevent the tube from rotating, cradle and tube are keyed together. The rifling torque reacts on the key and bearing whose moment arm extends from the key to the center of the assumed triangular distributed load on the, projected diameter. According to Figure 53, the key load is

$$F_r' = \frac{T}{d_t} \quad (78)$$

where T is the maximum rifling torque obtained from Equations 18 or 19. The shear stress on the key and the bearing stress on the keyway are, respectively,

$$\tau = \frac{F_r'}{tL} \quad (79a)$$

$$\sigma_{br} = \frac{F_r'}{hL} \quad (79b)$$

where

h = depth of keyway

L = length of key

t = thickness of key

141. Recoilless tubes exert little or no external forces. Both recoil force and generally rifling torque are balanced by the nozzle discharge. Therefore, supporting structures need only the rigidity and strength necessary to support the weight and hold the gun firmly in firing position. Light clamps or rings around the tube or lugs integral with the chamber provide attachments for the supports. Ease of handling rather than strength becomes the

design philosophy of the attachments. One of these provisions, as with other gun tubes, is the gunner's quadrant flats shown in Figure 54. Each tube must have flats on which to rest the gunner's quadrant during engineering tests. The flats are machined on collars integral with the tube and are spaced between chamber and trunnions, but located as close to the trunnions as convenient. The surface established by the two flats must be parallel to the trunnion axis laterally and to the bore axis longitudinally.

3. Muzzle Attachments

142. Muzzle attachments comprise muzzle brakes, flash suppressors or hidars, blast deflectors, and sights. Sights at the muzzle are usually confined to shoulder arms and machine guns and fit into dove-tailed slots or are clamped around the tube. Muzzle brakes, flash suppressors and blast deflectors are threaded or clamped to the muzzle. Threads, being the better arrangement, may be the interrupted type. If necessary, the wall thickness at the muzzle is increased to keep the root diameter within the limits commensurate with pressure-strength requirements. Axial loads predominate and are induced by recoil acceleration and propellant gas pressure.

L. GUN TUBE MATERIALS

143. Gun tube material must have diversified properties. It must have high strength to withstand the high propellant gas pressures. It must be ductile to be able to respond favorably to the repeated quickly applied and released loads. It must be resistant to the erosive action of hot propellant gases and the abrasive action of rotating bands. These properties must be maintained throughout the temperature range of -65°F to approximately 2000°F . The latter temperature is estimated as that of the bore surface after continuous firing of a machine gun. No one material meets all these requirements. If one material has the needed strength, it may be susceptible to erosion; if erosion resistant, it may be too brittle. Combinations in the form of liners and plating overcome these deficiencies to an appreciable extent.

1. Steel

144. Alloy steel is the nearest approach to an ideal gun tube material. Although some materials excel it in erosion resistance, it responds favorably to erosion activity when subjected to other than sustained automatic firing. Erosion resistant materials

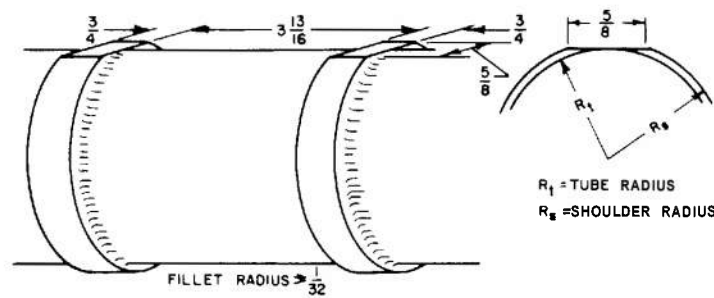


FIGURE 54. Gunner's Quadrant Flats.

used either as liners or as plating on the bore surface, increase tube life considerably. Alloy steel is unmatched in strength but does not necessarily have the best strength-weight ratio in the tensile strength range needed for gun tubes. However, massiveness in gun tubes is not always unfavorable; heavy tubes being correlated to low recoil accelerations. In this respect, some compromise must be reached between tube weight and recoil force.

Steel, like most other materials, undergoes a change in strength at elevated temperatures. A considerable loss in ultimate and yield strengths develops between 600° and 1300°F. The curves in Figure 55 illustrate the progressive strength decay with temperature rise for SAE 4150 and chrome-moly-vanadium steels.* The low strengths may be disturbing when one realizes that gun tubes reach these high temperatures, particularly in small arms after sustained firing. However, because of temperature gradients across the tube wall stresses are induced which function as autofrettage activity. These stresses actually help relieve pressure stresses since thermal stresses are compressive at the inside surface. Furthermore, the time interval of load application is short indicating that the strength of the material at elevated temperatures is greater under dynamic loading than it is under static loading. This phenomenon is demonstrated in machine gun barrels heated to temperatures where strength has decreased by 90%, but apparently the barrel is still strong enough to sustain the high pressures of propellant gases. Although considerable research is being conducted in the field of high rate-of-loading sufficient progress has not been made to understand and incorporate this phenomenon into a design criterion.

145. Various steels are designated for the different categories of gun tubes. Table 11 lists the chemical requirements of steels generally used for tubes.

* Reference 34, pages 20 and 36.

Tubes made from heavy stock require a high degree of hardenability so that the specified heat treatment, can develop the desired properties in the interior without developing excessive hardness on the exterior. Extreme hardness should be avoided to prevent brittleness. Figure 56 shows mechanical properties corresponding to various tempering temperatures. Best heat treating results are obtained when the blanks are held vertically during heating and quenching. With sufficient space between them, this position assures each blank a uniform exposure to heat and coolant to produce steel of near homogeneous properties. Decarburization and formation of adherent scale should be avoided. Heating should be done in furnaces having controlled atmosphere.

146. Steels used for artillery and recoilless tubes are similar to those of small arms except that the

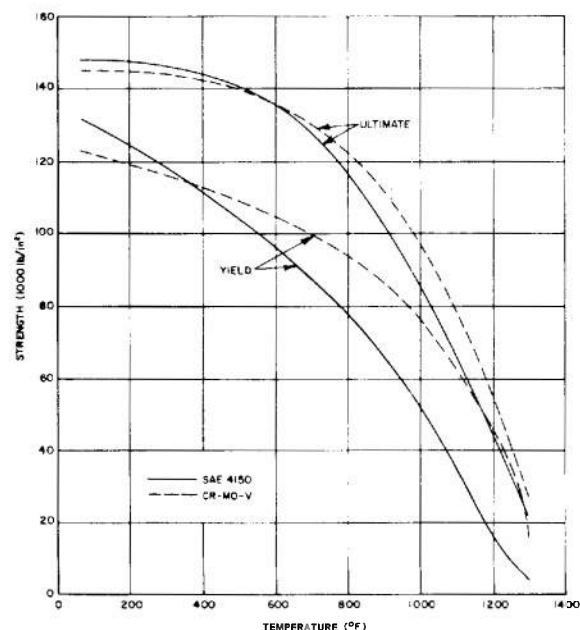


FIGURE 55 Effects of Temperature on Tensile Strength of SAE 4150 and Cr-Mo-V Steels.

TABLE 11. CHEMICAL REQUIREMENTS OF STEEL.
(Quantities shown in percent)

Steel	C	Mn	P(Max)	S(Max)	Si	Cr	Mo	V
ORD 1052	0.47-0.55	1.20-1.50	0.40	0.05	0.20-0.35	—	—	—
ORD 1155 ReS*	0.50-0.62	1.30-1.65	0.40	0.05 0.09	0.20-0.35	—	—	—
ORD 4150	0.48-0.55	0.75-1.00	0.40	0.04	0.20-0.35	0.80-1.10	0.15-0.25	—
ORD 4150 ReS*	0.47-0.55	0.70-1.00	0.40	0.05-0.09	0.20-0.35	0.80-1.15	0.15-0.25	—
Cr-Mo-V	0.41-0.49	0.60-0.90	0.10	0.04	0.20-0.35	0.80-1.15	0.30-0.40	0.20-0.30
ORD 4330V (Mod + Si)†	0.30-0.35	0.75-1.00	0.40	—	1.40-1.70	0.80-1.10	0.40-0.60	0.08-0.12

* Resulfurized

† 1.50 - 2.00 Ni; developed specifically for recoilless tubes.

phosphorous and sulfur contents do not exceed 0.015 percent thereby reducing the machineability but decreasing the brittleness. Processing the blanks follows a routine similar to that for small arms tubes. Tubular blanks are held upright with empty bores during heating and quenching for a uniform application of heat and coolant both internally and externally. When necessary, tube blanks are straightened while hot, by heating them to temperatures which do not exceed the tempering temperature.

Although not subjected to as elevated temperatures during firing as tubes in rapid fire weapons, artillery and recoilless tubes nevertheless reach tem-

peratures at which significant strength reductions occur. Figure 57 shows the effects of temperature on two gun steels. In conjunction with these curves, Table 12 lists the required reductions of area at ambient temperature and the Charpy V-notch impact requirements at -40°F for various ranges of yield strength for the modified SAE 4330 steel.

Other useful information includes thermal conductivity, specific heat, linear coefficient of thermal expansion, and the heat transfer coefficient. These are defined as

k , Btu/sec/ft²/°F/in, thermal conductivity
 c , Btu/lb/°F, specific heat
 α , in/in/°F, coefficient of linear expansion
 h , Btu/hr/ft²/°F, heat transfer coefficient

Heat transfer coefficients for various size tubes at various temperatures appear in Table 13. Curves for k , c , and α are plotted in Figure 58. Because all physical property data for gun steels are not available, the values shown by the curves are those for SAE 4130 and 4140 steels and may be considered as applying to gun steels as well. Differences in properties which may exist between those shown in the curves and those of gun steels will not be so large as to affect tube design.

2. Titanium Alloy

147. Titanium alloy†, as gun tube material, has some favorable qualities particularly for recoilless gun tubes where it has been used successfully. Some alloys have tensile strengths of over 160,000 psi. Titanium is 40 percent lighter than steel. At ambient temperatures, it is resistant to most corrosive media. It is readily shaped and heat treated. Increasing temperatures to 800°F increase toughness,

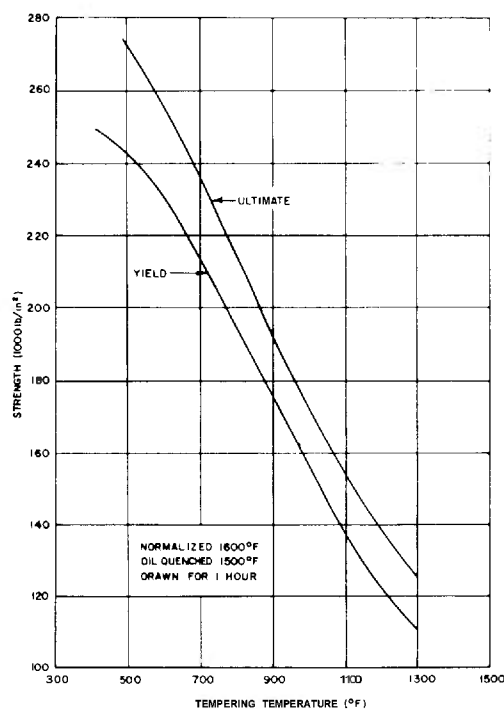


FIGURE 56. Effects of Tempering Temperature on Tensile Strength of SAE 4150 Steel.

* Reference 35, pages 218 and 221.

† Reference 37.

TABLE 12. REDUCTION OF AREA AND IMPACT REQUIREMENTS.
4330V (Mod + Si) Steel

Yield Strength 1000 psi	Percent Reduction of Area				Impact value at -40° ft-lb.			
	Average		Min. Single Value		Average		Min. Single Value	
	Trans.	Long	Trans.	Long	Trans.	Long	Trans.	Long
160	27	39	18	30	12	25	8	21
165*	25	38	17	29	11	23	8	20
170	23	38	16	29	10	21	7	18
175	21	37	15	29	10	19	7	16
180	20	37	14	29	10	17	7	14
185	20	36	14	28	10	15	7	12
190	20	36	14	28	10	15	7	12
195	20	35	14	27	10	15	7	12
200	20	35	14	27	10	15	7	12
205	20	35	14	27	10	15	7	12
210	20	35	14	27	10	15	7	12
215	20	34	14	26	10	15	7	12
220	20	34	14	26	10	15	7	12
225	20	34	14	26	10	15	7	12
230	20	34	14	26	10	15	7	12

* The upper limit in each range is one less than the lower limit in the succeeding range, e.g., 160—164, 999.

but tensile and yield strengths decrease, while the modulus of elasticity remains practically unaffected. The effects of aging processes on tensile strength are shown in Figure 59. Titanium also has many limita-

tions. It is a poor thermal conductor and therefore susceptible to high thermal stresses. Mechanical properties vary considerably, even within lots. Corrosion resistance at high temperatures is poor. Above 800°F, titanium has poor retention of mechanical properties (Figure 60). The coefficient of sliding friction is high while sliding surfaces gall and seize, wear poorly, and resist lubrication. Except for recoilless applications, these deficiencies render titanium practically useless as tube material. Not only in the origin of rifling region where temperatures are high and the severe abrasion of engraving

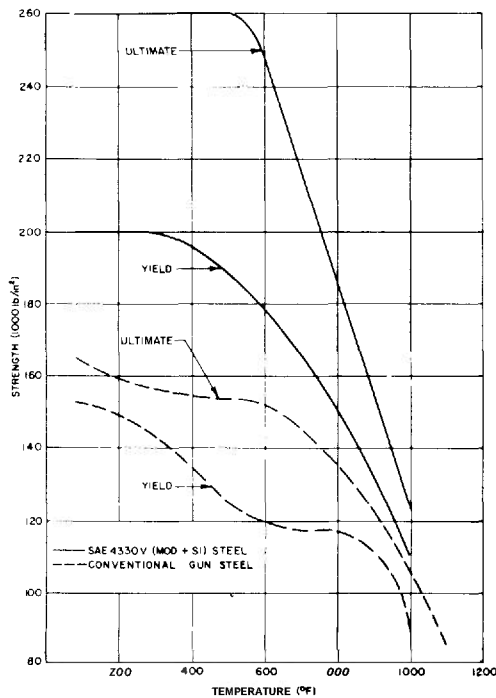


FIGURE 57. Effects of Temperature on Tensile Strength of Typical Steels for Recoilless Tubes.

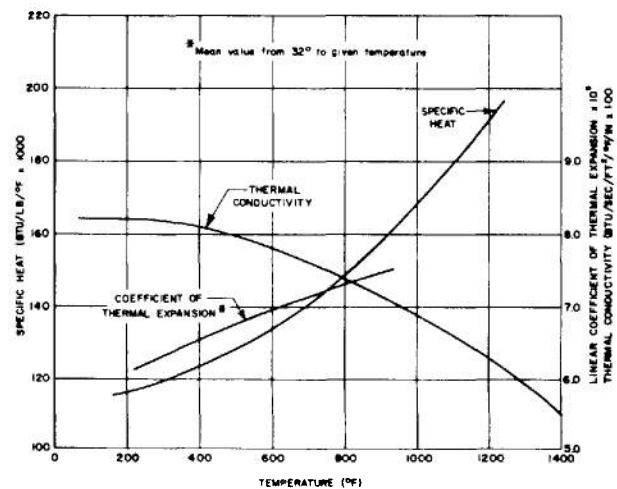


FIGURE 58. Physical Properties of Steel.

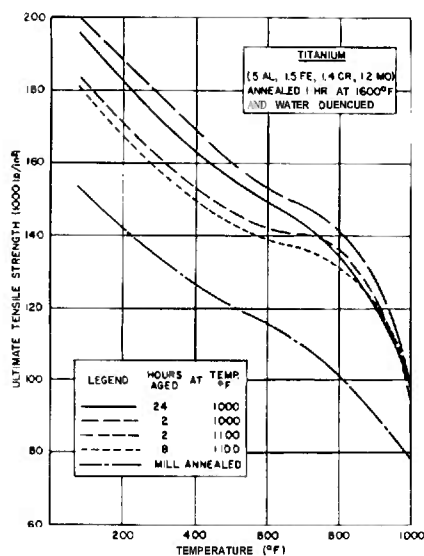


FIGURE 59. Effects of Aging Processes on Tensile Strength of Titanium at Various Temperatures.

takes place, but also in the rest of the bore the erosion rate is extremely high under normal firing conditions. Unless given a protective coating of some sort, titanium tubes are worthless. Since no satisfactory method for applying adherent coatings has been developed, any bore surface protection must be provided with liners.

For recoilless application, the advantages of titanium outweigh the disadvantages. Recoilless tubes erode at a rate less than either artillery or small arms tubes primarily because engraving action is eliminated by pre-engraved rotating bands and the propellant gases move at relatively low velocities. Low firing rates also keep temperatures at levels where tensile strength and erosion resistance are maintained. The adequate erosion and strength properties can be maintained only in the chamber

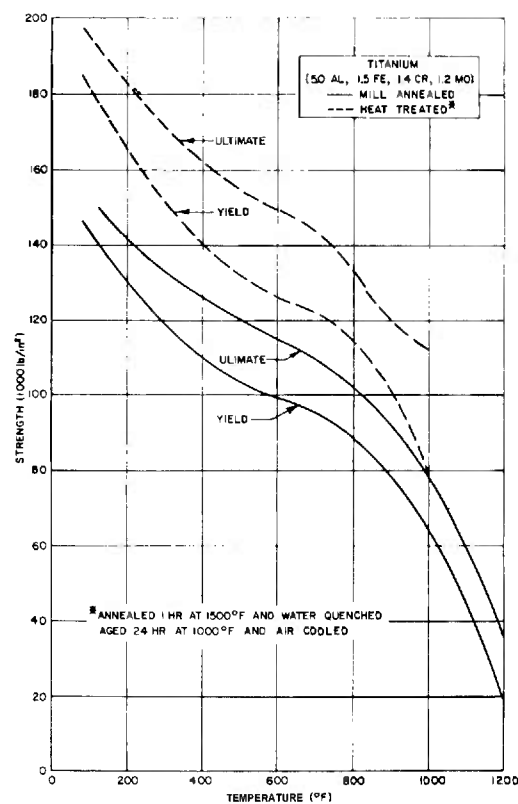


FIGURE 60. Effects of Temperature on Strength of Titanium Alloy.

and bore. In nozzles where gas velocities are considerably higher, titanium surfaces wear away rapidly. However, the protection offered by thin steel liners inhibits rapid erosion thereby converting the otherwise vulnerable titanium nozzle to one as effective as steel.

148. The chemical composition of titanium alloys should be selected and specified to meet physical

TABLE 13. HEAT TRANSFER COEFFICIENTS, h^* .
(For Horizontal bare steel tube in atmosphere at 80°F)

Tube OD (in)	Δt , °F., Temperature Difference from Tube Surface to Air														
	50	100	150	200	250	300	400	500	600	700	800	900	1000	1100	1200
.96	2.12	2.48	2.76	3.10	3.41	3.75	4.47	5.30	6.21	7.25	8.40	9.73	11.20	12.81	14.65
1.32	2.03	2.38	2.65	2.98	3.29	3.62	4.33	5.16	6.07	7.11	8.25	9.57	11.04	12.65	14.48
2.38	1.93	2.27	2.52	2.85	3.14	3.47	4.18	4.99	5.80	6.92	8.07	9.38	10.85	12.46	14.28
4.45	1.84	2.16	2.41	2.72	3.01	3.33	4.02	4.83	5.72	6.75	7.89	9.21	10.66	12.27	14.09
8.63	1.76	2.06	2.29	2.60	2.89	3.20	3.88	4.68	5.57	6.60	7.73	9.05	10.50	12.10	13.93
12.75	1.71	2.01	2.24	2.54	2.82	3.13	3.83	4.61	5.50	6.52	7.65	8.95	10.42	12.03	13.84
24.00	1.64	1.93	2.15	2.45	2.72	3.03	3.70	4.48	5.37	6.39	7.52	8.83	10.28	11.90	13.70

* Reference 36, page 179.

requirements. Interstitial impurities such as carbon, hydrogen, nitrogen, and oxygen if present in more than a few tenths of one percent promote brittleness and notch fatigue. Generally the maximum impurities tolerated are: carbon, 0.05%; hydrogen, 0.01%; nitrogen, 0.04%; oxygen 0.19%. Mechanical properties are obtained by heat treatment so that the values arranged in Table 14 will correspond with the specified strength limits.

3. Aluminum

149. Aluminum tubes (cal. .50) have been tested for expendable weapons. They were not durable, just a few fired rounds removed the rifling completely from the bore. By being able to last for several rounds, aluminum tubes are well suited for the expendable weapon. Pre-engraving may extend its life a little longer but, to prolong its life appreciably, the aluminum tube must be lined or plated with erosion resistant material. Even so, aluminum alloy tubes are limited to moderately elevated temperatures and hence, to slow fire. Some of the alloys weaken appreciably at 200°F; others maintain their strength fairly well to 400°F. Both temperatures are exceeded during extended firing, consequently discouraging the use of aluminum for gun tubes for any but special cases.

4. Plastics

150. As gun tube material, plastics, in their present state, are in the same category as aluminum, i.e., restricted to special applications such as the expendable tube. Plastics have poor retention of strength at moderately high temperatures but improve in this respect when reinforced with fibrous glass. At least one sporting gun currently on the market has a fiberglass barrel with a steel liner. Others are in the experimental stage. However, no data are available on their ability to withstand the high temperatures generated by prolonged, rapid fire.

In general, fiberglass reinforced plastics, *FRP*, offer many advantages that may be applied to gun

TABLE 14. MINIMUM MECHANICAL PROPERTY REQUIREMENTS OF TITANIUM ALLOYS. (MIL-T-46038)

Yield Strength (0.10% offset) 1000 psi	Ave Elongation %	Ave Reduction of Area %	Ave V-notch Charpy Impact (-40°F) ft-lb
120			
130*	14	29	15
140	12	26	12
150	11	23	11
160	10	21	10
170	8	18	8
180	8	18	8
190	7	16	7
200	7	14	7
210	6	13	6

* The upper limit in each range is one less than the lower limit in the succeeding range, e. g., 120,000 to 129,999.

tubes, provided that steel or other type liners are used to weather the erosive activity of propellant, and projectile. These advantages are summarized:

1. relatively high strength
2. high strength-weight ratio
3. usable in temperatures as high as 400° to 600°F
4. high impact strength
5. low specific gravity
6. chemically resistant
7. low cost

A review of the various resin types indicates that phenolic resin offers the best properties as gun tube material.* Table 15† shows the relative properties of several representative gun tube materials, including the specific strength and the ratio of tensile strength to specific gravity. The values in Table 15 are not optimum for the various materials, but are shown as mere approximations of one type of each material. Note that, the plastic material far sur-

* Table 10, Reference 38.

† Table 13, Reference 38.

TABLE 15. PROPERTIES OF REPRESENTATIVE GUN TUBE MATERIALS.

Material	Specific Gravity sp. gr.	Mod of Elasticity $E \times 10^{-6}$ psi	Actual Tensile Str. psi	Specific Str. TS/sp. gr. psi
FRP	1.9	5.7	152,000.	80,000.
Aluminum	2.7	9.7	81,000.	30,000.
Titanium	4.5	16.2	126,000.	28,000.
Steel	8.0	29.0	240,000.	30,000.

TABLE 16. THERMAL COEFFICIENT OF LINEAR EXPANSION OF STELLITE 21*.

Temp. Range °F	$\alpha \times 10^6$ per °F	Temp. Range °F	$\alpha \times 10^6$ per °F
70-600	7.83	70-1500	8.68
70-800	7.96	70-1600	8.72
70-1000	8.18	70-1800	8.90

* Reference 35, page 429.

passes the metals in specific strength. A titanium alloy is available with tensile strength of 200,000 psi. Its specific strength of 44,000 psi is better than steel but still far below that of the glass fiber reinforced plastic.

5. Stellite

151. Of the various high temperature resistant materials tested for small arms tube liners, Stellite has the best properties. Because of its high melting point and resistance to erosion, more rounds can be fired at faster rates than with other materials. Stellite 21 (MIL-C-13358) is the liner material currently being used. Although Stellite is brittle at ambient temperatures, the steel tube cover prevents expansion and resulting failure. At high temperatures, the mechanical properties of Stellite are ideally suited for liners. Tensile strength ranges from 120,000 psi at 70°F to 33,000 psi at 1800°F. Ductility improves with increase in temperature. Blank liners are received as tubular castings which are precision machined to fit the tube. Stellite liners are restricted to short lengths primarily because of

clearance limitations during shrink fit assembly (see Chapter 6-I, Liner Design). Stellite liners may not be the final solution; scarcity of cobalt and difficulty in processing are still major problems. Although machine gun tube performance has been improved remarkably, experimentation continues. New materials with improved characteristics are now available but are classified and will not be discussed here.*

Stellite 21 has the following chemical composition:

0.22% C, 62.2% Co, 27.4% Cr, 0.70% Fe
0.66% Mn 5.5% Mo 2.8% Ni 0.53% Si

Physical properties available include the density at 70°F of 0.229 lb/in³ and the thermal coefficient of linear expansion over several ranges of temperatures. Some are shown in Table 16.

The mechanical properties at various temperatures are listed in Table 17.

6. Chromium

152. Of the various metals plated to the surface of gun bores chromium was found superior to molybdenum, tungsten, tantalum, nickel, cobalt and copper†. The melting points of nickel, cobalt and copper are too low. Of the remaining, only chromium can be electrodeposited readily. Alloys of molybdenum and tungsten have been deposited on bore surfaces but low-hardness and uncertain adhesion make them inferior to chromium. This leaves chromium as the only metal that can be electrodeposited and can approach the chemical

* Reference 39.

† Reference 40, page 5.

TABLE 17. MECHANICAL PROPERTIES OF STELLITE 21.*

Form or 1 Condition	Temp. °F	UTS 1000 psi	YS 100 psi	Elong. %	Red Area %	E 10 ⁶ psi
A	Room	101.3	82.3	8.2	9.0	36.0
A	1000	69.1	30.1	16.4	25.3	33.0
B	1000	86.2	74.4	1.2	4.3	35.0
A	1200	74.2	38.0	5.7	36.0	33.7
B	1200	89.3	71.3	2.0	6.0	23.9
B	1350	79.3	61.5	3.8	9.0	24.2
B	1500	59.0	49.0	6.8	19.7	16.8
H	1600	41.6	32.8	19.3	23.2	15.4
A	1700	42.5	—	27.0	52.4	—
A	1800	33.3	—	35.0	52.4	—
C	1800	32.9	—	49.0	63.1	—

1. A: as cast, B: 1350°F, 50 hr. C: 1700°F, 16 hr.

* Reference 35, page 428.

TABLE 18. SURFACE FINISHES OF GUN TUBES, RMS.

Surface	Artillery	Recoilless	Small Arms
Exterior	125-250	63-250	63
Bore	8-16	16	32
Grooves	16-32	16	32
Chamber	32	3%	32
Breech Threads	16	16	32
Sliding	16-32	—	32
Shrink Fit	63	—	63

and physical properties required for plating gun bores. These properties include: erosion resistant, high melting point, high strength and hardness when heated, ductility when hot or cold, no abrupt volume change with temperature, and chemical resistant to propellant gases. Techniques have been developed which exploit the properties of chromium when applied to gun barrels.

M. MANUFACTURING PROCEDURES

153. The procedure for manufacturing gun tubes follows normal machine shop activity of turning, grinding, boring, honing, and broaching arranged in well-established, sequential order. However, the operations are unique in their application. Gun tubes, because of their large slenderness ratio, require considerable care in maintaining concentricities and

alignments. Inspections and tube straightening follow each series of machining operations to insure the two requirements. Surface finishes and tolerances, particularly in the bore, are demanding. Tolerance in the bore does not exceed 0.002 in. regardless of the diameter. Finishes normally associated with the various inner and outer surfaces of each tube type are listed in Table 18.

154. Tube blanks for large bore guns are either rough machine forgings or centrifugal castings, and for small bore guns the blanks are solid rolled forging bar stock heat treated to specifications. For each machining operation, the tube must be properly aligned by indicator to assure the cutting operation running true. After initial rough turning and boring, straightness is checked with the bore as the reference. This is done optically in small arms. Magnetic particle inspection at various stages of completion exposes any surface flaws which may be present. Artillery tubes are so inspected before coldworking or shrink fit and after final machining. Small arms tubes are magnetically inspected before machining, before reaming and rifling the bore, and after proof firing. Because of their small size, cutting tools for small arms present problems involving chip clearance and lubrication. These problems are discussed fully elsewhere.*

* Reference 39.

CHAPTER 7

MAINTENANCE

Maintenance of gun tubes is usually restricted to the preventive processes inasmuch as the tube wall, regardless of how slight its failure, cannot be repaired for further use. This limits corrective maintenance to the repair of the bore surface.

A. CORROSION INHIBITORS

155. Preventive maintenance begins at the completion of manufacture when corrosion inhibitors are applied. The exposed outer surfaces of large caliber tubes are painted. Those of small arms are phosphatized, a process which provides protection from normal exposure. Exposed sliding surfaces are oiled. Bore surfaces may be protected by oil or plating. These surfaces are oiled immediately after manufacture and after each firing session. Plating is used primarily as an erosion resistant measure, although it does prevent corrosion until worn off by propellant and projectile activity. Then the exposed surface must receive the same care as the unplated tube.

B. INSPECTION

156. Inspection is carried on throughout manufacturing to detect any flaws which may develop. Rifling is one of the critical items on the schedule, not only to insure good machining and correct size but also to check the angle of twist. The angle can be computed from Equations 9f or 9i for any position in the bore. It may be measured with a rotating cylinder equipped with radial pins which fit snugly in the grooves and ride on the edges of the lands. The cylinder is positioned in the bore by a rod attached to it. The rod indicates the bore travel and turns a dial which indicates the angular dis-

placement of the rifling which should correspond in degrees with the computed angle. Increasing twist rifling has such a small angular displacement adjacent to the origin that starting measurements at the muzzle becomes more practical from the viewpoint of correlating rifling twist with travel.

157. Frequent, diligent inspection of the bore while in service is essential from the viewpoint of safety as well as that of effectiveness. Visual inspection, aided or unaided by a borescope, followed by star and plug gaging are methods of inspection. The bore should be free of dirt, grit, rust and propellant fouling. Mild coppering, like mild erosion, is not detrimental. Only coppering severe enough to impede firing is detrimental. A clean bore is not necessarily shiny but may be a dull gray. A shiny, polished surface may indicate the use of abrasive cleansers. Scratches, nicks, pitting and scoring permit gas leakage which aggravates erosion and reduces muzzle velocity with a subsequent loss in range. These defects must be smoothed even with the original surface and all sharp edges rounded. Advancement of the forcing cone caused by erosion, and the spalling and crushing of the rifling lands are other damaging factors. The location, character, and extent of any damage determines whether the tube is still serviceable. Plug gaging helps to determine the extent of erosion at the origin of rifling and is sometimes correlated with accuracy life. Otherwise, no specific rules on serviceability exist for field inspection. Experience, therefore, becomes the qualifying trait in those who evaluate the condition of the tube. Where facilities are available, barrel life is determined by proof firing and is based on velocity drop and on loss of accuracy.

CHAPTER 8

SAMPLE PROBLEMS

A. MONOBLOC TUBE, ARTILLERY

1. Regular Tube*

158. A 100 mm gun tube is selected for the sample design problem of artillery tubes. The 100 mm bore avoids confusion with existing weapons. The problem is to determine the wall thickness of a regular tube at all points for the interior dimensions of chamber and bore and for the pressures along the tube shown in Figure 61. These pressures are the computed design pressures discussed in paragraph 112. For this analysis, the tube is assumed to be smooth bore and made of SAE 4150 steel having a yield strength of 160,000 lb/in². Artillery tube design procedures do not include stress concentrations induced by the rifling other than by adopting the compensating measure of extending the inside diameter to the grooves. This analysis, therefore, would also apply to a rifled tube have a groove diameter of 100 mm.

The design pressure is the maximum pressure to which any given tube section is subjected under any expected service or test condition. To ensure safe firing, the tube is designed for 105 percent of this pressure or $1.05p$. No permanent bore enlargement during firing being permitted, the equivalent stress is limited to the elastic limit, σ_L , of the material which, in this application, is 10,000 lb/in² less than the yield strength, or $\sigma_L = 150,000$ lb/in². Longitudinal stresses, being negligible, are omitted.

The required wall ratios and consequently the outside diameters are found by modifying Equation 55b. Substitute σ_e for Y and increase the pressure to incorporate a factor of safety of 1.05, then solve for σ_e .

$$\sigma_e = \frac{\sqrt{3W^4 + 1}}{W^2 - 1} 1.05p_m \quad (80)$$

where

p_m = computed pressure, based on *PIMP*

$p = 1.05p_m$ = design pressure

W = wall ratio.

If D_i is the inside diameter, the outside diameter is

$$D_o = WD, \quad (81)$$

* Submitted by Watervliet Arsenal.

The equivalent stress in this problem must not exceed the elastic limit, σ_L , 150,000 lb/in². The required wall ratio for any pressure along the bore may now be computed by Equation 80 or obtained from Table 10, where p/Y is equivalent to p/σ_L . Table 19 lists the design data of the theoretical tube.

159. The tabulated dimensions for the outside diameter establishes the contour of minimum wall thicknesses. This theoretical contour and the actual contour are shown in Figure 61. The walls of the tube are generally made thicker than the minimum requirements for practical reasons such as: provide compatibility with dimensions of mating components, provide the necessary rigidity to minimize droop, provide ease of manufacture with cylindrical or conical surfaces rather than curvatures along the length. Actual wall thicknesses exceed the design thickness everywhere except at the breech end where one-half inch continuous buttress threads appear over a length of five inches to provide for the attachment of the breech ring. This structure reinforces the gun tube, providing ample overall strength. For pressure stress calculations, the pitch diameter is assumed to be the effective outside tube diameter. The diameter of the chamber forward of the thread exceeds the thread major diameter so that ample clearance is provided when the tube slides through the recoil mechanism during assembly. The elastic strength pressure (*ESP*), the actual pressure that

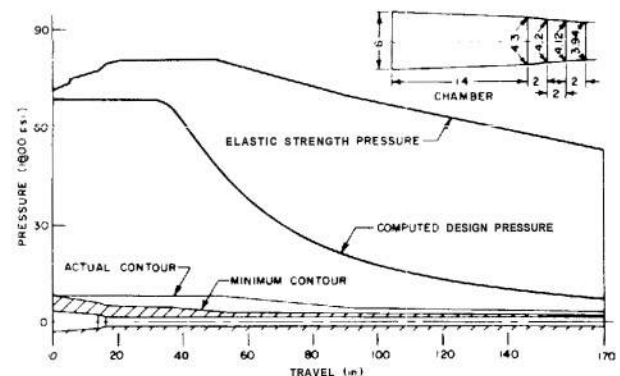


FIGURE 61. Design Data, Monobloc Artillery Tube.

TABLE 19. DESIGN DATA OF THEORETICAL MONOBLOC TUBE.

Dist. From Breech (in.)	p^* (psi)	p/σ_L	W	D_i (in.)	D_o (in.)
0	72100	.483	2.503	6.00	15.02
14	72100	.483	2.503	4.80	12.01
16	72400	.483	2.503	4.20	10.51
20	72400	.483	2.503	3.94	9.86
32	72400	.483	2.503	3.94	9.86
40	61600	.431	2.46	3.94	7.91
50	50100	.336	1.575	3.94	6.20
60	39900	.266	1.388	3.94	5.47
70	32600	.217	1.288	3.94	5.07
80	26300	.175	1.217	3.94	4.79
90	22100	.147	1.175	3.94	4.63
100	18900	.126	1.145	3.94	4.51
120	14200	.095	1.105	3.94	4.35
140	10500	.070	1.075	3.94	4.24
160	8400	.056	1.058	3.94	4.17
170	7600	.051	1.053	3.94	3.15

* See Table 21 for values of computed design pressure, p_m .

the tube can sustain at any section, is computed from Equation 55b, or interpolated from Table 10, by substituting ESP for p , and σ_L (150,000) for Y and leads to the factor of safety of the tube.

$$S_f = \frac{ESP}{p} \quad (82)$$

This and other design data of the actual tube appear in Table 20.

2. Autofrettaged Tube*

160. Theoretical wall ratios are to be determined for the 100 mm tube, prestressed by autofrettage practices. A factor of safety of 1.2 applied to the design pressures, instead of the customary 1.05, is prescribed by Watervliet Arsenal to allow for some uncertainties in the design procedures which have not been completely identified and rationalized. The tube outlines with corresponding design pressure data are similar to those of Figure 61. If p is substituted for ESP in Equation 64b, and the 1.2 factor of safety is included, the expression for natural logarithm of the wall ratio becomes

$$\ln W_f = \frac{1.2p}{1.08Y} = 1.11 \frac{p}{Y}$$

For SAE 4150 steel, having a yield strength of

* Submitted by Watervliet Arsenal.

TABLE 20. DESIGN DATA OF ACTUAL MONOBLOC TUBE.

Dist. From Breech (in.)	D_i (in.)	D_o (in.)	W	ESP/σ_L	ESP (psi)	p (psi)	S_f^*
0	6.00	15.0	2.50	.483	72400	72400	1.00
5	5.57	15.0	2.69	.496	74100	72400	1.03
5	5.57	15.4	2.76	.500	75000	72400	1.06
14	1.8	15.4	3.21	.520	78000	72400	1.08
16	4.2	15.4	3.67	.534	80100	72400	1.10
20	3.94	15.4	3.91	.539	80800	72400	1.11
50	3.94	15.4	3.91	.539	80800	72400	1.60
90	3.94	8.0	2.03	.433	64900	72400	2.93
170	3.94	6.5	1.65	.358	53700	72400	7.06

* Based on 1.05 computed design pressure.

160,000 psi before cold working, the expression becomes $\ln W_f = p/144,000$.

The values for pressure from the pressure-travel curve are now substituted for p at suitable intervals along the tube length and the values of $\ln W_f$ determined, as shown in Table 21. The values of W_f are then obtained by reference to a table of natural logarithms, and the required outside diameters calculated by referring to Table 21.

161. Following the same practice as that for the monobloc tube, preceding, the wall thicknesses are increased for practical considerations. Since the wall ratios are known, the ESP is readily computed from Equation 61b. The factor of safety becomes that of Equation 82. The factors of safety and other design data of the actual autofrettaged tube appear in Table 22.

B. JACKETED TUBE, ARTILLERY

1. Tube With Single Jacket†

162. A 100 mm single jacketed tube, i.e., liner with one jacket, is selected as an example of a shrink fit type tube construction. The shrink fit is determined first at the breech end where the wall ratio is critical. The selection of wall ratio here involves trial and error. Approximate values may be obtained by either Equation 29a or 37. Equation 29a, by yielding wall ratios larger than needed, is more conservative. Although Equation 37 is based on stresses developed in a closed cylinder, it yields wall ratios closer to the required value and hence, is used in the sample problem. After the tube wall ratio is estimated, the wall

† Submitted by Watervliet Arsenal.

ratios of tube and jacket are determined, to be followed by the calculations for the elastic strength pressure (*ESP*) for each component. The tube shown in Figure 62 is analyzed to learn whether it can sustain the pressures at various locations along its length measured from the breech.

The following are the design data at the breech:

$$D_i = 6.0 \text{ in.}, \text{ inside diameter}$$

$$p_m = 69,000 \text{ psi, computed design pressure, based on PIAP}$$

$$S_f = 1.05$$

$$p = 1.05 p_m = 72,400 \text{ psi}$$

$$\sigma_L = 150,000 \text{ lb/in}^2, \text{ elastic limit}$$

According to Equation 37,

$$W = \frac{1}{1 - \frac{1.732p}{2\sigma_L}} = 1.724$$

Therefore, $D_o = 1.724 D_i = 10.344 \text{ in.}$ To confine the outer diameter to nominal dimensions, increase D_o to 10.5 in and W to 1.73. According to Equations 29b and 29c, the liner and jacket wall ratios are

$$W_L = W_J = \sqrt{W} = 1.323$$

$$\text{and } D_J = 1.323 D_i = 7.94 \text{ in.}$$

163. The next problem is that of finding the interference necessary for shrink fit and the subsequent elastic strength pressure when this pressure will

TABLE 21. DESIGN DATA OF THEORETICAL AUTOFRETTAGED TUBE.

Dist. From Breech (in.)	p_m (psi)	$\ln W_f$	W_f	D_i (in.)	D_o (in.)
0	69000	.479	1.614	6.0	3.68
14	69000	.479	1.614	4.8	7.75
16	69000	.479	1.614	4.2	6.78
20	69000	.479	1.614	3.94	6.36
32	69000	.479	1.614	3.94	6.36
40	61500	.427	1.533	3.94	6.04
50	48000	.333	1.395	3.94	5.50
60	38000	.264	1.302	3.94	5.13
70	31000	.215	1.240	3.94	4.89
80	25000	.171	1.190	3.94	4.69
90	21000	.146	1.157	3.94	4.57
100	18000	.125	1.133	3.94	4.46
120	13500	.094	1.099	3.94	3.33
140	10000	.069	1.071	3.94	4.22
160	8000	.056	1.058	3.94	4.18
170	1200	.050	1.051	3.94	4.14

TABLE 22. DESIGN DATA OF ACTUAL AUTOFRETTAGED TUBE.

Dist. From Breech (in.)	D_i (in.)	D_o (in.)	W_f	$\ln W_f$	ESP (psi)	p_m (psi)	S_f^*
0	6.0	9.75	1.625	.485	83800	69000	1.21
5	5.57	9.75	1.750	.560	96800	69000	1.10
5	5.57	10.0	1.795	.585	101100	69000	1.16
14	4.8	10.0	2.083	.734	126800	69000	1.84
16	4.2	10.0	2.381	.868	150,000	69000	2.17
20	3.94	10.0	2.538	.931	160,900	69000	2.33
50	3.94	10.0	2.538	.931	160,900	48000	3.35
90	3.94	7.75	1.967	.676	116,800	21000	5.56
170	3.94	6.50	1.65	.501	86600	7200	12.0

* Based on computed design pressure.

induce the maximum equivalent stress. By designating the elastic strength pressure as the applied pressure ($p = ESP$), the tangential stress at the inner surface of the liner according to Equation 30b becomes

$$\sigma_t = ESP \frac{W^2 + 1}{W^2 - 1} - 2p_s \frac{W_L^2}{W_L^2 - 1}$$

The radial stress (Equation 30c) is

$$\sigma_r = -ESP$$

Substitute these expressions in Equation 24 and replace σ_L , on the assumption that the equivalent stress will be equal to the elastic limit, and then solve for ESP . Before proceeding, collect the complex expressions and condense them into simple terms so the final equations will be less complicated. The expressions and their numerical values for the first trial calculation are

$$D_i = 6.0 \text{ in., ID liner} \quad W_L = \frac{D_i}{D_i} = 1.323$$

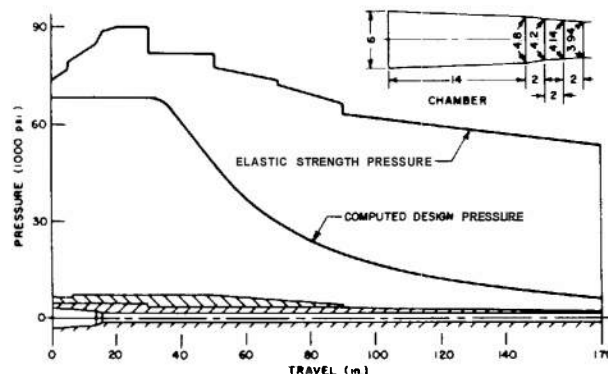


FIGURE 62. Design Data, Jacketed Artillery Tube.

$D_1 = 7.94$ in., OD inner, ID jacket

$$W_J = \frac{D_o}{D_1} = 1.323$$

$$D_o = 10.5 \text{ in., OD jacket} \quad W = \frac{D_o}{D_1} = 1.750$$

$$A = \frac{W_L^2}{W_L^2 - 1} = 2.333 \quad C = \frac{W_J^2 + 1}{W^2 - 1} = 1.334$$

$$B = \frac{W^2 + 1}{W^2 - 1} = 1.970 \quad F = \frac{W_J^2 - 1}{W^2 - 1} = 0.364$$

$$G = B^2 + B + 1 = 6.851$$

$$H = A + 2AB = 11.525$$

$$J = C^2 + CF + F^2 = 2.$$

The solution for the elastic strength pressure of the liner is

$$ESP_L = \frac{Hp_s + \sqrt{G\sigma_L^2 - 3A^2p_s^2}}{G} \quad (83)$$

The tangential stress at the inner surface of the jacket induced by the elastic strength pressure and the shrink fit pressure is, according to Equations 25 and 26,

$$\sigma_t = ESP \frac{W_J^2 + 1}{W^2 - 1} + p_s \frac{W_J^2 + 1}{W^2 - 1}$$

The radial stress, combining the effects of Equations 27a and 27b, is

$$\sigma_r = ESP \frac{W_J^2 + 1}{W^2 - 1} - p_s$$

By substituting these expressions in Equation 24 and collecting terms, the solution for ESP of the jacket becomes

$$ESP_J = \frac{\sigma_L}{\sqrt{J}} - \frac{p_s}{F} \quad (84)$$

The shrink fit pressure is obtained by solving for p_s in Equation 32c.

$$p_s = \frac{E}{2D_1} (W_L^2 - 1) F \delta \quad (85)$$

164. Only the interference remains to be determined. It becomes available by stressing the jacket to the limit as its most critical section, first by solving for the shrink fit pressure and then for the shrink fit interference. The total interference normally has a spread of 0.003 inch. The maximum interference is assigned to the analysis involving jacket whereas the minimum interference is confined to the liner analysis. Continuing with the numerical value estab-

lished earlier, and solving for p_s from Equation 84

$$p_s = F \left(\frac{\sigma_L}{\sqrt{J}} - \right) \\ = 0.364 \left(\frac{150,000}{1.548} - 72,450 \right) = 8870 \text{ psi}$$

Solving for δ_{max} as in Equation 85

$$\delta_{max} = \frac{2p_s D_1}{(W_L^2 - 1) E} \\ = \frac{2 \times 8870 \times 7.94}{.75 \times 0.364 \times 29.6 \times 10^6} = .017 \text{ in} \\ \delta_{min} = \delta_{max} - 0.003 = 0.014 \text{ in}$$

For the liner, substitute δ_{min} for δ in Equation 85

$$p_s = \frac{E}{2D_1} (W_L^2 - 1) F \delta_{min} \\ - \frac{29.6 \times 10^6}{2 \times 7.94} \times 0.75 \times 0.364 \times 0.014 = 7120 \text{ psi}$$

According to Equation 83

$$ESP = \frac{8.207 + \sqrt{1541 - 8.3}}{6.851} \times 10^4 = 69,000 \text{ psi}$$

Since this pressure stresses the liner to its limit, the liner is unable to contain an ESP of 72,400 psi without suffering permanent damage, therefore, a larger wall ratio is indicated. For the second trial, a 10.75 inch outside diameter is selected. The calculations for this section and all succeeding sections are arranged in sequence in Table 23.

2. Tube With Two Jackets

165. A tube for a heavy artillery gun is used to demonstrate the technique for determining the wall thickness and shrink fit conditions of a multilayered construction. Computations at the chamber section are given in this example. Calculations at other increments along the tube, if needed, are made in the same manner. The known design data are

$$D_i = 10.0 \text{ in., inside diameter}$$

$$n = 3, \text{ the number of layers}$$

$$p_m = 69,000 \text{ psi, computed design pressure, based on the PIMP}$$

$$S_f = 1.05, \text{ factor of safety}$$

$$p = S_f p_m = 72,400 \text{ psi}$$

$$\sigma_L = 150,000 \text{ lb/in}^2, \text{ elastic limit}$$

According to Equation 37, the wall ratio

$$W = \left[\frac{1}{1 - \frac{1.732p}{3\sigma_L}} \right]^{3/2} = 1.64$$

TABLE 23. ESP CALCULATIONS FOR SINGLE JACKETED, 100 MM TUBE.

Distance from Breech	0	5	5	14	16	20	30	30	50	50	70	70	90
D_1	6.0	5.571	5.571	4.8	4.2	3.94	3.94	3.94	3.94	3.94	3.94	3.94	3.94
D_2	8.0	8.0	8.0	8.0	8.0	8.0	7.75	7.75	7.75	7.75	7.75	7.75	7.75
D_0	0.75	10.75	11.0	11.0	11.0	11.0	11.0	11.0	11.0	11.0	9.625	9.625	8.25
W	1.792	1.930	1.975	2.292	2.619	2.792	2.792	2.792	2.792	2.792	2.443	2.443	2.094
W_L	1.333	1.436	1.436	1.667	1.905	2.030	1.967	1.967	1.967	1.967	1.967	1.967	1.967
W_f	1.344	1.344	1.375	1.375	1.375	1.375	1.419	1.419	1.419	1.242	1.242	1.065	1.065
J	2.287	1.942	1.942	1.562	1.380	1.320	1.349	1.349	1.349	1.349	1.349	1.349	1.349
β	1.905	1.734	1.689	1.470	1.341	1.294	1.294	1.294	1.403	1.403	1.403	1.391	1.391
ϵ	1.269	1.030	.997	.680	.493	.425	.444	.444	.414	.512	.512	.630	.630
F	.365	.296	.307	.210	.152	.131	.149	.149	.149	.109	.109	.109	.109
3.4^2	5.69	11.31	11.31	7.32	5.71	5.23	5.46	5.46	5.46	5.46	5.46	5.46	5.46
B^2	3.63	3.01	2.85	2.16	1.80	1.67	1.67	1.67	1.67	1.97	1.97	2.53	2.53
ϵ^2	1.61	1.06	.994	.462	.243	.181	.197	.197	.197	.262	.262	.397	.397
F^2	.133	.088	.094	.044	.023	.017	.022	.022	.022	.012	.012	.002	.002
AB	4.36	3.37	3.28	2.30	1.85	1.71	1.75	1.75	1.75	1.89	1.89	2.15	2.15
ϵF	.403	.305	.306	.143	.075	.056	.066	.066	.066	.056	.056	.025	.025
G	6.53	5.74	5.54	4.63	4.14	3.97	3.97	3.97	4.37	4.37	5.12	5.12	5.12
H	1.0	8.68	8.50	6.15	5.08	4.71	4.84	4.84	5.13	5.13	5.13	5.64	5.64
J	2.21	1.453	1.394	.649	.341	.254	.285	.285	.330	.330	.330	.124	.124
δ_{min}	.017	.017	.017	.017	.017	.017	.007	.003	.003	.003	.001	.001	.001
δ_{max}	.020	.020	.020	.020	.020	.020	.010	.006	.006	.006	.004	.004	.004
ps_L	8900	9900	10200	11800	12600	12800	5700	2450	1800	600	200	200	200
ESP_L	73400	77300	79200	85000	88800	90300	82300	78300	73800	72100	66500	66500	66500
ps_J	10400	11600	12100	13800	14800	15100	8200	4900	3600	2100	900	900	900
ESP_{φ}	72400	85100	87700	120000	160000	183000	226000	248000	228000	239000	208000	208000	208000

Therefore, $D_0 = 1.64 \times 10 = 16.40$ in. Increasing the OD to a nominal dimension, D_0 becomes 16.5 in. and W becomes 1.65. According to Equations 39a through 39e, the individual wall ratios of inner, intermediate tube, and outer tube are

$$W_{11} = W_{21} - W_{22} = W^{1/3} = 1.81$$

and of the inner and outer combinations of tubes are

$$W_{21} = W_{21} = W^{2/3} = 1.394$$

Thus $D_1 = 10$, $W_{11} = 11.81$ in and $D_2 = 10$ $W_{21} = 13.94$ in. From Equation 31, the total shrinkage pressure is

$$p_s = \frac{p^2}{4\sigma_L - 2p} = \frac{72,400^2}{600,000 - 144,900} = 11,520 \text{ psi}$$

According to Equation 40, the shrink fit pressure at each interface is

$$p_{s1} = p_{s2} = \frac{p_s}{2} = 5,760 \text{ psi}$$

166. The tangential and radial stresses due to shrink fit pressure at the various surfaces of the tube are computed by Equations 41a to 46b. From these shrink fit pressures and those induced by the design propellant gas pressure, the total effective

stress at the inner surface of the inner jacket exceeds the yield strength. The effective stresses at other regions are below the yield. To reduce the effective stress at the inner surface of the jacket to an acceptable value and also to realize a more efficient tube with respect to stress distribution, the shrink fit pressures are increased and the wall thickness of the three layers are modified according to the dimensions below.

$$D_1 = 10.0 \text{ in.} \quad D_1 = 11.67 \text{ in.}$$

$$D_0 = 16.75 \text{ in.} \quad D_2 = 13.75 \text{ in.}$$

$$W_{11} = 1.167 \quad W_{21} = 1.18$$

$$W_{21} = 1.375 \quad W_{21} = 1.438$$

$$W = 1.675 \quad W_{22} = 1.218$$

$$p_{s1} = 3300 \text{ psi} \quad p_{s2} = 6,750 \text{ psi}$$

According to Equations 41a and 41b, the stresses at the inner surface are

$$\sigma_{rs} = -2 \times 3300 \times \frac{1.36}{0.36} - 2 \times 6750 \times \frac{1.89}{0.89}$$

$$= -53,600 \text{ lb./in.}^2$$

$$\sigma_r = 0$$

Equations 42a and 42b yield the corresponding stresses on the outer surface

$$\begin{aligned}\sigma_{ts} &= -3300 \frac{2.36}{0.36} - 6750 \times 1.39 \frac{2.36}{0.89} \\ &= -46,500 \text{ lb/in}^2\end{aligned}$$

$$\sigma_{rs} = -3300 - 6750 \times 1.39 \frac{0.36}{0.89} = -7100 \text{ lb/in}^2$$

The two stresses (Equations 43a and 43b) on the inner surface of the inner jacket are

$$\begin{aligned}\sigma_{ts} &= 3300 \frac{2.39}{0.39} - 6750 \times 1.39 \frac{2.36}{0.89} \\ &= 20,200 - 24,800 = -4600 \text{ lb/in}^2\end{aligned}$$

$$\sigma_{rs} = -7100 \text{ lb/in}^2 \text{ (same as outer surface of liner)}$$

From Equations 44a and 44b, the two stresses on the outer surface of the inner jacket are

$$\begin{aligned}\sigma_{ts} &= 3300 \frac{2}{0.39} - 6750 \frac{2.89}{0.89} = 16,900 - 21,900 \\ &= -5000 \text{ lb/in}^2 \\ \sigma_{rs} &= -6800 \text{ lb/in}^2\end{aligned}$$

According to Equations 45a and 45b, the tangential and radial stresses at the inner surface of the outer jacket are

$$\begin{aligned}\sigma_{ts} &= 6750 \frac{2.48}{.48} = 34,900 \text{ lb/in}^2 \\ \sigma_{rs} &= -6800 \text{ lb/in}^2\end{aligned}$$

The stresses on the outer surface of the tube are found from Equations 46a and 46b.

$$\begin{aligned}\sigma_{ts} &= 6750 \frac{2}{.48} = 28,100 \text{ lb/in}^2 \\ \sigma_{rs} &= 0\end{aligned}$$

According to Equation 25, in terms of the wall ratios, the tangential pressure stress at any surface x of the composite tube is

$$\sigma_{tp} = p \frac{1}{W_x^2} \frac{W^2 + W_x^2}{W^2 - 1}$$

From Equation 27a, in terms of the wall ratios, the corresponding radial stress is

$$\begin{aligned}\sigma_{rp} &= -p \frac{1}{W_x^2} \frac{W^2 - W_x^2}{W^2 - 1} \\ W^2 &= 2.80\end{aligned}$$

At the inner surface of the liner, i.e., the bore surface, $W_x = 1$

$$\sigma_{tp} = 72,400 \frac{3.80}{1.80} = 153,000 \text{ lb/in}^2$$

$$\sigma_{rp} = -p = -72,400 \text{ lb/in}^2$$

At the interface between liner and inner jacket,

$$W_x^2 = W_{1i}^2 = 1.36$$

$$\sigma_{tp} = 72,400 \frac{1}{1.36} \times \frac{4.16}{1.80} = 123,000 \text{ lb/in}^2$$

$$\sigma_{rp} = -72,400 \frac{1}{1.36} \times \frac{1.44}{1.80} = -42,600 \text{ lb/in}^2$$

At interface between inner and outer jacket,

$$W_x^2 = W_{2i}^2 = 1.89$$

$$\sigma_{tp} = 72,400 \frac{1}{1.89} \times \frac{4.69}{1.80} = 100,000 \text{ lb/in}^2$$

$$\sigma_{rp} = -72,400 \frac{1}{1.89} \times \frac{2.91}{1.80} = -19,400 \text{ lb/in}^2$$

At the outer surface of the composite tube, $W_x = W$

$$\sigma_{tp} = 72,400 \frac{2}{1.80} = 80,500 \text{ lb/in}^2$$

$$\sigma_{rp} = 0$$

Combine the shrink fit with the pressure stresses at the various surfaces. Inner surface of liner

$$\sigma_t = \sigma_{tp} + \sigma_{ts} = 133,000 - 53,600 = 99,400 \text{ lb/in}^2$$

$$\sigma_r = \sigma_{rp} + \sigma_{rs} = -72,400 + 0 = -72,400 \text{ lb/in}^2$$

Outer surface of liner

$$\sigma_t = \sigma_{tp} + \sigma_{ts} = 123,000 - 46,500 = 76,500 \text{ lb/in}^2$$

$$\begin{aligned}\sigma_r &= \sigma_{rp} + \sigma_{rs} = -42,600 - 7100 \\ &= -49,700 \text{ lb/in}^2\end{aligned}$$

Inner surface of inner jacket

$$\sigma_t = \sigma_{tp} + \sigma_{ts} = 123,000 - 4600 = 118,400 \text{ lb/in}^2$$

$$\begin{aligned}\sigma_r &= \sigma_{rp} + \sigma_{rs} = -42,600 - 7100 \\ &= -49,700 \text{ lb/in}^2\end{aligned}$$

Outer surface of inner jacket

$$\sigma_t = \sigma_{tp} + \sigma_{ts} = 100,000 - 5000 = 95,000 \text{ lb/in}^2$$

$$\begin{aligned}\sigma_r &= \sigma_{rp} + \sigma_{rs} = -49,400 - 6800 \\ &= -56,200 \text{ lb/in}^2\end{aligned}$$

Inner surface of outer jacket

$$\begin{aligned}\sigma_t &= \sigma_{tp} + \sigma_{ts} = 100,000 + 34,900 \\ &= 134,900 \text{ lb/in}^2\end{aligned}$$

$$\begin{aligned}\sigma_r &= \sigma_{rp} + \sigma_{rs} = -19,400 - 6800 \\ &= -26,200 \text{ lb/in}^2\end{aligned}$$

Outer surface of tube

$$\sigma_t = \sigma_{tp} + \sigma_{ts} = 80,500 + 28,100 = 108,600 \text{ lb/in}^2$$

$$\sigma_r = \sigma_{rp} + \sigma_{rs} = 0$$

The critical stresses occur at the inner surfaces of all three tubes. According to Equation 24, the total mean effective stress at each location is:

Liner,	$\sigma_e = 149,500 \text{ lb/in}^2$
Middle Tube,	$\sigma_e = 149,600 \text{ lb/in}^2$
Outer Tube,	$\sigma_e = 149,800 \text{ lb/in}^2$

167. The required interference between liner and inner jacket and between outer and inner jacket are found by solving Equations 63a to 63d. Poisson's ratio for steel is 0.30, and $E = 29 \times 10^6 \text{ lb/in}^2$. From Equation 63a,

$$\delta_{oi} = -\frac{11.67 \times 3300}{29 \times 10^6 (136 - 100)} [136(1.0 - 0.3) + 100(1.0 + 0.3)] = -0.0083 \text{ in.}$$

From Equation 63b,

$$\delta_{oi} = \frac{11.67 \times 3300}{29 \times 10^6 (189 - 136)} [136(1.0 - 0.3) + 189(1.0 + 0.3)] = 0.0086 \text{ in.}$$

Since both outer diameter of liner and inner diameter of the inner jacket decreased under the assigned conditions and diametral interference needed between these two members is, according to Equation 63i

$$\delta_i = 0.0083 + 0.0086 = .0169 \text{ in.}$$

From Equation 63c,

$$\delta_{oi} = \frac{13.75 \times 6750}{29 \times 10^6 (189 - 100)} [189(1.0 - 0.3) + 100(1.0 + 0.3)] = -0.0094 \text{ in.}$$

From Equation 63d,

$$\delta_{oi} = \frac{13.75 \times 6750}{29 \times 10^6 (280 - 189)} [189(1.0 - 0.3) + 280(1.0 + 0.3)] = 0.0173 \text{ in.}$$

From Equation 63f, the diametral interference between the jackets is

$$\delta_i = .0094 + .0173 = .0267 \text{ in}$$

During assembly, when heated to 970°F, the increase in diameter at each interface is

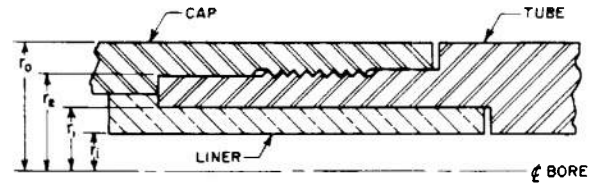


FIGURE 63. Schematic of Tube With Liner.

$$AD_1 = D_1 \alpha AT = 11.67 \times 7.5$$

$$\times 10^{-6} \times 900 = .0786 \text{ in}$$

$$AD_2 = D_2 \alpha AT = 13.75 \times 7.5$$

$$\times 10^{-6} \times 900 = .0927 \text{ in}$$

Where α is the mean linear coefficient of thermal expansion for steel through the temperature range of 32°–932°F*. The above diametral clearances are ample for the shrink fit process.

C. SMALL ARMS BARREL WITH SHRINK FITTED LINER AND CAP†

168. Shrink fit stresses are combined with pressure stresses for a shrink fitted small arms tube with stellite liner which is shown schematically in Figure 63. For brevity, stresses are computed in one location only. The design data are listed below.

- $r_i = .150 \text{ in.}$ internal radius (caliber .30)
- $r_1 = .250 \text{ in.}$ OR liner; IR tube
- $r_2 = .375 \text{ in.}$ OR tube; IR cap
- $r_o = .500 \text{ in.}$ OR cap
- $p_d = 32,000 \text{ psi.}$ design propellant gas pressure
- $E_J = 30 \times 10^6 \text{ psi.}$ modulus for steel (jacket)
- $E_L = 35 \times 10^6 \text{ psi.}$ modulus for stellite (liner)
- $\delta_1 = .00025 \text{ in.}$ interference between tube and liner‡
- $\delta_2 = .00045 \text{ in.}$ interference between tube and cap‡
- $\nu_J = 0.3,$ Poisson's ratio of steel
- $\nu_L = 0.3,$ Poisson's ratio of stellite

1. Shrink Fit Pressure

Shrink fit, pressure between tube and liner is calculated from Equation 73b. Here the various radii are

$$a = r_i = .150 \text{ in}$$

$$b = r_1 = .250 \text{ in}$$

$$c = r_2 = .375 \text{ in}$$

* Reference 35, page 221.

† Submitted by Springfield Armory.

‡ These interferences have been established by practice.

$$p_{s1} = \frac{.00025 \times 10^6}{.25 \left[\frac{1}{30} \left(\frac{.1406 + .0625}{.1406 - .0625} + .3 \right) + \frac{1}{35} \left(\frac{.0625 + .0225}{.0625 - .0225} - .3 \right) \right]} = 6720 \text{ psi}$$

The shrink fit pressure between tube and cap is determined by considering the liner-tube assembly a homogeneous unit and solving for the shrink fit pressure by Equation 73a. Here the various radii are

$$a = r_i = .150 \text{ in}$$

$$b = r_2 = .375 \text{ in}$$

$$c = r_o = .500 \text{ in}$$

$$p_{s2} = \frac{30 \times 10^6 \times 45 \times 10^{-5} (.1406 - .0225) (.250 - .1406)}{2 \times .0527 (.250 - .0225)} \\ = 7270 \text{ psi}$$

2. Shrink Fit Stresses

a. Inner Surface of Liner

From p_{s1} , based on first part of Equation 41a

$$\sigma_{ts1} = -p_{s1} \frac{2r_1^2}{r_1^2 - r_i^2} \\ = -6720 \frac{2 \times .0625}{.0625 - .0225} = -21,000 \text{ lb/in}^2$$

From p_{s2} , based on second part of Equation 41a

$$\sigma_{ts2} = -p_{s2} \frac{2r_2^2}{r_2^2 - r_i^2} \\ = -7270 \frac{2 \times .1406}{.1406 - .0225} = -17,300 \text{ lb/in}^2$$

b. Outer Surface of Liner

From p_{s1} , based on first part of Equation 42a

$$\sigma_{ts1} = -p_{s1} \frac{r_1^2 + r_i^2}{r_1^2 - r_i^2} \\ = -6720 \frac{.0625 + .0225}{.0625 - .0225} = -14,300 \text{ lb/in}^2$$

From p_{s2} , based on second part of Equation 42a

$$\sigma_{ts2} = -p_{s2} \frac{r_2^2 r_1^2 + r_i^2}{r_1^2 r_2^2 - r_i^2} \\ = -7270 \frac{.1406 .0625 + .0225}{.0625 .1406 - .0225} \\ = -11,800 \text{ lb/in}^2$$

c. Inner Surface of Tube

From p_{s1} , based on first part of Equation 43a

$$\sigma_{ts1} = p_{s1} \frac{r_2^2 + r_1^2}{r_2^2 - r_1^2} \\ = 6720 \frac{.1406 + .0625}{.1406 - .0625} = 17,500 \text{ lb/in}^2$$

Note that this stress exists before the cap is assembled. The stress from p_{s2} is the same as for the outer surface of the liner,

$$\sigma_{ts2} = -11,800 \text{ lb/in}^2$$

d. Outer Surface of Tube

From p_{s1} , based on first part of Equation 44a

$$\sigma_{ts1} = p_{s1} \frac{2r_1^2}{r_2^2 - r_1^2} \\ = 6720 \frac{2 \times .0625}{.1406 - .0625} = 10,800 \text{ lb/in}^2$$

From p_{s2} , based on second part of Equation 44a

$$\sigma_{ts2} = -p_{s2} \frac{r_2^2 + r_i^2}{r_2^2 - r_i^2} \\ = -7270 \frac{.1406 + .0225}{.1406 - .0225} = -10,000 \text{ lb/in}^2$$

e. Inner Surface of Cap

The cap is affected only by p_{s2} , based on Equation 45a

$$\sigma_{ts2} = p_{s2} \frac{r_o^2 + r_2^2}{r_o^2 - r_2^2} \\ = 7270 \frac{.250 + .1406}{.250 - .1406} = 26,000 \text{ lb/in}^2$$

f. Outer Surface of Cap

Based on Equation 46a

$$\sigma_{ts2} = p_{s2} \frac{2r_2^2}{r_o^2 - r_2^2} \\ = 7270 \frac{2 \times .1406}{.250 - .1406} = 18,700 \text{ lb/in}^2$$

3. Pressure Stresses

The formulas for the pressure stresses are based on Equation 26.

a. Inner Surface of Liner

$$\sigma_{tp} = p_d \frac{r_o^2 + r_i^2}{r_o^2 - r_i^2}$$

$$= 32,000 \frac{.250 + .0225}{.250 - .0225} = 38,300 \text{ lb/in}^2$$

b. Interface Between Liner and Tube

$$\sigma_{tp} = p_d \frac{r_i^2 r_o^2 + r_1^2}{r_1^2 r_o^2 - r_i^2}$$

$$= 32,000 \frac{.0225 \cdot .250 + .0625}{.0625 \cdot .250 - .0225} = 15,800 \text{ lb/in}^2$$

c. Interface Between Tube and Cap

$$\sigma_{tp} = p_d \frac{r_i^2 r_o^2 + r_2^2}{r_2^2 r_o^2 - r_i^2}$$

$$= 32,000 \frac{.0225 \cdot .250 + .1406}{.1406 \cdot .250 - .0225} = 8,800 \text{ lb/in}^2$$

d. Outer Surface of Cap

$$\sigma_{tp} = p_d \frac{2r_i^2}{r_o^2 - r_i^2}$$

$$= 32,000 \frac{2 \times .0225}{.250 - .0225} = 6,300 \text{ lb/in}^2$$

4. Combined Stresses

The stresses are combined for each surface and are listed in Table 24 and plotted in Figure 64. The total stress

$$\sigma = \sigma_{ts_1} + \sigma_{ts_2} + \sigma_{tp}$$

D. SMALL ARMS BARREL WITH COMBINED PRESSURE AND THERMAL STRESSES*:

169. Stresses are computed to determine the total effective stress at the inner surface of the outer tube of a two-piece barrel subjected to propellant gas pressure, shrink fit pressure, and a temperature gradient through the wall. The design data are

TABLE 24. COMBINED SHRINK FIT AND PRESSURE STRESSES (lb/in²).

Part	Surface	σ_{ts_1}	σ_{ts_2}	σ_{tp}	σ
Liner	Inner	-21,000	-17,300	38,300	0
	Outer	-14,300	-11,800	15,800	-10,300
Tube	Innrr	17,500	-11,800	15,800	21,500
	Outer	10,800	-10,000	8,800	9,600
Cap	Inner		26,000	8,800	34,800
	Outer		18,700	6,300	25,000

* Submitted by Springfield Armory.

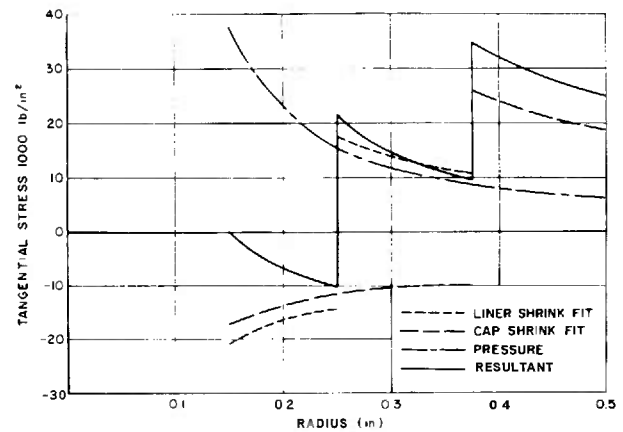


FIGURE 64. Tangential Stress of Shrink Fitted Tube.

r_i = .250 in, internal radius (caliber .50)

r_1 = .375 in, radius at interface

r_o = .500 in, outer radius

ΔT = 1400°F, temperature drop across total wall

p_d = 35,000 psi, design propellant gas pressure

E = 30×10^6 lb/in², modulus of steel

α = 7×10^{-6} in/in/°F, coefficient of linear expansion of steel

ν = .3, Poisson's ratio for steel

δ = .00025 in., interference at the interface

According to Equation 73a, the shrink fit pressure is

$$p_s = \frac{30 \times 10^6 \times 25 \times 10^{-3} (.1406 - .0625) (.250 - .1406)}{2 \times .0527 (.250 - .0625)}$$

$$= 3,240 \text{ lb/in}^2$$

1. Propellant Gas Pressure Stresses, from Equations 26 and 27a,

$$\sigma_{tp} = p_d \frac{r_i^2}{r_1^2} \times \frac{r_o^2 + r_1^2}{r_o^2 - r_i^2}$$

$$= 35,000 \frac{.0625}{.1406} \times \frac{.250 + .1406}{.250 - .0625} = 32,400 \text{ lb/in}^2$$

$$\sigma_{rp} = -p_d \frac{r_i^2}{r_1^2} \times \frac{r_o^2 - r_1^2}{r_o^2 - r_i^2}$$

$$= 35,000 \frac{.0625}{.1406} \times \frac{.250 - .1406}{.250 - .0625} = -9100 \text{ lb/in}^2$$

2. Shrink Fit Pressure Stresses, from Equation 34a (in terms of tube radii), and Equation 34b,

$$\sigma_{ts} = p_s \frac{r_o^2 + r_1^2}{r_o^2 - r_1^2}$$

$$= 3240 \frac{.250 + .1406}{.250 - .1406} = 11,600 \text{ lb/in}^2$$

$$\sigma_{rs} = -p_s = -3,240 \text{ lb/in}^2$$

3. Thermal Stresses

The temperature variation across the wall is assumed to be logarithmic although there is a temperature discontinuity at the interface. According to Equation 48a, the tangential thermal stress

$$\begin{aligned}\sigma_{tt} &= \frac{30 \times 7 \times 1400}{2(1 - .3).693} [1 - .288 - \frac{1}{3}(1 + 1.78).693] \\ &= 21,200 \text{ lb/in}^2\end{aligned}$$

From Equation 49a, the radial thermal stress

$$\begin{aligned}\sigma_{rr} &= \frac{30 \times 7 \times 1400}{2(1 - .3).693} [\frac{1}{3}(1.78 - 1).693 - .288] \\ &= -32,700 \text{ lb/in}^2\end{aligned}$$

From Equation 50a, the axial thermal stress

$$\begin{aligned}\sigma_{aa} &= \frac{30 \times 7 \times 1400}{2(1 - .3).693} (1 - .576 - \frac{2}{3} \times .693) \\ &= -11,500 \text{ lb/in}^2\end{aligned}$$

According to Equations 51, 52 and 53,

$$\begin{aligned}\sigma_t &= 32,400 + 11,600 + 21,200 = 65,200 \text{ lb/in}^2 \\ \sigma_r &= -9100 - 3200 - 32,700 = -45,000 \text{ lb/in}^2 \\ \sigma_a &= -11,500 \text{ lb/in}^2\end{aligned}$$

In Equation 23,

$$\begin{aligned}\sigma_t - \sigma_r &= 110,200 \text{ lb/in}^2 \\ \sigma_r - \sigma_a &= 33,500 \text{ lb/in}^2 \\ \sigma_a - \sigma_t &= -76,700 \text{ lb/in}^2 \\ 2\sigma_e^2 &= 1.914 \times 10^{10} (\text{lb/in}^2)^2\end{aligned}$$

Therefore, the total equivalent stress

$$\sigma_e = 97,800 \text{ lb/in}^2$$

This equivalent stress does not conform to the discussion of paragraph 109, indicating that some dimensional changes are necessary or a yield strength of 195,000 lb/in² is required.

E. RECOILLESS GUN*

1. Gun Tube

170. A 120 mm tube is selected for the sample design problem for recoilless tubes. Only the computed pressure-travel curve and the *CMP* read from it are available. The computed wall thickness will be that for a preliminary design (see paragraph 114).

* Based on material submitted by Frankford Arsenal.

Given design data

$$\begin{aligned}CMP &= 12,500 \text{ psi, at } \frac{5}{8} \text{ in. of projectile travel} \\ p_{muz} &= 3,545 \text{ psi, pressure at muzzle} \\ D_i &= 4.742 \text{ in., groove diameter plus tolerance} \\ Y &= 153,000 \text{ lb/in}^2, \text{ yield strength at ambient temperature (Fig. 57)} \\ T_a &= 125^\circ\text{F, atmospheric temperature} \\ T_h &= 600^\circ\text{F, elevated temperature of tube.}\end{aligned}$$

Material is conventional gun steel

Follow the outlined procedure of paragraph 115.

1. *CMP* is listed in the design data
2. According to Equation 56g

$$\begin{aligned}PIMP &= 1.05 CMP + \frac{\Delta p}{\Delta T} (T_a - 70^\circ) + 3\Delta_{CMP} \\ &= 1.05 \times 12,500 + 20(125 - 70) \\ &\quad + 3 \times 0.03 \times 12,500 \\ &= 13,125 + 1100 + 1125 = 15,350 \text{ psi}\end{aligned}$$

where

$$\frac{\Delta p}{\Delta T} = 20 \text{ psi/}^\circ\text{F}$$

$$\Delta_{CMP} = 3\% \text{ of } CMP$$

3. Applying Equation 56e

$$ESP_{hot} = 1.15 PIMP = 17,650 \text{ psi}$$

4. From Figure 58, $Y_h = 120,000 \text{ lb/in}^2$ at 600°F

$$5. \quad \frac{ESP_{hot}}{Y_h} = 0.147$$

6. From Table 10, the corresponding value of W for a $p/Y = 0.147$ is 1.175.

7. According to Equation 55e

$$\begin{aligned}W_a &= 1.0555W - 0.0555 \\ &= 1.240 - 0.055 = 1.184 \text{ in.}\end{aligned}$$

8. From Equation 56d

$$D_o = D_i W_a = 4.742 \times 1.184 = 5.615 \text{ in}$$

The same procedure is followed to find the wall thickness at the muzzle; for preliminary design

$$\begin{aligned}p_{muz} &= 3545 \text{ psi} & ESP_{hot}/Y_h &= 0.0492 \\ PIMP_{muz} &= 5140 \text{ psi} & \Pi &= 1.0515 \\ ESP_{hot} &= 5910 \text{ psi} & W_a &= 1.055 \\ Y_h &= 120,000 \text{ lb/in}^2 & D_o &= 5.00\end{aligned}$$

For a test barrel, assume $p = 2.5 \text{ CMP} = 31,200 \text{ psi}$

$$\frac{p}{Y} = \frac{31,200}{165,000} = 0.204$$

From Table 10, by interpolation

$$W = 1.265$$

$$D_o = D_i W = 4.742 \times 1.265 = 6.00 \text{ in}$$

As stated in paragraph 116 for economy the test barrel is constructed with a uniform outside diameter and no allowance is made for eccentricity. After firing the test gun, sufficiently accurate information becomes available to design a prototype tube according to the method discussed in paragraph 115.

a. Gimbal Ring Analysis

171. A steel gimbal ring is shrunk on a titanium tube of a recoilless gun. The problem requires the stresses at the points of discontinuity, 4 and 5 of Figure 13, in tube and ring. The known data defined in paragraph 118 are

$$E = 16.5 \times 10^6 \text{ lb/in}^2 \quad p = 7245 \text{ lb/in}^2$$

$$E_r = 30 \times 10^6 \text{ lb/in}^2 \quad t_1 = 0.1565 \text{ in}$$

$$r_1 = 2.429 \text{ in} \quad t_2 = 0.148 \text{ in}$$

$$r_2 = 2.425 \text{ in} \quad t_3 = 0.178 \text{ in}$$

$$r_3 = 2.440 \text{ in} \quad t_4 = 0.063 \text{ in}$$

$$r_r = 2.530 \text{ in} \quad \nu = 0.33$$

$$\Delta r = 0.004 \text{ in} \quad \nu_r = 0.29$$

The computed design data follow. The shrink fit pressure (Equation 57a)

$$p_s = \frac{A_r''}{\frac{r_2^2}{E t_s} + \frac{r_r^2}{E_r t_r}} = \frac{0.004 \times 10^6}{\frac{5.9}{2.44} + \frac{6.4}{1.89}} = \frac{4000}{5.80} = 690 \text{ lb/in}^2$$

From Equation 57b,

$$D = \frac{E t^3}{12(1 - \nu^2)}$$

$$D_1 = 5.9 \times 10^3 \text{ lb-in} \quad D_2 = 8.7 \times 10^3 \text{ lb-in}$$

$$D_3 = 5.0 \times 10^3 \text{ lb-in} \quad D_4 = 6.82 \times 10^3 \text{ lb-in}$$

From Equation 57c,

$$\lambda = \sqrt[4]{\frac{3(1 - \nu^2)}{r^2 t^2}}$$

$$\lambda_1 = 2.08/\text{in} \quad \lambda_3 = 1.94/\text{in}$$

$$\lambda_2 = 2.13/\text{in} \quad \lambda_r = 3.22/\text{in}$$

According to Equations 57d and 57e, respectively,

$$\bar{E} = \frac{16.5 \times 10^6}{.891} = 18.52 \times 10^6 \text{ lb/in}^2$$

$$\bar{E}_r = \frac{30 \times 10^6}{.916} = 32.8 \times 10^6 \text{ lb/in}^2$$

From Equations 57f and 57g

$$r = \frac{2.425 + 2.530}{2} = 2.478 \text{ in}$$

$$\begin{aligned} E_e t_e &= (16.5 \times 0.148 + 30 \times 0.063) 10^6 \\ &= 4.33 \times 10^6 \text{ lb/in} \end{aligned}$$

The flexural rigidity equivalent (Equation 57h)

$$\begin{aligned} D &= \frac{343 \times 4.81 + 1076 \times .158}{12(27.45 + 20.65)} \\ &\quad + \frac{607(8.18 + 5.21 + 1.48)}{12(27.45 + 20.65)} 10^3 \\ &= \frac{10850}{577} \times 10^3 = 18.8 \times 10^3 \text{ lb-in} \end{aligned}$$

According to Equation 57j

$$\begin{aligned} C &= \frac{2315 - (9.06 + 5.98)'}{6.14 \times 48.1} \times 10^5 \\ &= \frac{2089}{295.5} \times 10^5 = 7.08 \times 10^5 \text{ lb/in}^3 \end{aligned}$$

The λ equivalent (Equation 57i)

$$\beta = \left(\frac{C}{4D_e} \right)^{1/4} = \left(\frac{708000}{75200} \right)^{1/4} = 9.42^{1/4} = 1.752 \text{ in}$$

Equating the expressions for δ_4 in Equations 57k and 57n and substituting for the known values

$$\begin{aligned} &\frac{7245 \times 5.9}{16.5 \times 10^6 \times .1565} + \frac{2.08 M_4 - Q_4}{2 \times 9.0 \times 5.9 \times 10^3} \\ &= \frac{7245 \times 6.14}{4.33 \times 10^6} - \frac{690 \times 5.88}{16.5 \times 10^6 \times .148} \\ &\quad + \frac{1.752 M_4 + Q_4}{2 \times 5.38 \times 18.8 \times 10^3} M_4 - 1.31 Q_4 = -755 \end{aligned}$$

Equating the expressions for θ_4 in Equations 57m and 57o and substituting for the known values

$$\begin{aligned} &\frac{2 \times 2.08 M_4 - Q_4}{2 \times 4.32 \times 5.9 \times 10^3} = -\frac{2 \times 1.752 M_4 + Q_4}{2 \times 3.07 \times 18.8 \times 10^3} \\ &M_4 = 0.098 Q_4 \end{aligned}$$

$$Q_4 = 622 \text{ lb/in} \quad M_4 = 61.1 \text{ lb-in/in} \quad \delta_4 = .01192 \text{ in}$$

Equating the expressions for δ_s in Equations 57p and 57r and substituting the known values

$$\begin{aligned} & \left(10.27 - 1.66 + \frac{1.752M_5 + Q_5}{202.5}\right) \frac{1}{10^3} \\ &= \frac{7245 \times 5.95}{16.5 \times 10^6 \times .178} + \frac{1.94M_5 - Q_5}{2 \times 7.3 \times 8.7 \times 10^3} \\ & - M_5 + 1.942Q_5 = 922 \end{aligned}$$

Equating the expressions for θ_s in Equations 57r and 57t and substituting the known values

$$\begin{aligned} \frac{4.16M_5 + Q_5}{51.0} 10^{-3} &= -\frac{2 \times 1.94M_5 - Q_5}{2 \times 3.76 \times 8.7 \times 10^6} \\ M_5 &= 0.0742Q_5 \end{aligned}$$

$$Q_5 = 519 \text{ lb/in} \quad M_5 = 38.5 \text{ lb-in/in} \quad \delta_s = .01117 \text{ in}$$

Before starting the actual stress computation, find the factors of Equations 58e, 58f and 58g which determine the distribution of loads and moments in the gimbal ring region.

$$\begin{aligned} B &= \frac{(0.33 - 0.29)18.52 \times 32.8 \times 10^6 \times 0.148 \times 0.063(0.148 + 0.063)}{2.478(18.52 \times 0.148 + 32.8 \times 0.063)} = 4020 \text{ lb/in} \\ H &= \frac{1}{2} \left(\frac{18.52 \times 0.0219 - 32.8 \times 0.00397}{18.52 \times 0.148 + 32.8 \times 0.063} \right) = 0.0286 \text{ in} \\ J &= \frac{3 \times 0.276(0.134 - 0.0377) - 4(0.060 + 0.0082)(0.910 + 5.97)}{12 \times 2.487 \times 4.82} = -2320 \text{ lb} \end{aligned}$$

Sufficient data are now available to compute the stresses in the members according to Equations 58a through 58p. Maximum stresses occur at the inner surface and are tensile except for the radial stresses. At Station 4, tube Region 1, from Equations 58a, 58b, 58c, 58d,

$$\begin{aligned} \sigma_a &= \frac{6M_4}{t_1^2} = \frac{6 \times 61.1}{0.1565^2} = 15,000 \text{ lb/in}^2 \\ \sigma_{tm} &= \nu\sigma_r = 0.33 \times 15000 = 4,950 \text{ lb/in}^2 \\ \sigma_{ts} &= \frac{E\delta_4}{r_1} = \frac{16.5 \times 10^6 \times 0.01192}{2.429} = 81,000 \text{ lb/in}^2 \\ \sigma_t &= \sigma_{tm} + \sigma_{ts} = 86,000 \text{ lb/in}^2 \\ \sigma_r &= -p = -7245 \text{ lb/in}^2 \end{aligned}$$

By Equation 23

$$\begin{aligned} \sigma_e^2 &= \frac{1}{2}[(\sigma_t - \sigma_r)^2 + (\sigma_r - \sigma_s)^2 + (\sigma_a - \sigma_t)^2] \\ &= 71 \times 10^8 \\ \sigma_e &= 84,300 \text{ lb/in}^2 \end{aligned}$$

Similarly, at Station 4, tube Region 2, inner surface

$$\begin{aligned} \sigma_a &= \frac{18.52 \times 10^6}{18.8 \times 10^3} \left[-61.1(0.0286 - 0.148) \right. \\ & \quad \left. + 0.01192 \left(0.33 \frac{18.8 \times 10^3}{2.425} - 2320 \right. \right. \\ & \quad \left. \left. - \frac{4020 \times 0.148}{2} \right) \right] \\ &= 986[7.29 + 0.01192(2550 - 2320 - 298)] \\ &= 6400 \text{ lb/in}^2 \end{aligned}$$

where $At = -0.148$ in, measured inward from interface

$$\begin{aligned} \sigma_{tm} &= \nu\sigma_a = 0.33 \times 6400 = 2100 \text{ lb/in}^2 \\ \sigma_{ts} &= \frac{E\delta_4}{r_2} = \frac{16.5 \times 10^6 \times 0.01192}{2.425} = 81,100 \text{ lb/in}^2 \\ \sigma_t &= \sigma_{tm} + \sigma_{ts} = 83,200 \\ \sigma_r &= -p = -7245 \text{ lb/in}^2 \\ \sigma_s &= 84,400 \text{ lb/in}^2 \end{aligned}$$

Analysis of gimbal ring at Station 4, inner surface, when At measured from the interface is zero. From Equation 58h

$$\begin{aligned} \sigma_a &= \frac{32.8 \times 10^6}{18.8 \times 10^3} \left[-61.1 \times 0.0286 \right. \\ & \quad \left. + 0.01192 \left(0.29 \frac{18.8 \times 10^3}{2.53} - 2320 \right) \right] \\ &= 1745[-1.75 + 0.01192(2155 - 2320)] \\ &= -6500 \text{ lb/in}^2 \end{aligned}$$

From Equation 58i

$$\sigma_{tm} = \nu\sigma_a = 0.29(-6500) = -1900 \text{ lb/in}^2$$

Since the derivation of deflections (paragraph 118) did not consider the effects of shrink fit pressure on the gimbal ring deflection, this deflection is determined separately. Thus, from Equations 58m and 58k

$$\delta_{rs} = \frac{p_s r_r^2}{E_r t_r} = \frac{690 \times 6.4}{30 \times 10^6 \times 0.063} = 0.00234 \text{ in}$$

$$\sigma_{t\delta} = \frac{E_r(\delta_r + s_{\theta})}{r_r} = \frac{30 \times 10^6(0.01192 + 0.00234)}{2.53}$$

$$= 169,000 \text{ lb/in}^2.$$

$$\sigma_t = \sigma_{tm} + \sigma_{t\delta} = 167,100 \text{ lb/in}^2$$

From Equation 58r,

$$p_r = 7245 \frac{1.89 \times 6.4}{1.89 \times 6.4 + 2.44 \times 5.9} = 3310 \text{ lb/in}^2$$

The total radial stress at the interface

$$\sigma_r = -p_{2r} = -(p_r + p_s) = -(3310 + 690)$$

$$= -4000 \text{ lb/in}^2$$

$$\sigma_s = 172,300$$

Analysis of gimbal ring at Station 4, outer surface, when At measured from the interface is t_r . From Equation 58h

$$\sigma_s = \frac{32.8 \times 10^6}{18.8 \times 10^3} \left[-61.1(0.0286 + 0.063) \right.$$

$$+ 0.01192 \left(0.29 \frac{1.88 \times 10^3}{2.53} - 2320 \right.$$

$$\left. \left. + \frac{4020 \times 0.063}{2} \right) \right]$$

$$= 1745[-5.60 + 0.01192(2155 - 2320 + 127)]$$

$$= -10,600 \text{ lb/in}^2$$

$$\sigma_{tm} = \nu_r \sigma_s = 0.29(-10,600) = -3100 \text{ lb/in}^2$$

$$\sigma_{t\delta} = 169,000 \text{ lb/in}^2 \text{ (same as for inner surface)}$$

$$\sigma_t = \sigma_{tm} + \sigma_{t\delta} = 165,900 \text{ lb/in}^2$$

$$\sigma_r = 0$$

$$\sigma_s = 171,500 \text{ lb/in}^2$$

The stresses at Station 5 are obtained similarly.

b. Threads

172. Compute the four stresses involved in a threaded joint according to the procedure discussed in paragraph 139. The dimensions and other design data of Figure 52 are

$$F_u = 4260 \text{ lb/in, unit load on oic thread}$$

$$C = 0.005 \text{ in, clearance}$$

$$d_t = 0.070 \text{ in, depth of thread}$$

$$p_t = 0.0250 \text{ in, pitch}$$

$$r = 0.016 \text{ in, fillet and corner radii}$$

$$t = 0.153 \text{ in, wall thickness at root of thread}$$

$$w = 0.143 \text{ in, width of thread at root diameter}$$

The direct shear stress according to Equation 77b

$$\tau = \frac{2F_u}{p_t} = \frac{2 \times 4260}{0.250} = 34,100 \text{ lb/in}^2$$

The bearing stress (Equation 77c)

$$\sigma_{br} = \frac{F_u}{t_t - C - 2r} = \frac{4260}{0.033} = 129,100 \text{ lb/in}^2$$

The net tensile stress through the wall according to Equation 77d

$$\sigma_n = k_c \frac{2F_u}{t} = 2.1 \frac{2 \times 4260}{.153} = 117,000 \text{ lb/in}^2$$

where

$$k_c = 2.1^*, \text{ the stress concentration factor.}$$

From Equation 77e, the fillet bending stress

$$\sigma_f = 3k_c \frac{F_u(d_t + C)}{w^2} = 3 \times 2.8 \frac{4260 \times 0.075}{0.0204}$$

$$= 131,500 \text{ lb/in}^2$$

which is well within the yield strength of 153,000 lb/in² where

$$k_c = 2.8^\dagger, \text{ the stress concentration factor.}$$

2. Chamber

a. Chamber Volume

173. The known data (paragraph 67) involving the design of the chamber of a 120 mm recoilless rifle are

$$A_b = 17.35 \text{ in}^2, \text{ bore area}$$

$$E = F(\gamma - 1) = 1.46 \times 10^6 \text{ ft-lb/lb}$$

$$F = 365,000 \text{ ft-lb/lb, specific impetus}$$

$$\omega = 0, \text{ ratio of momentums, rifle to projectile, i.e., momentum of rifle is zero}$$

$$v_m = 650 \text{ ft/sec, muzzle velocity}$$

$$W_p = 50 \text{ lb, projectile weight}$$

$$\Delta = 0.5 \text{ gm/cc, loading density}$$

$$\Delta_p = 1/30. \text{ lb/in}^3, \text{ bag density of propellant}$$

$$\gamma = 1.25, \text{ ratio of specific heats.}$$

From Equation 4a, the muzzle energy

$$K = \frac{1}{2} \left(\frac{W_p}{g} \right) v_m^2 = \frac{50}{64.4} 423,000 = 328,000 \text{ ft-lb}$$

According to Equation 4b (with $\omega = 0$), the propellant charge

$$C \approx \frac{2K}{E} \left(1 + \frac{(1 - \omega)\sqrt{2gE}}{v_m} \right)$$

$$= \frac{6.56}{14.6} \left(1 + \frac{9700}{650} \right) = 7.15 \text{ lb}$$

* Reference 32.

† Reference 33.

The required chamber volume (Equation 4c)

$$V_c = 27.7 \frac{C}{A} = 27.7 \frac{7.15}{0.5} = 396 \text{ in}^3$$

The propellant bag space determined from Equation 4d is

$$V_c = \frac{C}{\Delta_p} = 30 \times 7.15 = 214 \text{ in}^3$$

From Equation 4e, the required chamber length

$$L_o = \frac{V_c}{A_c} = 17.0 \text{ in}$$

where

$$A_c = \frac{A_b}{1.45} = 11.96 \text{ in}^2$$

Assuming the main portion of the chamber to be a conical frustum and the length of the nozzle entrance to be 0.44 in, the length of the frustum is

$$L'_o = 17.0 - 0.44 = 17.46 \text{ in}$$

The volume of the frustum according to Equation 4g is

$$V'_o = \frac{\pi L'_o}{3} (r_a^2 + r_a r_b + r_b^2) = \frac{17.46\pi}{3} 26.0 = 475 \text{ in}^3$$

where

$r_a = 3.5 \text{ in}$, large radius of frustum,

$r_b = 2.35 \text{ in}$, small radius of frustum, bore radius

Thus,

$$\frac{A_o}{A_t} = \frac{38.48}{11.96} = 3.22$$

which meets the requirement of Equation 5b. The volume of the nozzle entrance (Equation 4g)

$$\begin{aligned} V_e &= \pi \left(ab^2 + ar^2 - \frac{a^3}{3} - ab\sqrt{r^2 - a^2} - br^2 \sin^{-1} \frac{a}{r} \right) \\ &= \pi(2.54 + 0.85 - 0.028 - 0 - .73) \\ &= 1.87\pi = 6 \text{ in}^3 \end{aligned}$$

Where the dimensions of Figure 21 are

$$a = 0.44 \text{ in}$$

$$b = 2.40 \text{ in}$$

$$r = .44 \text{ in}$$

The nozzle entrance volume increases the chamber volume to

$$V_o = V'_o + V_e = 475 + 6 = 481 \text{ in}^3$$

which meets the requirement of Equation 4c by being greater than 396 in³.

b. Conical Section —Discontinuity Stresses (paragraph 120)

174. The known data involving the chamber design are

$E = 16.5 \times 10^6 \text{ lb/in}^2$, modulus of elasticity of titanium alloy

$L_c = 1.60 \text{ in}$, length of conical section

$p = 15,640 \text{ lb/in}^2$, internal design pressure

$\bar{r} = 2.835 \text{ in}$, mean radius of conical section

$\bar{r}_t = 2.50 \text{ in}$, mean radius of tube

$\bar{r}_c = 3.170 \text{ in}$, mean radius of chamber

$t = 0.41 \text{ in}$, wall thickness of conical section

$t_t = 0.40 \text{ in}$, wall thickness of tube

$t_c = 0.40 \text{ in}$, wall thickness of chamber

$\beta = 21.2^\circ$, slope of conical surface of chamber

$\nu = 0.33$, Poisson's ratio for titanium

From Equations 59b and 59c

$$\begin{aligned} \Delta_1 &= \frac{p}{E} \left(\frac{\bar{r}^2}{t} - \frac{\bar{r}_t^2}{t_t} \right) \\ &= \frac{15640}{16.5 \times 10^6} \left(\frac{8.04}{0.44} - \frac{6.25}{0.40} \right) = 0.00252 \text{ in} \end{aligned}$$

$$\begin{aligned} \Delta_2 &= \frac{p}{E} \left(\frac{\bar{r}^2}{t} - \frac{\bar{r}_c^2}{t_c} \right) \\ &= \frac{15640}{16.5 \times 10^6} \left(\frac{8.04}{0.44} - \frac{10.05}{0.40} \right) = -0.006 \text{ in} \end{aligned}$$

From Equations 59d, 59e, 59f

$$\begin{aligned} C &= \frac{12\pi^2}{E(Lt^3 + L^3 t \tan \beta)} \\ &= \frac{12 \times 8.04}{16.5 \times 10^6 (0.136 + 0.700)} = 7.0 \times 10^{-6} \text{ lb} \end{aligned}$$

$$\begin{aligned} C_c &= \frac{\bar{r}_c \bar{r}}{EtL} = \frac{3.17 \times 2.83}{16.5 \times 10^6 \times 0.44 \times 1.6} \\ &= 0.774 \times 10^{-6} \text{ in}^2/\text{lb} \end{aligned}$$

$$\begin{aligned} C_t &= \frac{\bar{r}_t \bar{r}}{EtL} = \frac{2.5 \times 2.83}{16.5 \times 10^6 \times 0.44 \times 1.6} \\ &= 0.61 \times 10^{-6} \text{ in}^2/\text{lb} \end{aligned}$$

From Equations 57b and 57c

$$\begin{aligned} D_c &= \frac{12(1 - \nu^2)}{16.5 \times 6.4 \times 10^4} = 98,700 \text{ lb-in} \\ &= \frac{12 \times 0.891}{16.5 \times 6.4 \times 10^4} \end{aligned}$$

$$D_t = \frac{Et_t^3}{12(1-\nu^2)} = 98,700 \text{ lb-in}$$

$$\lambda_c = \sqrt[4]{\frac{3(1-\nu^2)}{\bar{r}_c^2 t_c^2}} = \sqrt[4]{\frac{3(1-0.109)}{10.05 \times 0.16}} = 1.136 \text{ in}$$

$$\lambda_t = \sqrt[4]{\frac{3(1-\nu^2)}{\bar{r}_t^2 t_t^2}} = \sqrt[4]{\frac{3(1-0.109)}{6.25 \times 0.16}} = 1.278 \text{ in}$$

Substituting the known and computed values in Equations 59g to 59j

$$1.675Q_2 - 5.6Q_1 - 15.92M_2 + 7.0M_1 = 0$$

$$5.6Q_2 - 2.50Q_1 - 7.0M_2 + 14.92M_1 = 0$$

$$8.70Q_2 - 3.87Q_1 - 1.67M_2 + 5.6M_1 = -6460$$

$$-3.87Q_2 + 7.51Q_1 + 5.6M_2 - 2.50M_1 = 2520$$

The solution of the four simultaneous equations yields

$$Q_1 = -185 \text{ lb/in} \quad M_1 = 444 \text{ lb-in/in}$$

$$Q_2 = -1080 \text{ lb/in} \quad M_2 = 145 \text{ lb-in/in}$$

The radial deflections are computed from Equations 59k and 59m

$$\begin{aligned} \delta_1 &= \frac{15640 \times 6.25}{16.5 \times 10^6 \times 0.40} \\ &+ \frac{444}{2 \times 1.63 \times 98700} - \frac{182}{2 \times 2.08 \times 98700} \\ &= .01482 + .00138 - .00044 = 0.01576 \text{ in} \end{aligned}$$

$$\begin{aligned} \delta_2 &= \frac{15640 \times 10.05}{16.5 \times 10^6 \times 0.40} \\ &+ \frac{145}{2 \times 1.29 \times 98700} - \frac{1080}{2 \times 1.47 \times 98700} \\ &= .02380 + .00057 - .00373 = 0.02064 \text{ in} \end{aligned}$$

Stress computations are shown for the tube where it joins the conical section. The axial bending stress according to Equation 58a

$$\sigma_a = \frac{6M_1}{t_t^2} = \frac{6 \times 444}{0.16} = 16,600 \text{ lb/in}^2$$

The tangential bending stress according to Equation 58b

$$\sigma_{tm} = \nu \sigma_a = 0.33 \sigma_a = 5,500 \text{ lb/in}^2$$

The tangential stress derived from the radial deflection from Equation 58c

$$\sigma_{ts} = \frac{E\delta_1}{\bar{r}_t} = \frac{16.5 \times 10^6 \times 0.01576}{2.5} = 104,000 \text{ lb/in}^2$$

Total tangential stress

$$\sigma_t = \sigma_{tm} + \sigma_{ts} = 109,500 \text{ lb/in}^2$$

The radial stress (Equation 58d)

$$\sigma_r = -p = -15,600 \text{ lb/in}^2$$

According to Equation 23, the effective stress

$$\sigma_e = 112,000 \text{ lb/in}^2$$

c. *Toroidal Section—Discontinuity Stresses* (paragraph 121)

175. The known data for the toroidal section shown in Figure 45 arc

$E = 16.5 \times 10^6 \text{ lb/in}^2$, modulus of elasticity of titanium alloy

$p_c = 15,640 \text{ lb/in}^2$, design pressure at C

$p_n = 4,860 \text{ lb/in}^2$, design pressure at n

$p_o = 2,400 \text{ lb/in}^2$, design pressure at O

$p_t = 8,680 \text{ lb/in}^2$, design pressure at nozzle throat

$\bar{r}_c = 1.124 \text{ in}$, mean radius at C

$\bar{r}_n = 2.419 \text{ in}$, mean radius at n

$\bar{r}_o = 2.612 \text{ in}$, mean radius at O

$r_t = 1.935 \text{ in}$, radius of throat

$t_c = 0.45 \text{ in}$, wall thickness at C

$t_n = 0.652 \text{ in}$, wall thickness at n

$t_o = 0.492 \text{ in}$, wall thickness at O

$\alpha = 15^\circ 15'$, half angle of nozzle

$\nu = 0.33$, Poisson's ratio for titanium

From Equations 57b and 57c

$$\begin{aligned} D_c &= \frac{Et_c^3}{12(1-\nu^2)} \\ &= \frac{16.5 \times 10^6 \times 0.0913}{12(1-0.109)} = 1.406 \times 10^5 \text{ lb-in} \end{aligned}$$

$$\begin{aligned} D_n &= \frac{Et_n^3}{12(1-\nu^2)} \\ &= \frac{16.5 \times 10^6 \times .277}{12(1-0.109)} = 4.28 \times 10^5 \text{ lb-in} \end{aligned}$$

$$\lambda_c = \sqrt[4]{\frac{3(1-\nu^2)}{\bar{r}_c^2 t_c^2}} = \sqrt[4]{\frac{3(1-0.109)}{17 \times 0.203}} = 0.939 \text{ in}$$

$$\lambda_n = \sqrt[4]{\frac{3(1-\nu^2)}{\bar{r}_n^2 t_n^2}} = \sqrt[4]{\frac{3(1-0.109)}{5.85 \times 0.425}} = 1.018 \text{ in}$$

From Equation 60a,

$$\begin{aligned} \delta_n &= \frac{4860 \times 5.85}{0.652 \times 16.5 \times 10^6 \times 0.965} \\ &- \frac{1.018M_n + Q_n}{2 \times 1.055 \times 4.28 \times 10^5} \\ &= 0.00274 - (1.13M_n + 1.11Q_n)10^{-6} \end{aligned}$$

From Equation 60b,

$$\theta_n = \frac{\left(\frac{2400 \times 6.82}{0.492}\right) - \left(\frac{4860 \times 5.8}{0.652}\right)}{16.5 \times 10^6 \times 0.965 \times 1.0} + \frac{2 \times 1.018 M_n + Q_n}{2 \times 1.036 \times 4.28 \times 10^5}$$

hence

$$x_n - x_o = 1.0 \text{ in., distance between } n \text{ and } O$$

$$\theta_n = (-650 + 2.3 M_n + 1.13 Q_n) 10^{-6}$$

From Equation 60c,

$$\delta_c = \frac{15640 \times 17}{16.5 \times 10^6 \times 0.45} - \frac{0.939 M_c - Q_c}{2 \times 0.828 \times 1.406 \times 10^5} = 0.0358 - (4.0331 - 4.28 Q_c) 10^{-6}$$

From Equation 60d

$$\theta = -\frac{2 \times 0.939 M_c - Q_c}{2 \times 0.883 \times 1.406 \times 10^5} = -(7.58 M_c - 4.03 Q_c) 10^{-6}$$

To obtain the design data of the toroidal section, the area is divided into narrow radial strips Δy wide. The length of each strip, Δr , is measured from a sketch drawn to scale (see Figure 46). Numerical integration provides the location of neutral axis and mean radius. The detailed computations are omitted. From Equation 60j, the neutral axis location is given by

$$y_c = \frac{\sum \frac{y_n \Delta r \Delta y}{r}}{\sum \frac{\Delta r \Delta y}{r}} = \frac{1.165}{0.71} = 1.64 \text{ in}$$

The distance from the neutral axis to Station n

$$y_n = 2.708 - y_c = 1.068 \text{ in}$$

The mean radius according to Equation 60k

$$\bar{r} = \frac{\sum r \Delta r \Delta y}{\sum \Delta r \Delta y} = \frac{51.9 \times 0.125}{16.83 \times 0.125} = 3.09 \text{ in}$$

Continuing with the numerical integration process, the unit moment in terms of θ is determined from the stresses on the cross sectional area and according to Equation 60h, is

$$M_T = \frac{E\theta}{2} \sum \frac{y^2}{\Delta r} \Delta u = \frac{16.5 \times 10^6 \times 0.320}{3.09} = 1.71 \times 10^6 \theta \text{ lb-in/in}$$

The effects of the pressure on the toroid are determined next. The pressures are obtained for a gas

constant of 1.226.* Detailed calculations are shown for one increment, to be followed by the total effects. The increment adjacent to the cylinder,

$$\Delta r_p = 0.010 \text{ in}$$

$$\Delta y_p = 0.167 \text{ in}$$

$$y_p = 1.553 \text{ in}$$

$$r_p = 3.895 \text{ in}$$

$$p_i = 15,335 \text{ lb/in}^2 \text{ (obtained from gas tables)}$$

The incremental axial force, according to Equation 60m

$$\Delta F_n = 2\pi r_p \Delta r_p p_i = 3750 \text{ lb}$$

The loads on the remaining increments are computed similarly. The total axial load

$$F_a = \sum \Delta F_i = 516,000 \text{ lb}$$

The total axial force on the nozzle, when the nozzle is assumed to be conical

$$F_n = A_n p_n = \pi(r_e^2 - r_{ni}^2) p_n = 22.9 \times 1200 = 27,500 \text{ lb}$$

where

$$p_n = 1200 \text{ lb/in}^2, \text{ average nozzle pressure (Reference 19)}$$

$$r_e = 3.42 \text{ in, exit radius}$$

$$r_{ni} = 2.10 \text{ in, inner radius at Station } n.$$

The total axial force at the cylinder, Equation 60p

$$F_c = F_a - F_n = 488,500 \text{ lb}$$

The distance of the center of pressure from the axis, according to Equation 60n is

$$r_p = \frac{\sum r_p \Delta F_i}{\sum \Delta F_i} = \frac{1596000}{516000} = 3.093 \text{ in}$$

That \bar{r}_p almost equals \bar{r} is purely coincidental. The unit moment at the mean radius produced by the axial loads

$$M_a = \frac{F_c(\bar{r}_c - \bar{r}_p) - F_n(\bar{r}_n - \bar{r}_n)}{2\pi r} = \frac{488500 \times 1.031 - 27500 \times 0.674}{19.41} = 25,100 \text{ lb-in/in}$$

(negative indicates counterclockwise direction)

The total moment on the toroid produced by radial pressure forces are computed according to Equa-

* Reference 37.

tion 60r. For the same increment as that for the axial direction

$$\Delta M_r = -2\pi r \Delta y p_c / y_p = -97,100 \text{ lb-in}$$

The summation of the remaining increments

$$\Sigma \Delta M_r = -432000 \text{ lb-in}$$

The unit moment about the mean radius

$$M_r = \frac{\Sigma \Delta M_r}{2\pi \bar{r}} = -\frac{432000}{19.41} = -22,300 \text{ lb-in/in}$$

The resultant unit moment due to pressure forces on the mean circumference

$$M_p = M_n + M_r = 2,800 \text{ lb-in/in}$$

Substituting values in Equation 60t

$$M_T = 2800 + M_c - M_n + 1.64Q_c + 1.068Q_n$$

Earlier M_T was found to equal $1.71 \times 10^6 \theta$, therefore

$$\theta = 0.585 \times 10^{-6} M_T = (1640 + 0.585M_c - 0.585M_n + 0.96Q_c + 0.625Q_n)10^{-6}$$

The radial deflection at n from Equation 60w

$$\begin{aligned} \delta_n &= 1.068\theta + \frac{3.09(2.419Q_n - 4.124Q_c)}{16.5 \times 10^6 \times 2.10} \\ &= (1752 + 0.625M_c - 0.625M_n \\ &\quad + 0.659Q_c + 0.884Q_n)10^{-6} \end{aligned}$$

Equating this deflection to that for the nozzle and collecting terms

$$1.994Q_n + 0.659Q_c + 0.508M_n + 0.625M_c = 988$$

The radial deflection at c from Equation 60v

$$\begin{aligned} \delta_c &= 1.64\theta + \frac{3.09(2.419Q_n - 4.124Q_c)}{16.5 \times 10^6 \times 2.10} \\ &= (-2690 - 0.96M_c + 0.96M_n \\ &\quad - 1.943Q_c - 0.809Q_n)10^{-6} \end{aligned}$$

Equating this deflection to that for the cylinder and collecting terms

$$-0.809Q_n - 6.223Q_c + .96M_n + 3.07M_c = 38490$$

According to Equation 60x, $8 = \theta_n = 8$. Two more equations become available by substituting the above expressions of θ for c_n and c , and collecting terms.

$$\begin{aligned} 0.505Q_n - 0.96Q_c + 2.885M_n - 0.585M_c &= 2290 \\ -0.625Q_n + 3.07Q_c + 0.585M_n - 8.165M_c &= 1640 \end{aligned}$$

The solution to the four simultaneous equations has

$$Q_n = 6,580 \text{ lb/in} \quad M_n = -4,720 \text{ lb-in/in}$$

$$Q_c = -10,170 \text{ lb/in} \quad M_c = -4,865 \text{ lb-in/in}$$

$$\theta = \theta_n = 8_s = -0.004 \text{ radian}$$

$$\begin{aligned} \delta_n &= 0.00274 + (1.13 \times 4720 - 1.11 \times 6580)10^{-6} \\ &= 0.00078 \text{ in} \end{aligned}$$

$$\begin{aligned} \delta_c &= 0.0358 + (4.03 \times 4865 - 4.28 \times 10170)10^{-6} \\ &= 0.0119 \text{ in} \end{aligned}$$

All data are now available to compute the stresses by means of Equations 58a through 58d and Equation 23, following the procedures illustrated in paragraph 171.

3. Nozzle

a. Design

176. Two parameters for the nozzle design of the 120 mm recoilless rifle, namely the approach area and the throat area, have been determined in the earlier chamber analysis. Other known data are

$\omega = 0$, ratio of momentums

$p_o = 15,600 \text{ lb./in}^2$, stagnation pressure

$r_a = 3.5 \text{ in.}$, radius of approach area

$r_t = 1.95 \text{ in.}$, throat radius

$\gamma = 1.25$, ratio of specific heats

$\phi = 90 - \alpha = 75^\circ 29'$, complement of nozzle slope

The value of p_e for design purposes here includes a 1.15 factor of safety, thus $p_e = 1.15 \text{ PIMP}$. Since $A_e/A_t = 1.45$ and $A_n/A_t = 3.22$, the ratio p_e/p_o , according to Figure 22, is 1.02. Therefore, the ratio

$$\frac{A_e p_e}{A_t p_o} = 1.45 \times 1.02 = 1.48$$

Locating this ratio on the $\omega = 0$ curve of Figure 23 indicates the ratio $A_e/A_t = 2.3$. According to Equation 5c

$$A_e = \left(\frac{A_e}{A_t}\right)A_t = 2.3 \times 11.96 = 26.3 \text{ in}^2,$$

theoretical nozzle exit area $r_e = 2.90 \text{ in.}$, corresponding exit radius

$$L_n = \frac{r_e - r_t}{\tan \alpha} = \frac{2.96 - 1.95}{.259} = 3.67 \text{ in}$$

where

$$\alpha = 14^\circ 31', \text{ nozzle slope}$$

TABLE 25. NOZZLE STRESSES.

Station x	-5.75	-5.37	-3.65	-1.91	0	.66
r	3.410	3.340	2.895	2.445	1.950	3.060
r/r_t	1.762	1.712	1.485	1.254	1.000	1.568
r_1	∞	∞	∞	∞	.44	-1.11
r_t/r_1	0	0	0	0	4.43	-1.758
ϕ	75°29'	75°29'	75°29'	75°29'	90°	37°05'
$\sin \phi$.968	.968	.968	.968	1.00	.603
F/F_t	1.242	1.232	1.188	1.124	.80	2.04
ψ	1.551	1.511	1.481	1.405	1.00	2.548
p/p_o	.0576	.0628	.0973	.1704	.555	.962
$\psi_e - \psi$	0	.010	.067	.146	.551	-.997
η_a	0	-.003	-.022	-.060	-.276	.528
η_t	.1050	.1112	.1492	.221	-.667	.083
f_e	.1050	.1128	.1612	.256	.581	.192
t_r	.021	.023	.033	.052	.118	.100
t_n	.150	.165	.236	.300	.625	.375
W_a	1.043	1.050	1.082	1.123	1.320	1.122
W_t	1.042	1.048	1.078	1.117	1.303	1.116
t_e	0.144	0.160	0.226	0.286	0.591	0.355
σ_e	22,200	21,600	21,700	27,200	29,900	42,200

From past experience this length of nozzle appears far too short. Increased to a length of 5.75 in., the exit radius becomes

$$r_e = r_t + L_n \tan \alpha = 1.95 + 5.75 \times .259 = 3.44 \text{ in}$$

b. Stresses

The nozzle contour is now complete and with a computed wall thickness, the effective stress may be computed at each station. Refer to Figure 48 for illustration. For instance, at Station -1.91, $r = 2.445$. From Equation 61a,

$$\frac{A}{A_t} = \left(\frac{r}{r_t}\right)^2 = 1.254^2 = 1.572$$

$$\frac{F}{F_t} = 1.124^*.$$

From Equation 61b

$$\begin{aligned} \psi &= (1 + \gamma) \left(\frac{2}{1 + \gamma} \right)^{\gamma/(\gamma-1)} \frac{F}{F_t} \\ &= 2.25 \left(\frac{2}{2.25} \right)^{1.25/.25} 1.124 \\ &= 1.25 \times 1.124 = 1.405 \end{aligned}$$

At the exit,

$$\frac{A_e}{A_t} = \left(\frac{r_e}{r_t}\right)^2 = 1.762^2 = 3.11$$

* Reference 27.

$$\frac{F_e}{F_t} = 1.242^\dagger \text{ and}$$

$$\frac{p}{p_o} = 0.1704^\dagger$$

From Equation 61c,

$$\psi_e = 1.25 \frac{F_e}{F_t} = 1.25 \times 1.242 = 1.551$$

The axial stress factor (Equation 61d)

$$\eta_a = \frac{\psi_e - \psi}{2 \frac{r}{r_t} \sin \phi} = \frac{1.551 - 1.405}{2 \times 1.254 \times .968} = -0.060$$

The tangential stress factor (Equation 61e),

$$\eta_t = \frac{r/r_t \left(\frac{p}{p_o} + \frac{r_t}{r_1} \eta_a \right)}{\sin \phi} = \frac{1.254}{.968} (0.1704 + 0) = 0.221$$

where

$$r_t/r_1 = 1.95/\infty = 0$$

According to Equation 61f, the equivalent stress factor

$$\begin{aligned} f_e &= \sqrt{\eta_a^2 + \eta_a \eta_t + \eta_t^2} \\ &= 0.01 \sqrt{36 + 133 + 488} = 0.256 \end{aligned}$$

To compute the wall thickness, the yield strength at elevated temperature is assumed to be the same as that for the tube.

$$Y = 150,000 \text{ lb/in}^2$$

† Reference 27.

From Equation 61g,

$$t_r = \frac{f_s p_o}{Y} f_s = \frac{1.95 \times 15,600}{150,000} f_s = 0.203 f_s = 0.052 \text{ in}$$

This wall is too thin for handling. Therefore, it is increased to the dimensions shown in Table 25. Continuing the calculations for Station -1.91, the apparent wall ratio (Equation 61k) for a nominal wall thickness of $t_n = 0.30$ in. is

$$W_a = \frac{r + t_n}{r} = \frac{2.445 + 0.30}{2.445} = 1.123$$

The actual wall ratio (Equation 61m)

$$W = .947 W_a + 0.053 = 1.064 + 0.053 = 1.117$$

The effective wall thickness (Equation 61n)

$$t_e = r(W - 1) = 2.445 \times .117 = 0.286$$

The effective stress now becomes (Equation 61j)

$$\sigma_e = f_s \frac{p_o t}{t_e} = .256 \frac{15,600 \times 1.95}{.286} = 27,200 \text{ lb/in}^2$$

Effective stresses at other stations are computed similarly with all data listed in Table 25.

GLOSSARY

(In general, terms are defined with specific reference to their use in respect to guns.)

- autofrettage. ("self-hooping") A method of tube manufacture, using cold working, i.e., prestressing by radial expansion which see.
- ballistic cycle. Elapsed time from ignition of propellant to time that action of propellant gases on the projectile ceases.
- barrel. Common terminology for gun tube of small arms. *See:* tube, gun.
- band, rotating. Soft metal band around projectile near its base. The rotating band centers the projectile and makes it fit tightly in the bore, thus preventing the escape of gas, and by engaging the rifling, gives projectile its spin.
- band, rotating, preengraved. A rotating band fitted to or integral with a projectile and containing grooves to fit the rifling of the weapon. The grooves are formed during manufacture of the projectile. This practice is followed in the manufacture of ammunition for recoilless weapons.
- bolt, gun. As applied to small arms, that portion of the gun which carries the firing pin, and which closes the rear of the chamber during burning of the propellant; bolt.
- bore. The interior of a gun tube.
- bore, smooth. Bore of a gun with smooth surface, i.e., not rifled.
- bore, tapered. Bore of a gun tube with a diameter which decreases along all or part of the length of bore.
- bourellet. The cylindrical surface of a projectile on which the projectile bears while in the bore of the weapon.
- breech. The rear part of the bore of a gun, especially the opening that permits the projectile to be inserted at the rear of the bore.
- breechblock. A movable steel block in the mechanism of a breech-loading gun that seals the breech opening of the tube during firing.
- breech ring. Breechblock housing, screwed or shrunk on the rear of a cannon, in which the breechblock engages.
- built-up gun. Gun (tube) assembled by shrinkage method. Consists of two or more concentric cylinders shrunk one on another.
- bullet. The projectile fired, or intended to be fired, from a small arm.
- caliber. The diameter of the bore of a gun tube. In a rifled bore it is measured on the surface of the lands.
- cannon. A complete assembly, consisting of a tube and a breech mechanism, firing mechanism or base cap, which is a component of a gun, howitzer, or mortar. It may include muzzle appendages. The term is generally limited to calibers greater than 30 mm.
- cap. The shrunk-on retainer of a small arms lined tube. It contains the chamber.
- centering cylinder. A cylindrical section in the forward portion of the chamber, and of a reduced diameter, which seats the rotating band.
- chamber. Region of a gun tube in which the charge is placed.
- choke bore. A tapered bore with diameter decreasing towards the muzzle.
- cold-worked gun. Gun produced by cold working, that is, by radial expansion, which see.
- complete round. All of the ammunition components necessary to fire a weapon once.

GLOSSARY—(continued)

cook-off. The deflagration or detonation of ammunition caused by the absorption of heat from its environment. Usually it consists of the accidental and spontaneous discharge of, or explosion in, a gun or firearm, caused by an overheated chamber or barrel igniting a fuze, propellant charge, or bursting charge.

cooling, boundary layer. Cooling of gun tube by insulating bore surface from heat of propellant gases.

cooling, transpiration. Cooling of gun tube by injecting a coolant through porous walls.

coppering. Metal fouling left in the bore of a weapon by the rotating band or jacket of a projectile.

cradle. The nonrecoiling structure of a weapon that houses the recoiling parts and rotates about the trunnions to aim the gun.

crush-up. In small arms, longitudinal interference between case and chamber, designed to prevent cartridge cases from pulling apart during gun firing.

drum. Rotatable cylinder containing a group of chambers equally spaced radially about the axis; a component of a revolver type weapon.

engraving. The process by which the rotating bands of projectiles or jackets of bullets are cut by the rifling.

erosion. The enlargement or wearing away of the bore of a weapon by the movement of high-temperature gases and residues generated from the burning of the propellant, by chemical action and by friction between the projectile and the bore.

extraction. Process by which the cartridge cases are pulled from the chamber of a gun.

fixed ammunition. Ammunition with primer and propellant contained in a cartridge case permanently crimped or attached to a projectile. Loaded into the weapon as a unit. Usually termed a cartridge.

forcing cone. Conical section which includes tapered

beginning of the lands at the origin of the rifling of a gun tube. The forcing cone allows the rotating band of the projectile to be gradually engaged by the rifling thereby centering the projectile in the bore.

free run. Travel of a projectile from its original position in the gun chamber until it engages with the rifling in the gun bore.

frequency ratio. In automatic weapons, ratio of natural frequency of gun tube to firing rate.

gas wash. Erosion caused by propellant gas activity.

groove. One of the helical grooves forming the rifling.

gun. 1. General term for a piece of materiel, consisting essentially of a tube or barrel, for throwing projectiles by force, usually the force of an explosive. The general term embraces such weapons as are sometimes specifically designated as gun, howitzer, mortar, cannon, firearm, rifle, shotgun, carbine, pistol, revolver. 2. Specific term for a weapon with relatively long tube, usually over 30 calibers, which fires a projectile with relatively high initial velocity, and with a comparatively flat trajectory (fired at low angles of elevation).

gun, Gatling type. A gun having several tubes rigidly attached together which rotate about a common axis and fire in rotation.

gun, revolver type. A gun having several chambers rigidly attached together which rotate about a common axis and fire in rotation through a common tube.

howitzer. Normally, cannon with a medium length barrel between that of a mortar and a gun in length, operating with a relatively high angle of fire, and using a medium muzzle velocity.

interior ballistics. The science which deals with the motion of the projectile and accompanying phenomena in a gun tube.

jacket. One of the outer layers of a multilayer gun tube.

GLOSSARY—(continued)

jacket, bullet. A metal shell surrounding a metal core, the combination comprising a bullet for small arms.

land. One of the raised ridges in the bore of a rifled gun tube.

liner. 1. Inside layer of a multilayer gun tube.
2. An inside cylinder of a small arms tube designed for withstanding erosion and heat damage to prolong tube life.

loading. Process of placing the round in the chamber.

mortar. Weapon which, in comparison to gun or howitzer of the same caliber, has the shortest tube length. Usually designed to fire at very high elevations and to obtain very short ranges by combinations of reduced propelling charge and very high elevations.

muzzle. The end of a gun tube from which the projectile is discharged.

muzzle brake. Device attached to the muzzle which utilizes escaping gases to reduce recoil forces.

muzzle velocity. Velocity of the projectile as it leaves the muzzle. Also called "initial velocity."

nozzle. A convergent-divergent structure forming the rear portion of a recoilless weapon. Flow of propellant gases through the nozzle produces the counterrecoil force to prevent rearward movement of the gun.

nozzle, bar breech. A nozzle with a bar across its opening to retain the round and to house the firing mechanism.

nozzle, central orifice. A nozzle with passageway centrally located.

nozzle, kidney-shaped. A nozzle with two or more kidney-shaped passageways symmetrically located.

nozzle index. The sum of the products of the chord by width of all nozzle openings.

origin of rifling. The position in a rifled gun bore

at which the rifling begins. More specifically, the plane, perpendicular to the axis of the gun bore, in which the rifling starts.

pressure, rotating band. The pressure generated between rotating band and gun tube.

pressure, computed maximum. (*CMP*) The maximum pressure computed from interior ballistics equations, developed in the gun to achieve rated muzzle velocity during operation at 70°F.

pressure, elastic strength. (*ESP*) The pressure that will produce an equivalent stress (based on distortion-energy criteria) at some point in the tube that is equal to the minimum elastic limit of the material at ambient temperature (+70°F).

pressure factor. The ratio of design pressure to the allowable stress for the material.

pressure, permissible individual maximum. (*PIMP*) Pressure which should not be exceeded by the maximum pressure of any individual round under any service condition.

pressure, propellant gas. Pressure in a gun tube exerted by the propellant gas.

pressure, rated maximum. (*RMP*) Pressure which should not be exceeded by the average of maximum pressures achieved by firing a group of the specified projectiles at the specified muzzle velocity.

propellant. A low explosive substance which, through burning, can be made to produce gases at controlled rates and to provide the energy necessary to propel a projectile.

radial expansion. A method of making gun tubes by expanding steel cylinders under internal pressure until the interior diameter has been permanently enlarged. This method is also known as cold-working and autofrettage. (The latter is a French term meaning "self-hooping.")

receiver. The basic unit of a firearm, especially a small arm, which contains the operating mechanism of the weapon and to which the barrel and other components are attached.

GLOSSARY—(continued)

- recoil. In small arms or artillery, the rearward motion of the gun or tube, due to firing. In recoilless weapons, the residual impulse between gun tube and nozzle which may move the gun rearward or forward. If the impulses balance, no motion occurs and the gun is truly recoilless.
- recoil system, double. A recoil system composed of two complete systems, a primary system and a secondary system.
- recoil system, primary. The system of the double recoil type which permits recoil of the tube and its components.
- recoil system, secondary. The system of the double recoil type which permits the top carriage to recoil.
- recoil system, single. A recoil system that has only the gun tube and its components as recoiling parts.
- recoilless. Of a gun: built so as to completely or nearly eliminate recoil, by discharging part of the propellant gases to the rear.
- rifling. Spiral grooves in the bore of a weapon designed to give a spin to the projectiles for greater accuracy and carrying power. Rifling includes both the grooves and the ridges between, called lands.
- rifling torque. Torque induced by the rifling acting on the projectile.
- rifling, wear compensating. Rifling designed to compensate for wear. It has zero twist for a short distance from the origin, followed by increasing twist.
- semifixed ammunition. Ammunition in which the cartridge case is not permanently fixed to the projectile, so that the zone charge within the cartridge case can be adjusted to obtain the desired range; loaded into the weapon as a unit.
- separated ammunition. Separated ammunition is characterized by the arrangement of the propelling charge and the projectile for loading into the gun. The propelling charge, contained in a primed cartridge case that is sealed with a closing plug, and the projectile are loaded into the gun in one operation. Separated ammunition is used when the ammunition is too large to handle as fixed ammunition.
- separate loading ammunition. Ammunition in which the projectile, propellant charge (bag loaded) and primer are handled and loaded separately into the gun. *Slo* cartridge case is utilized in this type of ammunition.
- slope, chamber. The diametral taper of the chamber.
- slope, forcing cone. The diametral taper of the forcing cone.
- small arms. Guns which do not exceed a caliber of 30 mm.
- strain compensation. The practice of providing an interference between projectile and bore to preclude excessive clearances when the tube dilates because of propellant gas pressure.
- stress, allowable working. The maximum stress to which a structure is intended to be subjected during normal performance.
- stress concentration. The presence of localized stresses in a structure, which are significantly larger than the stresses existing in immediate neighboring areas. The larger stresses are usually due to discontinuities in the structure.
- stress, axial. Principal stress in the longitudinal direction.
- stress, equivalent. The resultant stress obtained by combining the principal stresses according to some theory of failure. The theory now employed in gun tube design is that of Hencky-von Mises for the strain energy concept.
- stress, pressure. Stress induced in a gun tube by the propellant gas.
- stress, principal. One of three mutually perpendicular stresses on an element which is oriented such that no shear stress appears on the faces of the element.

GLOSSARY—(continued)

- stress, radial. Principal stress in the radial direction.
- stress, shrink fit. Stress induced by shrink fit.
- stress, tangential. Principal stress in the tangential direction.
- stress, thermal. Stress induced by a temperature gradient across a wall.
- travel, projectile. Distance traveled by the projectile in the bore.
- tube, gun. (Often shortened to tube.) Hollow cylindrical structure in which the projectile receives its motion and initial direction. Tubes for small arms are commonly called barrels.
- tube, jacketed. *See* : tube, multilayered.
- tube, monobloc. Tube made of one piece of material.
- tube, multilayered. A tube composed of two or more concentric tubes assembled by shrink fit.
- tube, quasi two-piece. Built-up small arms tube comprising barrel, liner, and cap assembled by threaded connection with shrink fit.
- twist, angle of. Angle formed by rifling and longitudinal line on bore surface.
- twist, increasing. Rifling in which the degree of twist increases from the origin of rifling to the muzzle; gain-twist, gaining twist.
- twist, left hand. Rifling in which the twist is such as to impart a left hand rotation to the projectile when viewed from the origin.
- twist, right hand. Rifling in which the twist is such as to impart a right hand rotation to the projectile when viewed from the origin.
- twist (of rifling). Inclination of the spiral grooves (rifling) to the axis of the bore of a weapon. It is expressed as the number of calibers of length in which the rifling makes one complete turn.
- twist, uniform. Rifling in which the degree of twist is constant from the origin of rifling to the muzzle, the path of the groove being a uniform spiral; constant twist.
- whip. Motion of tube in plane normal to its longitudinal axis during firing.
- wire-wrapped. Term applied to guns manufactured by wrapping wire under tension on a central tube.

REFERENCES

1. Al. J. Pascual, et al. *Transient Thermal Stresses in Gun Tubes, Part II*, Watervliet Arsenal Technical Report WVT-RR-6208, May 1962.
2. Gunther Cohn, *Cook-off in Aircraft Guns*, The Franklin Institute Report F-A2144-2, Contract DA-36-034-504-ORD-1, April 1960.
3. National Defense Research Committee. *Hyper-velocity Guns and the Control of Gun Erosion*, Washington, D. C., 1946.
4. D. E. Wente, et al, *An Investigation of the Effects of Natural Frequency of Vibration of the Barrel upon the Dispersion of an Automatic Weapon*, Report So. 311, U. S. Army Ordnance Experimental Station, Purdue University, April 1, 1955.
5. J. P. Den Hartog, *Mechanical Vibrations*, Fourth Edition, McGraw-Hill Book Company, Inc., N. Y., 1956.
6. ORDP 20-302, Materials Handbook, *Copper and Copper Alloys*.*
7. ORD-L784, TN2-8051, *Study of Pressure Gradients in Recoilless Rifle Chamber*, Aircraft Armaments, Inc., for Frankford Arsenal, September 1959. (Confidential)
8. J. J. Donnelly and H. H. Kahn, *Interior Ballistics Designs for FA-1 System for Davy Crockett*, Frankford Arsenal Report No. MR-678, June 1958. (Secret)
9. D. J. Katsanis, *A New Concept of the Ballistic Efficiency of Recoilless Rifles*, Frankford Arsenal Report R312, March 1956.
10. S. G. Hughes, *Summary of Interior Ballistics Theory for Conventional Recoilless Rifles*, Frankford Arsenal Report R-1140, Project TS4-4014.
11. H. W. Leipman and A. Roshko, *Elements of Gas Dynamics*, John Wiley and Sons, N. Y., 1937.
12. Alexander Hammer, *Barrel Research and Development at Springfield Armory*, 1955.
13. *A Study of Past and Present Designs of Rotating Band and Rifling, Part I*, Franklin Institute Laboratories Report No. 307, Contract W-36-034-OED-7380, June 1946.
14. ORDP 20-247 (C), Engineering Design Handbook, Artillery Ammunition Series, *Section 4, Design for Projection (U)*.*
15. ORDP 20-175, Engineering Design Handbook, Explosives Series, *Solid Propellants, Part One*.*
16. ORDP 20-106, Engineering Design Handbook, *Elements of Armament Engineering, Part 1, Sources of Energy*.*
17. OCM Item 29196, 27 September 1945.
18. Seeley and Smith, *Advanced Mechanics of Materials*, Second Edition, John Wiley and Sons, N. Y., 1952.
19. R. L. Strub, *Distribution of Mechanical and Thermal Stresses in Multilayer Cylinders*, Transactions ASME, January 1953.
20. C. M. King, *The Design of Gun Tubes*, Frankford Arsenal Report MR-608, Project TS4-4020, July 1955.
21. A. M. Stott, *Simplified Method of Utilizing Disfortiori Energy Concept for the Design and Stress Analysis of Tubes and Chambers*, Frankford Arsenal Technical Note TS-1110, January 1961.
22. *Stress Analysis for Recoilless Rifle XM28, (Spotter and Gimbal Brackets Calculations)*, Technik, Inc., Report 61-10 for Frankford Arsenal, April 1961.
23. *Stress Analysis Nozzle Section, XM-64, Recoilless Rifle*, Ordnance Engineering Associates, Project SO.2041, Progress Report for Frankford Arsenal, 28 February 1961. (Confidential)
24. R. J. Ronrk, *Formulas for Stress and Strain*, Third Edition, McGraw-Hill Book Company, Inc., S. Y., 1954.
25. S. Timoshenko, *Strength of Materials, Part II*, Second Edition, D. Van Nostrand Company, Inc., N. Y., 1945.
26. *Minimum Weight Design of Nozzle for Isentropic Flow*, Technik, Inc., Report 61-3, Contract DA-30-069-ORD-3081 for Frankford Arsenal, January 1961.
27. J. H. Keenan and J. Kaye, *Gas Tables*, John Wiley and Sons, N. Y., 1948.
28. Hoffman and Sachs, *Introduction to the Theory of Plasticity for Engineers*, McGraw-Hill Book Company, Inc., N. Y., 1953.
29. C. W. Musser, et al, *Strain Compensated Barrels*, Frankford Arsenal Report No. R-1008, May 1951.
30. *Screw-Thread Standards for Federal Services*, Na-

* See inside back cover for additional information pertaining to Engineering Design Handbooks.

REFERENCES—(continued)

- tional Bureau of Standards Handbook H28, Part I.
31. Watertown Arsenal Laboratories, *Quarterly Progress Report to Frankford Arsenal on XM-28 and XM-29*, 17 March 1959.
32. R. E. Petersen, *Stress Concentration Design Factors*, John Wiley and Sons, N. Y., 1953.
33. T. J. Dolan and E. L. Broghamer, *A Photoelastic Study of Stresses in Gear Tooth Fillets*, University of Illinois Experimental Station Bulletin 335, 1942.
34. *Elevated-Temperature Properties of Wrought Medium-Carbon Alloy Steels*, ASTM Special Technical Publication No. 199, Philadelphia, 1957.
35. ASME Handbook, *Metals Properties*, McGraw-Hill Book Company, Inc., N. Y., 1954
36. W. H. McAdams, *Heat Transmission*, Third Edition, McGraw-Hill Book Company, Inc., S. Y., 1954.
37. ORDP 20-305, Materials Handbook, *Titanium and Titanium Alloys*."
38. ORD 20-309, Materials Handbook, *Plastics*.*
39. Gunther Cohn, *Barrels for Automatic Weapons*, Franklin Institute Report FA-2461, May 1961. (Confidential)
40. R. J. Girad and E. F. Koetsch, *Production Hard Chromium Plating of the M14 Rifle Barrel*, Springfield Armory.

* See inside back cover for additional information pertaining to Engineering Design Handbooks.

ENGINEERING DESIGN HANDBOOK SERIES

The Engineering Design Handbook Series is intended to provide a compilation of principles and fundamental data to supplement experience in assisting engineers in the evolution of new designs which will meet tactical and technical needs while also embodying satisfactory producibility and maintainability.

Listed below are the Handbooks which have been published or submitted for publication. Handbooks with publication dates prior to 1 August 1962 were published as 20-series Ordnance Corps pamphlets. AMC Circular 310-38, 19 July 1963, redesignated those publications as 706-series AMC pamphlets (i.e., ORDP 20-138 was redesignated AMCP 706-138). All new, reprinted, or revised Handbooks are being published as 706-series AMC pamphlets.

General and Miscellaneous Subjects

<u>Number</u>	<u>Title</u>
106	Elements of Armament Engineering, Part One, Sources of Energy
107	Elements of Armament Engineering, Part Two, Ballistics
108	Elements of Armament Engineering, Part Three, Weapon Systems and Components
110	Experimental Statistics, Section 1, Basic Concepts and Analysis of Measurement Data
111	Experimental Statistics, Section 2, Analysis of Enumerative and Classificatory Data
112	Experimental Statistics, Section 3, Planning and Analysis of Comparative Experiments
113	Experimental Statistics, Section 4, Special Topics
114	Experimental Statistics, Section 5, Tables
134	Maintenance Engineering Guide for Ordnance Design
135	Inventions, Patents, and Related Matters
136	Servomechanisms, Section 1, Theory
137	Servomechanisms, Section 2, Measurement and Signal Converters
138	Servomechanisms, Section 3, Amplification
139	Servomechanisms, Section 4, Power Elements and System Design
170(C)	Armor and Its Application to Vehicles (U)
252	Gun Tubes (Guns Series)
270	Propellant Actuated Devices
290(C)	Warheads--General (U)
331	Compensating Elements (Fire Control Series)
355	The Automotive Assembly (Automotive Series)

Ammunition and Explosives Series

175	Solid Propellants, Part One
176(C)	Solid Propellants, Part Two (U)
177	Properties of Explosives of Military Interest, Section 1
178(C)	Properties of Explosives of Military Interest, Section 2 (U)
210	Fuzes, General and Mechanical
211(C)	Fuzes, Proximity, Electrical, Part One (U)
212(S)	Fuzes, Proximity, Electrical, Part Two (U)
213(S)	Fuzes, Proximity, Electrical, Part Three (U)
214(S)	Fuzes, Proximity, Electrical, Part Four (U)
215(C)	Fuzes, Proximity, Electrical, Part Five (U)
244	Section 1, Artillery Ammunition--General, with Table of Contents, Glossary and Index for Series
245(C)	Section 2, Design for Terminal Effects (U)
246	Section 3, Design for Control of Flight Characteristics
247(C)	Section 4, Design for Projection (U)
248	Section 5, Inspection Aspects of Artillery Ammunition Design
249(C)	Section 6, Manufacture of Metallic Components of Artillery Ammunition (U)

Ballistic Missile Series

<u>Number</u>	<u>Title</u>
281(S-RD)	Weapon System Effectiveness (U)
282	Propulsion and Propellants
284(C)	Trajectories (U)
286	Structures

Ballistics Series

140	Trajectories, Differential Effects, and Data for Projectiles
160(S)	Elements of Terminal Ballistics, Part One, Introduction, Kill Mechanisms, and Vulnerability (U)
161(S)	Elements of Terminal Ballistics, Part Two, Collection and Analysis of Data Concerning Targets (U)
162(S-RD)	Elements of Terminal Ballistics, Part Three, Application to Missile and Space Targets (U)

Carriages and Mounts Series

340	Carriages and Mounts--General
341	Cradles
342	Recoil Systems
343	Top Carriages
344	Bottom Carriages
345	Equilibrators
346	Elevating Mechanisms
347	Traversing Mechanisms

Materials Handbooks

301	Aluminum and Aluminum Alloys
302	Copper and Copper Alloys
303	Magnesium and Magnesium Alloys
305	Titanium and Titanium Alloys
306	Adhesives
307	Gasket Materials (Nonmetallic)
308	Glass
309	Plastics
310	Rubber and Rubber-Like Materials
311	Corrosion and Corrosion Protection of Metals

Military Pyrotechnics Series

186	Part Two, Safety, Procedures and Glossary
187	Part Three, Properties of Materials Used in Pyrotechnic Compositions

Surface-to-Air Missile Series

291	Part One, System Integration
292	Part Two, Weapon Control
293	Part Three, Computers
294(S)	Part Four, Missile Armament (U)
295(S)	Part Five, Countermeasures (U)
296	Part Six, Structures and Power Sources
297(S)	Part Seven, Sample Problem (U)